FREE RADICAL COPOLYMERIZATION OF HYDROXY-FUNCTIONAL MONOMERS: KINETIC AND SEMIBATCH STUDIES

By

KUN LIANG

A thesis submitted to the Department of Chemical Engineering

In conformity with the requirements for the degree of

Doctor of Philosophy

Queen's University

Kingston, Ontario, Canada

February, 2013

Abstract

Acrylic resins used as polymeric binders in automotive coatings are complex copolymers containing reactive functional (often hydroxyl) groups. A better understanding of the copolymerization kinetics of these monomers is required in order to ensure uniform distribution of the functional groups among the polymer chains over the course of production. Free radical copolymerization propagation kinetics of styrene (ST) with 2-hydroxyethyl methacrylate (HEMA) and 2-hydroxyethyl acrylate (HEA) have been investigated both in bulk and solution, using pulsed-laser polymerization (PLP) combined with size exclusion chromatography (SEC) and proton NMR. All of the solvents examined (*n*-butanol, toluene and DMF) affect ST/HEMA copolymer composition relative to bulk polymerization, while the effects on propagation rates suggest that hydrogen bonding interactions need to be explicitly considered. Semibatch reactions of ST/HEMA, butyl acrylate (BA)/HEMA and butyl methacrylate (BMA)/HEMA have been carried out in xylene, DMF and 1-pentanol at 110 and 138 °C. The variation in monomer composition for the three solvents agrees with the kinetic studies. It was found that polymer molecular weight is strongly affected by solvent choice and operating conditions, partially due to branching reactions caused by impurities from commercial HEMA monomers. PLP and ^{13}C-NMR analysis indicate that no backbiting occurred during polymerization of HEA, and it is shown that H-bonding disrupts the backbiting mechanism found for other acrylates. Thus, semibatch production in *n*-butanol can reduce branching and increase molecular weight of BA homopolymers by a factor of five compared to polymerization in xylene.

Acknowledgement

I would like to express my gratitude towards my supervisor, Dr. Robin Hutchinson, for his guidance, support, and encouragement throughout my Ph.D. study at Queen's University. I will never forget the brightness he brought to me when my life was in confusion. His extensive knowledge and charming character help me grow very fast as a researcher and as a person.

I would also like to thank Dr. Davide Maoscatelli of Politecnico di Milano and his group for the great cooperation on many projects, Dr. Sabine Beuermann of University of Potsdam and Dr. Michael Buback of Göttengen University for the technical discussions. I also really appreciate the help from my lab mates. They leave me endless pleasant memories in my lab experience and there are too many of them to list here.

Finally, to my lovely family, thanks for the spiritual and material support that I am able to pursue the work I am really interested in. Special thanks to my daughter, Chloe, the biggest surprise for my last year's study, for not ruining my data in the computer, and to my beloved wife, Connie, for firmly holding my hand and standing beside me.

Table of Contents

List of Tables

List of Figures

Nomenclature

Symbol	Units	Definition
A	L/(mol· s)	Frequency factor of propagation rate coefficient
BA		*n*-Butyl acrylate
BMA		*n*-Butyl methacrylate
$C_4\%$		Quaternary carbon level per 100 monomer units in the chain
Cs_i		Transfer rate coefficient to solvent
D_n		Dead polymer of length *n*
d*n*/d*c*		Specific refractive index increment
DRI		Differential refractometer detector
E_a	J/mol	Activation energy of propagation
FT-IR		Fourier transform infrared spectroscopy
f		Initiator decomposition efficiency
f_i		Mole fraction of monomer *i*
F_i^{inst}		Instantaneous polymer composition *i*
GC		Gas chromatography
GMA		Glycidyl methacrylate
HEA		2-Hydroxyethyl acrylate

HEMA		2-Hdroxyethyl methacrylate
[I]	mol/L	Initiator concentration
K, a		Mark-Houwink parameters
k_{bb}	1/s	Backbiting rate constant
k_{d}	1/s	Initiator decomposition rate constant
k_{piii}	L/(mol· s)	Propagation rate constant for monomer i
$k_{p_{iij}}$	L/(mol· s)	Propagation rate coefficient for addition of monomer *j* to radical *ii* (i, j = 1, 2, 3)
$k_{p,cop}$	L/(mol· s)	Average propagation rate constant in copolymerization
k_{p}^{MCR}	L/(mol· s)	Propagation rate constant for mid-chain radical
k_{p}^{av}	L/(mol· s)	Averaged propagation rate constant
k_{SD}	L/(mol· s)	Segmental diffusion termination rate coeffficient
k_{tc}	L/(mol· s)	Termination rate coefficient by combination
$k_{t,cop}$	L/(mol· s)	Termination rate coefficient in copolymerization
k_{td}	L/(mol· s)	Termination rate coefficient by disproportionation
k_{TD}	L/(mol· s)	Translational diffusion termination rate coefficient
k_{tii}	L/(mol· s)	Termination rate coefficient of monomer i
k_{trij}^{mon}	L/(mol· s)	Transfer rate coefficient to monomer
L_0		Chain length

LS		Light scattering detector
[M]	mol/L	Monomer concentration
M_i		Monomer i (i = 1, 2)
MMA		Methyl methacrylate
M_n		Number averaged molecular weight
M_w		Weight averaged molecular weight
MW		Polymer molecular weight
MWD		Molecular weight distribution
PDI		Polymer polydispersity index
$P_{n,m}$		Radicals with terminal unit 1 containing n units of monomer 1 and m units of monomer 2
P_{ij}		Probability of radical j with i penultimate unit
PLP		Pulsed laser polymerization
$Q_{n,m}$		Radicals with terminal unit 2 containing n units of monomer 1 and m units of monomer 2
R		Primary radical species
r_1, r_2		Monomer reactivity ratios
s_1, s_2		Radical reactivity ratios
[S]	mol/L	Solvent concentration
SEC		Size exclusion chromatography

ST		Styrene
T	K	Temperature
t_0	s	Time interval between laser flashes
TBPA		tert-Butyl peroxyacetate
U_i		Macromonomer with chain length i
ß		Fraction of radicals terminated prior to the next pulse
ρ	g/L	Density

List of Publications

1. Liang, K.; Marco, D.; Moscatelli, D.; Hutchinson, R. A. "An Investigation of Free-Radical Copolymerization Propagation Kinetics of Styrene and 2-Hydroxyethyl Methacrylate", *Macromolecules* 2009, 42, 7736-7744.

2. Liang, K.; Hutchinson, R. A. "Solvent Effects on Free Radical Copolymerization Propagation Kinetics of Styrene and Methacrylates", *Macromolecules* 2010, 43, 6311-6320.

3. Liang, K.; Hutchinson, R. A. "The Effect of Hydrogen Bonding on Intramolecular Chain Transfer in Polymerization of Acrylates", *Macromolecular Rapid Communications* 2011, 32, 1090-1095.

4. Liang, K.; Hutchinson, R. A.; Barth, J.; Samrock, S.; Buback, M. "Reduced Branching in Poly(butyl acrylate) via Solution Radical Polymerization in *n*- Butanol", *Macromolecules* 2011, 44, 5843-5845.

5. Liang, K.; Hutchinson, R. A. "Solvent Effects in Semibatch Free Radical Copolymerization of 2-Hydroxyethyl Methacrylate and Styrene at High Temperatures", *Macromolecular Symposia* 2012, accepted.

6. Mavroudakis, E.; Liang, K.; Moscatelli, D.; Hutchinson, R. A. "A Combined Computational and Experimental Study on the Free-Radical Copolymerization of Styrene and Hydroxyethyl Acrylate", *Macromolecular Chemistry and Physics* 2012, 213, 1706.

7. Dossi, M.; Liang, K.; Hutchinson, R. A.; Moscatelli, D. "An Investigation of Free Radical Copolymerization Propagation Kinetics of Vinyl Acetate and Methyl Methacrylate", *The Journal of Physical Chemistry B* 2010, 114, 4213.

8. Lessard, B.; Guillaneuf, Y.; Mathew, M.; Liang, K.; Clement, J.; Gigmes, D.; Hutchinson, R. A.; Maric, M. "Understanding the Controlled Polymerization of Methyl Methacrylate with Low Concentrations of 9-(4-Vinylbenzyl)-9H-Carbazole Comonomer by Nitroxide Mediated Polymerization: The Unexpected Pivotal Role of Reactivity Ratios." *Macromolecules* 2013, 46, 805.

Chapter 1 Introduction

Acrylic copolymers, the base polymer components for automotive coatings, are manufactured from a mixture of monomers selected from methacrylates, acrylates and styrene. The low molecular weight (MW) copolymer chains are synthesized via solution high-temperature semibatch free radical copolymerization.[1] Good reactor control is required to ensure that the copolymer composition and distribution of reactive functional groups is uniform among the copolymer chains produced over the course of the batch. This uniformity is required, as the functional groups on the low MW chains react on the surface of the vehicle, crosslinking to form the final high MW coating.[2] The goal of the research is to improve understanding of the kinetics of hydroxyl-functional monomers during high temperature polymerization, because of their important role in modern automotive coatings.[3-5]

Extensive research has been done upon copolymerization of styrene (ST) with alkyl methacrylates/acrylates, including recent efforts in our group.[6,7,14] A general family type behavior is observed when examining homopropagation kinetics,[8] monomer reactivity ratios,[9,14] and even their conformity to the implicit penultimate unit effect model of copolymerization rate.[10,14] For example, Müller and Buback studied the copolymerization of methyl acrylate (MA) or dodecyl acrylate (DA) with either methyl methacrylate (MMA) or dodecyl methacrylate (DMA), and showed that copolymer composition for all four systems is well represented by a single pair of

monomer reactivity ratios.[11] However, hydroxy-functional monomers, such as 2-hydroxyethyl methacryate (HEMA) and 2-hydroxyethyl acrylate (HEA), show some deviation from these generalities. Buback and Kurz[12] have measured propagation rate coefficients (k_p) for the homopolymerization of HEMA by the pulsed laser polymerization (PLP)/ size exclusion chromatography (SEC) technique, finding that the k_p value for HEMA is higher than alkyl methacrylates by a factor of two. Meanwhile, there are few reported studies of polymerizations involving HEA, which is partly due to the difficulties in analysis of its polymers stemming from the fact that its polymerization typically leads to high molecular weight products through crosslinking reactions caused by impurities and/or transfer reactions. Beuermann et al.[13] have shown the difficulties to determine the propagation rate coefficient (k_p) of butyl acrylate (BA) by PLP because of side reactions, such as backbiting. However, it will be shown later in this work that poly(HEA) presents a beautiful PLP structure without any backbiting effect. These phenomena suggest the need to perform detailed studies of the polymerization kinetics of HEMA and HEA to compare them to the better known behavior of alkyl (meth)acrylates, and to study their incorporation into acrylic resins under conditions similar to those used commercially in coatings. As part of this study, the effect of solvent on free-radical copolymerization kinetics will be examined, via specialized kinetic experiments as well as in a starved-feed semibatch lab-scale reactor under operating conditions similar to those used in industry.

1.1 Thesis Objective

The motivation of automotive coatings industry is to increase production rates and to produce new polymeric materials with existing equipment, as well as the desire to further decrease the amount of volatile organic solvent in the recipe. In the coatings industry, free radical polymerization is most widely applied in manufacture due to the high production rate and mature control system. Currently resins consist of functionalized low MW (<5,000 $g \cdot mol^{-1}$) acrylic polymers produced at high (>120 °C) temperatures, a strategy adopted to decrease solvent content in the "high-solids" mixture to 30 wt% or less without increasing solution viscosity.[2] In order to increase the cohesion strength of the low MW resins, functional monomers, such as GMA, HEMA and HEA, are introduced to the coating recipe to form, via reaction with an added crosslinking agent, a high MW network on the surface of vehicle. Therefore, the studies in this thesis targeted the improved understanding of free radical copolymerization kinetics of hydroxyl functional monomers. The primary goals of the study were:

1. Design and apply PLP-SEC-NMR technique to HEMA or HEA copolymerization systems, to measure monomer reactivity ratios and propagation rate coefficients.

2. Gain improved understanding of ST/HEMA and ST/HEA kinetics in bulk (ST=styrene), comparing to other alkyl methacrylate/acrylate systems.

3. Explore the solvent effect on copolymerization kinetics of methacrylates or acrylates and generate a universal explanation for the solvent effect on all the systems.

4. Verify the solvent effect in semibatch reaction and investigate other possible influences.

1.2 Thesis Outline

This thesis is written based on the published articles previously listed and summaries of unpublished results. Some editing has been done to improve the flow of the thesis.

Chapter 2 presents a literature review of the relevant technical areas for the research conducted. A general overview of the kinetics of free radical polymerization, especially propagation kinetics and short chain branching, is given as technical background. Some recent advances on the research of methacrylates and acrylates polymerization kinetics are also discussed. In addition, a comprehensive review of solvent effect on polymerization is necessary to motivate our study.

Chapter 3 combines two studies: ST/HEMA copolymerization in bulk and solvent effect studies on ST/methacrylates by PLP. Monomer reactivity ratios and propagation rate coefficients in bulk and solvents are determined. More consideration is given to the H-bonding effect between HEMA monomers or between monomer and solvent.

Chapter 4 focuses on semibatch reactions of ST/HEMA vs. ST/BMA in different solvents. Some effects of H-bonding will be covered, as well as the verification of long chain branching caused by the impurity of HEMA monomer.

Chapter 5 studies the influence of H-bonding and solvent choice on BMA/HEMA copolymerization, using both semibatch reactions as well as the PLP/SEC/NMR technique.

Chapter 6 combines ST/HEA copolymerization in bulk and solvent and the study of acrylate homopolymerization by PLP. H-bonding effect on acrylate backbiting will be checked in details by ^{13}C-NMR. Semibatch reactions of BA homopolymerization in different solvents are discussed, and the main cause of the significant decrease of branching density in *n*-butanol (BuOH) compared to polymerization in xylene is investigated.

Chapter 7 studies the influence of H-bonding and solvent choice on BA/HEMA copolymerization, using both semibatch reactions as well as the PLP/SEC/NMR technique.

Chapter 8 is an overall summary of this thesis and the recommended future work.

1.3 Summary of Original Contributions

With the aid of the PLP-SEC-NMR technique, we are able to determine monomer reactivity ratios and propagation rate coefficients accurately with ST/methacrylates or acrylates copolymerization in different solvents under a wide range of conditions, especially for hydroxyl functional monomers. The improved understanding of polymerization kinetics of HEMA and HEA will enable the optimization of the structure of acrylic polymers and polymerization recipes to meet the requirements of the coatings industry. More importantly, we generate a universal explanation for the solvent effect on copolymerization kinetics, which can be applied to all the

examined methacrylates or acrylates systems. In addition, the improved understanding of solvent effect helps to explore the complexities in the semibatch reactions.

References

1. Grady, M. C.; Simosick W. J.; Hutchinson R. A. *Macromol Symp.* **2002,** *182,* 149.
2. Adamsons, K.; Blackman, G.; Gregorovich, B.; Lin, L.; Matheson, R. *Prog. Org. Coat.* **1998**, *34*, 64.
3. Zimmt, W. S. *Chemtech.* **1981**, *11*, 681.
4. Bauer, D. R.; Dickie, R. A. *J. Coat Technol*. **1986**, *58*, 41.
5. Tilak, G. Y. *Prog. Org. Coat*. **1985**, *13*, 333.
6. Li, D. ; Li, N.; Hutchinson, R. A. *Macromolecules.* **2006**, *39*, 4366.
7. Wang, W.; Hutchinson, R. A. *Macromolecules.* **2008**, *41*, 9011.
8. Beuermann, S.; Buback, M.; Davis, T. P.; Gilbert, R. G.; Hutchinson, R. A.; Kajiwara, A.; Klumperman, B.; Russell, G. T. *Macromol. Chem. Phys.* **2000,** *201*, 1355.
9. Davis, T. P.; O'Driscoll, F. K.; Piton, M. C.; Winnik, M. A. *Macromolecules.* **1990**, *23*, 2113.
10. Buback, M. *Macromol. Symp.* **2009**, *275-276*, 90.
11. Buback, M.; Müller, E. *Macromol. Chem. Phys.* **2007**, *208*, 581.
12. Buback, M.; Kurz, C. *Macromol. Chem. Phys.* **1998,** *199*, 2301.
13. Beuermann, S.; Paquet, D. A., Jr.; McMinn, J. H.; Hutchinson, R. A. *Macromolecules*. **1996**, *29*, 4206.
14. Liang, K; Dossi, M; Moscatelli, D; Hutchinson, R. A. *Macromolecules.* **2009**, *42*, 7736.

Chapter 2 Literature Review

2.1 Free Radical Copolymerization Kinetics

The kinetic understanding of free-radical copolymerization processes provides a powerful synthetic route for efficiently producing polymers in wide applications. The evaluation and analysis of reaction rates and MWDs resulting from free-radical copolymerization are far from simple, due to the coupled nature of the different reactions. In this work, a penultimate model is applied based on the set of kinetic mechanisms including initiation, propagation, termination, transfer to monomer and solvent, as shown in Table 2.1.

Table 2.1 Basic Kinetic mechanisms of free-radical M_1 and M_2 copolymerization

Initiation		
$I \xrightarrow{k_d} 2fR$	$Rate = k_d I$	(2.1)
$R + M_1 \xrightarrow{k_{p111}} P_{0,1}$	$Rate = k_{p111} R M_1$	(2.2)
$R + M_2 \xrightarrow{k_{p222}} Q_{0,1}$	$Rate = k_{p222} R M_2$	(2.3)
Propagation		
$P_{n,m} + M_1 \xrightarrow{k_{p111}} P_{n+1,m}$	$Rate = k_{p111} P_{n,m} \mathrm{P}_{11} M_1$	(2.4)

$P_{n,m} + M_1 \xrightarrow{k_{p211}} P_{n+1,m}$	$Rate = k_{p211} P_{n,m} \mathrm{P}_{21} M_1$	(2.5)
$P_{n,m} + M_2 \xrightarrow{k_{p112}} Q_{n,m+1}$	$Rate = k_{p112} P_{n,m} \mathrm{P}_{11} M_2$	(2.6)
$P_{n,m} + M_2 \xrightarrow{k_{p212}} Q_{n,m+1}$	$Rate = k_{p212} P_{n,m} \mathrm{P}_{21} M_2$	(2.7)
$Q_{n,m} + M_1 \xrightarrow{k_{p221}} P_{n+1,m}$	$Rate = k_{p221} Q_{n,m} \mathrm{P}_{22} M_1$	(2.8)
$Q_{n,m} + M_1 \xrightarrow{k_{p121}} P_{n+1,m}$	$Rate = k_{p121} Q_{n,m} \mathrm{P}_{12} M_1$	(2.9)
$Q_{n,m} + M_2 \xrightarrow{k_{p222}} Q_{n,m+1}$	$Rate = k_{p222} Q_{n,m} \mathrm{P}_{22} M_2$	(2.10)
$Q_{n,m} + M_2 \xrightarrow{k_{p122}} Q_{n,m+1}$	$Rate = k_{p122} Q_{n,m} \mathrm{P}_{12} M_2$	(2.11)
Chain Transfer to Monomer		
$P_{n,m} + M_1 \xrightarrow{k_{tr11}^{mon}} P_{1,0} + D_{n,m}$	$Rate = k_{tr11}^{mon} P_{n,m} M_1$	(2.12)
$P_{n,m} + M_2 \xrightarrow{k_{tr12}^{mon}} Q_{0,1} + D_{n,m}$	$Rate = k_{tr12}^{mon} P_{n,m} M_2$	(2.13)
$Q_{n,m} + M_1 \xrightarrow{k_{tr21}^{mon}} P_{1,0} + D_{n,m}$	$Rate = k_{tr21}^{mon} Q_{n,m} M_1$	(2.14)
$Q_{n,m} + M_2 \xrightarrow{k_{tr22}^{mon}} Q_{0,1} + D_{n,m}$	$Rate = k_{tr22}^{mon} Q_{n,m} M_2$	(2.15)
Chain Transfer to Solvent		
$P_{n,m} + S \xrightarrow{cs_1 k_{p111}} S^* + D_{n,m}$	$Rate = cs_1 k_{p111} P_{n,m} S$	(2.16)
$Q_{n,m} + S \xrightarrow{cs_2 k_{p222}} S^* + D_{n,m}$	$Rate = cs_2 k_{p222} Q_{n,m} S$	(2.17)

$S^* + M_1 \xrightarrow{k_{p111}} P_{1,0}$	$Rate = k_{p111} S^* M_1$	(2.18)
$S^* + M_2 \xrightarrow{k_{p222}} Q_{0,1}$	$Rate = k_{p222} S^* M_2$	(2.19)
Termination by Combination		
$P_{n,m} + P_{r,q} \xrightarrow{k_{tc11}} D_{n+r,m+q}$	$Rate = k_{tc11} P_{n,m} P_{r,q}$	(2.20)
$P_{n,m} + Q_{r,q} \xrightarrow{k_{tc12}} D_{n+r,m+q}$	$Rate = k_{tc12} P_{n,m} Q_{r,q}$	(2.21)
$Q_{n,m} + Q_{r,q} \xrightarrow{k_{tc22}} D_{n+r,m+q}$	$Rate = k_{tc22} Q_{n,m} Q_{r,q}$	(2.22)
$Q_{n,m} + P_{r,q} \xrightarrow{k_{tc21}} D_{n+r,m+q}$	$Rate = k_{tc21} Q_{n,m} P_{r,q}$	(2.23)
Termination by Disproportionation		
$P_{n,m} + P_{r,q} \xrightarrow{k_{td11}} D_{n,m} + D_{r,q}$	$Rate = k_{td11} P_{n,m} P_{r,q}$	(2.24)
$P_{n,m} + Q_{r,q} \xrightarrow{k_{td12}} D_{n,m} + D_{r,q}$	$Rate = k_{td12} P_{n,m} Q_{r,q}$	(2.25)
$Q_{n,m} + Q_{r,q} \xrightarrow{k_{td22}} D_{n,m} + D_{r,q}$	$Rate = k_{td22} Q_{n,m} Q_{r,q}$	(2.26)
$Q_{n,m} + P_{r,q} \xrightarrow{k_{td21}} D_{n,m} + D_{r,q}$	$Rate = k_{td21} Q_{n,m} P_{r,q}$	(2.27)

2.1.1 Initiation

Initiation is the first step in the chain reaction that constitutes radical polymerization. The most

commonly used thermal initiators are azo-compounds and peroxides. They are often characterized by a decomposition rate (k_d) or half-life and an initiator efficiency (f). According to the starved-feed policy used to produce solvent-borne coatings, the initiator should be chosen to have a half-life at the reaction temperature that is short relative to the total feeding time.[1] Thus, *tert*-butyl peroxyacetate (TBPA) and dibenzoyl peroxide (BPO) with a half-life of 9 min at 138 and 110 ºC respectively, are chosen to initiate polymerizations in the semibatch reactions in this work. Although initiator efficiency is sufficient for representing polymerization rate, there are recent studies on the chemistry of initiator decomposition pathways that are helpful to improve the understanding of initiator effect on polymer molecular weight, especially at high initiator levels.

Buback et al.[2] indicate that the oxygen-centered radical, if produced, undergoes fast decarboxylation before starting chain growth, as determined by the end group analysis of the resultant polymers using electrospray ionization mass spectrometry (ESI-MS). Oxygen-centered radicals do not only initiate a chain by adding to the double bond of a monomer, but also abstract hydrogen from monomer, solvent and polymer, and may also undergo β-scission to form carbon-centered radicals.[3] Solomon et al.[4] investigated the initiation pathways of *t*-butoxy radicals during low-conversion MMA bulk polymerization at 60 °C and found that methacrylate systems seem especially prone to attack from initiator-derived oxygen-centered radicals. The hydrogen atoms along the backbone of poly(acrylates) are also readily attacked by oxygen-centered radicals. As the concentration of monomer is kept low in starved-feed

polymerizations, the oxygen-centered radicals formed by peroxide decomposition have an opportunity to abstract hydrogen from the solvent and polymer present in the system, as well as initiate new chains by addition to available monomer. Wang et al.[5] proved that H-abstraction from a methacrylate ester group found on an existing polymer chain will lead to an increase in polymer MW through branching, and decrease the number of new chains initiated.

It is well known that styrene can undergo self-initiation polymerization at higher temperatures.[6,7] However, under starved-feed and high initiator levels (2 wt% /monomer) conditions, this reaction is negligible and not considered in this work.[8]

2.1.2 Propagation

The propagation of radical polymerization comprises a sequence of radical additions to monomer carbon-carbon double bonds. Accurate measurement of propagation rate coefficient (k_p) is essential to study the kinetics of polymerization. Methods for measurement of k_p have been reviewed by Stickler,[9] van Herk,[10] and Beuermann and Buback.[11] Generally k_p is assumed to be chain-length independent, and chains grow quickly with a short lifetime (normally a fraction of a second) with many propagation steps followed by a transfer or termination step.

For the binary system of copolymerization, there are eight monomer addition propagation reactions if the penultimate effects are taken into consideration. $P_{n,m}$ is a living polymer (concentration= $P_{n,m}$) radical, with n units of M_1 and m units of M_2 and terminal group M_1, while

$Q_{n,m}$ is a polymer living radical (concentration= $Q_{n,m}$), with n units of M_1 and m units of M_2 and terminal group M_2. P_{ij} represents the fraction of radical *j* with *i* unit present in the penultimate position, and is introduced to track the penultimate unit in a terminal radical without introducing additional radical species. From these definitions, it is clear that $P_{11}+P_{21}=1$ and $P_{12}+P_{22}=1$. k_{pijk} is the rate coefficient for addition of monomer *k* to radical *ij*, leading to the following definitions of monomer (r_i) and radical (s_i) reactivity ratios for the implicit penultimate propagation model:

$$\begin{aligned} r_1 &= k_{p111}/k_{p112} = k_{p211}/k_{p212}; & s_1 &= k_{p211}/k_{p111} \\ r_2 &= k_{p222}/k_{p221} = k_{p122}/k_{p121}; & s_2 &= k_{p122}/k_{p222} \end{aligned} \tag{2.28}$$

Merz et al.[12] first developed the penultimate model to describe the copolymer-averaged propagation rate coefficient, $k_{p,cop}$:

$$k_{p,cop} = \frac{\overline{r_1} f_1^2 + 2 f_1 f_2 + \overline{r_2} f_2^2}{\left(\frac{\overline{r_1} f_1}{\overline{k_{11}}}\right) + \left(\frac{\overline{r_2} f_2}{\overline{k_{22}}}\right)} \tag{2.29}$$

If the penultimate unit does not affect the selectivity of the radicals, $\overline{r_1} = r_1$ and $\overline{r_2} = r_2$; Fukuda[13] named this case the Implicit Penultimate Effect (IPUE) model. In addition, $\overline{k_{11}}$ and $\overline{k_{22}}$ can be expressed as functions of monomer fraction,

$$\overline{k_{11}} = \frac{k_{p111}(r_1 f_1 + f_2)}{r_1 f_1 + (f_2/s_1)} \qquad \overline{k_{22}} = \frac{k_{p222}(r_2 f_2 + f_1)}{r_2 f_2 + (f_1/s_2)} \tag{2.30}$$

From previous studies on ST/BMA[14] and ST/GMA,[15] it is found that the terminal model adequately describes copolymer composition, and that the monomer reactivity ratios do not exhibit observable temperature dependence. In the terminal model, the radical reactivity depends only on

the terminal unit of the growing chain such that the mole fraction of monomer-1 in the copolymer (F_1^{inst}) is a function of monomer mole fractions (f_1 and f_2) and the monomer reactivity ratios:

$$F_1^{inst} = \frac{r_1 f_1^2 + f_1 f_2}{r_1 f_1^2 + 2 f_1 f_2 + r_2 f_2^2} \tag{2.31}$$

It is noted that these two models can be applied to both bulk and solution copolymerization systems.

2.1.3 Termination

The most important mechanism to terminate the propagating radicals in free radical polymerization is by combination or disproportionation. The apparent rate coefficient is affected not only by pressure and temperature, but also by system viscosity, a function of solvent choice, polymer concentration and MW. This complex behavior, as well as experimental difficulties in measuring k_t, has led to a large scatter in reported values.[16] Significant advances in the knowledge of termination kinetics came with the development of pulsed laser methods.[11] Termination is now generally accepted as a diffusion-controlled process and consists of three consecutive steps: translational diffusion of the two radicals (k_{TD}), segmental diffusion of the radical sites (k_{SD}) and chemical reaction (k_{CR}). Thus, the diffusion controlled termination rate coefficient k_t is expressed as Eq 2.32.

$$1/k_t = 1/k_{TD} + 1/k_{SD} + 1/k_{CR} \tag{2.32}$$

where k_{TD}, k_{SD} and k_{CR} are the corresponding rate coefficients. k_{CR} is significantly greater than k_{TD} and k_{SD} even at low conversions, and thus it is not a rate limiting factor.

Termination normally begins with segmental diffusion control; as the viscosity of reaction medium increases with conversion, translational diffusion then becomes the rate limiting process; at very high conversions, the termination is dominated by reaction diffusion in which the free radical sites come to contact through the propagational growth of the chain ends. Because of the low polymer MWs and high reaction temperature, the viscosity of the semibatch system remains low throughout the entire course of polymerization,[17] such that the termination process is controlled by segmental diffusion.[11,18] Thus, termination rate coefficient for homo- and co-polymerization in this work are assumed constant for each experiment.

For copolymerization, the penultimate model combined with the geometric mean approximation, provides a good fit to different systems,[19] including experimental acrylate-methacrylate $k_{t,cop}$ measured by pulsed-laser techniques.[20] The simplified form of termination penultimate model can be written as

$$k_{t,cop}^{0.5} = k_{t11,11}^{0.5} p_{11} + k_{t21,21}^{0.5} p_{21} + k_{t22,22}^{0.5} p_{22} + k_{t12,12}^{0.5} p_{12} \quad (2.33)$$

where $k_{tij,kl}$ (i,j,k,l=1,2) represents the termination of two radicals ending in monomer units ij and kl, and p_{ij} and p_{kl} are the relative populations of the four types of penultimate free radicals as calculated from the propagation rate coefficients and reactivity ratios, with $p_{11}+p_{21}+p_{22}+p_{12}=1$. In these previous efforts, the values of $k_{t12,12}$ and $k_{t21,21}$ were fit to the available $k_{t,cop}$ data. Wang et

al.[21] also checked the accuracy of the penultimate model by fitting the experimental profiles of semibatch reaction of ST/DMA (dodecyl methacrylate) copolymerization.

2.1.4 Backbiting/Short Chain Branching

In addition to the mechanisms listed in Table 2.1, the existence of intramolecular chain transfer to polymer was speculated by Scott and Senogles[22] to explain the dependence of the polymerization rate for acrylates on monomer concentration. The evidence of extensive chain transfer to polymer was first discovered by Lovell et al.[23] in the emulsion copolymerization of BA with MMA and acrylic acid by ^{13}C-NMR, although they did not make distinction between the intermolecular chain transfer and intramolecular chain transfer. In recent studies, the presence of the mid-chain radical resulting from backbiting was directly observed by ESR and also confirmed by ^{13}C-NMR analysis of the quaternary carbons in the solution polymerization of BA.[24] First found in ethylene homopolymerization, where it is responsible for the formation of short chain branches, backbiting is a process in which the propagating chain-end radical wraps around and abstracts a hydrogen atom from a unit on its own backbone via the formation of a six-membered ring. Monomer adds to the resulting tertiary radical at a much slower rate than the chain-end radical.[25]

Because of the lower reactivity of the tertiary radical, the backbiting process slows down the polymerization rate.[26] Plessis et al.[27,28] developed a complete kinetic model that accounts for the two radical species and reported a much lower apparent propagation rate for the

homopolymerization of BA and 2-ethyhexyl acrylate than the estimated k_p values. A similar observation was also reported by Azukizawa et al.[26] and Yamada et al.[29] for the polymerization of phenyl acrylate and cyclohexyl acrylate. These results are consistent with evidence that backbiting is indeed an important process for acrylate polymerization.

Acrylate polymerization kinetics deviate from the expected free-radical polymerization behavior due to the occurrence of backbiting reaction that converts a chain-end radical to a less reactive mid-chain radical (MCR).[24] Due to the slower addition of monomer to the MCR (with rate coefficient k_p^{MCR}), the observed rate of acrylate polymerization is significantly lower[25,30,31] than would be expected from the chain-end propagation rate coefficient (k_p) measured by pulsed laser polymerization (PLP).[32] The backbiting rate coefficient (k_{bb}) and its temperature dependence has been evaluated for *n*-butyl acrylate (BA) by various techniques, including analysis of short-chain branching (SCB) frequency,[30,33] and by specialized pulsed-laser techniques that also provide an estimate of k_p^{MCR}.[34] MCR formation occurs at mild conditions, even at 0 °C,[33,35] and leads to significant SCB levels (>5 branches per 100 repeat units) in poly(BA) produced under starved-feed high temperature (>100 °C) semibatch reaction conditions often used to produce acrylic polymers for coatings applications.[17,30,46] At these higher temperatures, the MCR formed by backbiting not only propagates and terminates, but can also undergo β-scission to produce a chain-end radical and a terminally-unsaturated polymer chain (a macromonomer)[17,37] detectable by proton NMR.[30,37,38]

Although acrylates undergo backbiting at low temperature, higher reaction temperatures will increase the likelihood of backbiting and tend to increase the incidence of fragmentation due to the higher activation energy for fragmentation relative to propagation.[39] Busch and Müller[40] have developed a mechanistic model including backbiting to simulate high temperature acrylate polymerization reactions, and Peck and Hutchinson[30] used a similar model to describe their experimental study of higher temperature semibatch BA homopolymerization. The latter model has been extended to represent the copolymerization of BA with BMA,[41] assuming that the backbiting reaction only involves acrylate radicals and acrylate units on the polymer chain such that the presence of BMA greatly decreases the probability of its occurrence. Wang and Hutchinson[42] also indicated in the ST/BMA/BA terpolymerization model that the backbiting rate coefficient is slightly affected by the identity of the penultimate unit on the chain, as shown by ^{13}C -NMR measure of quarternary carbons in the polymer chain.

Detailed models of high-temperature BA solution polymerization (including reaction of the macromonomer produced by β-scission) have been formulated to describe experimental results over a range of operating conditions.[40,43] It is also useful to examine analytical expressions for the averaged propagation rate coefficient (k_p^{av}, Eq 2.34) and branching level (BL, Eq 2.35) derived under the assumption that the majority of midchain radicals formed by backbiting result in formation of a branchpoint.[25,35]

$$k_p^{av} = \frac{k_p}{1 + \frac{k_{bb}}{k_p^{MCR}[M]}} \quad (2.34)$$

$$BL = \frac{k_{bb}}{k_p[M] + k_{bb}} \quad (2.35)$$

BL increases with reduced monomer concentration [M], and with increased temperature due to the higher activation energy of k_{bb} compared to k_p.[38-40] As branching increases, polymerization rate (proportional to k_p^{av}) decreases, as does average polymer chain length.[35,40]

It is possible to produce BA with low SCB levels by polymerizing at low temperatures, high monomer concentrations and low conversions.[44] BL can also be reduced by adding a powerful chain-transfer agent to the system; however, such a reduction is accompanied by a drastic decrease in polymer molecular weight (MW).[45] As both MW and SCB impact poly(BA) rheology,[44] it would be beneficial to independently control these properties under industrially-relevant synthesis conditions.

2.2 Pulsed Laser Polymerization (PLP)/Size Exclusion chromatography (SEC)

Pulsed laser polymerization (PLP) has emerged as the most reliable and simple method for determining propagation rate coefficient k_p and its temperature dependence while making very few assumptions, provided adequate care is taken with size exclusion chromatography (SEC) analysis of the polymer molecular weight distributions (MWDs).[11] In PLP experiments, a mixture of

monomer and photoinitiator is exposed to successive laser pulses at a constant repetition rate, usually between 10 and 100 Hz. Initiation of new chains occurs at each laser flash; these chains propagate and terminate in the dark period between pulses, with the radical concentration and the rate of termination decreasing with time. Growing macroradicals that escape termination all have the same chain length which increases linearly with time. There is a high probability that these surviving radicals are terminated at the next laser flash, which generates a new population of radicals. Thus, a significant fraction of dead chains formed has a chain length L_0 corresponding to a chain lifetime equal to the time between pulses, t_0 (Eq 2.36, where [M] is the monomer concentration).

$$L_0 = k_p[M]t_0 \tag{2.36}$$

Because radicals have a certain probability of surviving the laser flash and of terminating at a later laser flash, the polymers with chain length of L_i ($=i \times L_0$; i=2,3,...) will also be formed. Good PLP structure, namely, clear primary and secondary inflection points in the first-derivative curves of the MWD with the position of the secondary inflection point at twice the value of the primary, is an important consistency check for analysis. PLP/SEC technique has been successfully used to measure k_p for styrene,[46] acrylates[47,48] and methacrylates,[49-51] as compiled by IUPAC working party on modeling polymerization kinetics to accurately determine k_p.

The PLP technique allows control of when radicals are initiated, and thus is a valuable tool for the study of propagation rate coefficient. Genkin and Sokolov[52] provided a theoretical

analysis of the fundamental features of the molecular weight distribution resulting from periodic pulsed initiation. Olaj et al.[53] simplified the analysis, and was the first to experimentally implement the technique. From Eq 2.34, and known values of monomer concentration and time between two pulses, k_p can be directly determined from the structure of the MWD produced, without the knowledge of any other kinetic parameter. Olaj et al.[53] demonstrated that the low molecular weight inflection point of the primary peak in either the number or weight distribution is the best measure of L_0. As explained, if all growing radicals added new monomer at exactly the same moment, and termination by new short radicals occurred instantly, one would have a spike distribution of chain lengths. However, termination is not instantaneous, and some chains will be terminated after a short chain has grown a bit, which leads to some spread of the distribution towards longer chain lengths. Furthermore, the addition of a monomer unit does not occur exactly at the same moment on each growing radical and the distribution of chain length is broadened universally. The inflection point is the memory of the infinitely steep drop-off that was the original spike, and thus provides a measure of k_p that is within a few percent of the true value. The deviation of this approximation is usually insensitive to the termination mechanism.

Theoretically, the inflection point from the first derivative plot of MWD is used to calculate k_p, by rearranging Eq 2.36

$$k_p = \frac{MW_0}{1000\rho\emptyset_{mix}t_0} \tag{2.37}$$

where MW_0 is the polymer MW at the first inflection point, ρ (g/cm^3) is monomer density in

bulk system and $\emptyset_{mix}$ is the monomer volume faction in mixture (=1 for bulk system). An important check for the data is that the MW on the second inflection point should be observed at very close to twice the value of the first inflection point. The relationship between the propagation rate coefficient and reaction temperature is determined by fitting data to the Arrhenius equation

$$k = Aexp^{(-\frac{E_a}{\mathrm{RT}})} \tag{2.38}$$

Where k is the rate coefficient i.e. k_p (L/mol·s), A is a frequency factor and E_a is the activation energy (kJ/mol).

Although PLP-SEC technique has been applied to produce benchmark values for many common monomers, including styrene, a range of methacrylate monomers, and methacrylic acid because of its reliability and simplicity, there are significant difficulties in obtaining k_p values for acrylates by PLP; rather than producing well-structured distributions, the PLP-generated polyacrylate MWDs are broad and indistinct. For *n*-butyl acrylate (BA), the PLP-SEC technique has failed to yield values at temperatures above 30 °C with a pulse-repetition rate of 100 Hz;[55] recently, this temperature range has been extended to 70 °C using a laser repetition rate of 500 Hz.[56] Dating back to the PLP study in 1991, Davis et al.[57] failed to estimate k_p values for homopolymerization of methyl acrylate and BA. All the literature results of the acrylate family at temperatures at or above 30 °C give broadened or no PLP structure, such that the k_p values apparently depend on the laser frequency, pulse energy and photoinitiator concentration. Lyons et

al.[58] concluded that chain transfer to monomer, high termination rate and intramolecular chain transfer to polymer could be the main cause of the failure of PLP-SEC. The problem could be obviated by carrying out measurements at very low temperature and with high laser frequency so that laser pulses are the dominant origin of chain starting and stopping. Interference from excessive chain transfer reactions, or from termination reactions which are too fast or too slow, results in unsuitable MWDs for k_p determination. Beuermann et al.[48] also considered the situations in which a good PLP condition was not met and described the experimental techniques to get better MWD.

In order to establish the appropriate level of termination, β, the fraction of radicals that are terminated prior to the next pulse, is considered. Assuming termination by combination without chain length dependence, β is given by

$$\beta = \frac{[\Delta R\cdot]}{[R\cdot]_{max}} = \frac{k_t[R\cdot]_{max}t_0}{1+k_t[R\cdot]_{max}t_0} \tag{2.39}$$

where k_t is the termination rate coefficient, $[\Delta R\cdot]$is the increased radical concentration after each pulse and $[R\cdot]_{max}$ is the maximum radical concentration in the experiment, which is a function of $[\Delta R\cdot]$

$$[R\cdot]_{max} = [\Delta R\cdot][\frac{1}{2} + \left(\frac{1}{4} + \frac{1}{k_t[\Delta R\cdot]t_0}\right)^{0.5}] \tag{2.40}$$

In order to get ideal MWD from PLP, the experimental conditions must be chosen carefully to reach the intermediate termination rate. It can be found from Eq 2.39 that the high termination limit is approached when $t_0 \gg 1/k_t[R\cdot]_{max}$ and the low end is approached when this

inequality is reversed. As a result, β can be controlled by changing t_0 or by varying experimental conditions that influence either k_t or $[\Delta R\cdot]$ which can be adjusted by changing initiator concentration or laser pulse energy.

On the other hand, overwhelming evidence has emerged that the loss of PLP structure is due to the effect of intramolecular chain transfer to polymer (backbiting), as summarized in a 2004 IUPAC benchmark paper for butyl acrylate,[55] and more recently reviewed by van Herk.[59] As described previously (Ch 2.1.4), the propagating chain-end radical abstracts a hydrogen atom from a CH unit on its own backbone, favored through the formation of a six-membered ring, with the resulting mid-chain radical capable of undergoing propagation or termination. As addition to the mid-chain radical is much slower than to the chain-end radical, the relationship between chain length and chain lifetime is disrupted, causing the loss of the typical PLP structure. In this case, it would be helpful to improve the PLP structure by reducing the branching level of acrylates.

2.3 Solvent Effect on Copolymerization Kinetics

A number of studies on solution copolymerization have found that solvent does not affect the relative consumption of the two monomers, and thus does not influence copolymer composition. However, this generality starts to break down as the polarity of the monomer and/or solvent increases. For example, Barb et al.[60,61] first concluded that the propagation mechanism of styrene and maleic anhydride was affected in solvents by comonomer complexation. Klumperman et

al.[62,63] also observed the variation in reactivity ratios in solution copolymerization of styrene with maleic anhydride and styrene with acrylonitrile, with the variation of solvent polarity. O'Driscoll et al.[64] studied the homo- and copolymerizations of ST and MMA in the presence of several levels of benzyl alcohol (BzOH). They found that MMA incorporation into the copolymer increases with addition of BzOH for monomer mixtures with low MMA content, but that BzOH has little to no effect on copolymer composition when f_{MMA} is high. The results were fit by decreasing the value of r_{ST} with increasing BzOH, and explained by the argument that BzOH forms a strong complex with radical chain ends terminating in MMA, but a weak complex with those terminating in styrene. In contrast to complexation arguments, Harwood et al.[65] proposed the "bootstrap model" based upon the study of styrene/methacrylic acid, styrene/acrylic acid and styrene/acrylamide systems. It was hypothesized that solvent does not modify the inherent reactivity of the growing radical, but affects the monomer partitioning such that the concentrations of the two monomers at the reactive site (and thus their ratio) differs from that in bulk.

The most dramatic effects of solvent on copolymer composition involve systems with highly polar monomers such as maleic anhydride, acrylonitrile and acrylamide. Various complexation models have been proposed to describe these effects, as summarized by Coote et al.[81] and by Kamachi et al.[82] For more "common" systems, such as copolymerization of styrene with acrylates or methacrylates, solvent effects are not observed, or are very subtle. Ito and Otsu[66] studied ST copolymerized with methyl methacrylate (MMA) in various mono-substituted benzene solvents. Fitting their composition data to the terminal model, they report a small decrease in the values of

the ST reactivity ratio (r_{ST}) with increasing solvent polarity which was correlated to a small shift of the MMA carbonyl stretching frequency to lower wave numbers. It was proposed that a more polarized structure of the ester becomes important in the transition state when the solvents become more protic, resulting in increased reactivity. Fujihara et al.[67] extended the study of ST/MMA to a larger range of solvents, including *N, N*-dimethyl formamide (DMF) and ethanol (EtOH). They found a small decrease in r_{ST} values for copolymerization in DMF compared with benzene, with no change in r_{MMA}, a result also reported by Bontà et al.[68] However, the variation results in only very small shifts in composition when examined on a Mayo-Lewis plot of copolymer vs. comonomer composition. Later O'Driscoll et al.[64] questioned the statistical significance of these small shifts when reporting new results for ST/MMA copolymerization in benzyl alcohol (BzOH) at 30 °C. The decrease observed in EtOH, however, was more significant, with r_{ST} decreasing from 0.5-0.6 in bulk and other solvents to 0.4 in EtOH.[67]

While ST/MMA copolymer composition shows negligible or very minor dependence on solvent choice (with the possible exception of polymerization in alcohols), the same is not true for ST/HEMA. Lebduška et al.[69] used dilatometry to investigate ST/HEMA copolymerizations in DMF, toluene, isopropyl alcohol and *n*-butanol (BuOH). The data were fit using the Mayo-Lewis terminal model, with reactivity ratios found to differ in the polar solvents (r_{ST} =0.53 and r_{HEMA} =0.59 in DMF, isopropyl alcohol and BuOH) and the non-polar toluene (r_{ST} =0.50 and r_{HEMA}=1.65), values that are significantly different from the bulk values of r_{ST} =0.27 and r_{HEMA} =0.48 reported by Schoonbrood et al.[70] Sánchez-Chaves et al.[71] analyzed HEMA/ST copolymers produced in DMF

using proton NMR. From low conversion experiments, the monomer reactivity ratios were also determined according to the terminal model and the comparison with previous results of Lebduška et al.[69] and Schoonbrood et al.[70] revealed a noticeable solvent effect that was qualitatively explained by the bootstrap model.

Most of these studies of solvent effects on copolymerization kinetics focus solely on copolymer composition. However, it is expected that any solvent influence on monomer reactivity ratios should also affect copolymerization rate. These influences may be complex, as there are many systems for which the terminal model provides a good representation of copolymer composition, but not the variation in the copolymer-averaged propagation rate coefficient, $k_{p,cop}$, as a function of monomer composition. According to the IPUE, solvent effects may influence $k_{p,cop}$ through six parameters, the homopropagation rate coefficients and radical reactivity ratios in addition to the monomer reactivity ratios that control copolymer composition. Solvent does affect homopropagation kinetics for some systems, as recently reviewed by Beuermann.[72] These variations have been systematically studied using the PLP/SEC technique. The magnitude of the change in k_p is relatively small (up to 20%) for polymerization in solvents which do not undergo specific interaction with either monomer or polymer.[72] Previously Hutchinson et al. has observed solvent effects of this magnitude for MMA and DMA in 2-heptanone and octyl acetate,[73] but none for BMA in the same solvents[73] or for GMA in xylene.[15] A more significant solvent effect is observed for ST homopropagation in DMF, with k_p reduced by 15-25% compared to bulk polymerization.[74]

The effect of solvent on homopropagation kinetics is more pronounced for systems with H-bonding. Zammit et al.[75] report that k_p of MMA in 70 mol% BzOH is 70% higher compared to bulk values at 25 °C, with the increase smaller (25%) for 30 mol% BzOH. ST k_p values also were found to increase in BzOH, but to a smaller extent, with a 50% increase in 70 mol% BzOH. A study by Morrison et al.,[76] however, found that neither EtOH nor methanol has an effect on ST homopropagation k_p values, but did increase the k_p of MMA by up to 40%. Similarly, Beuermann reports that the k_p of BMA in *n*-butanol ([BMA]=0.8 mol·L^{-1}) is 45% higher than that in bulk at 80 °C, with a reduction in the propagation activation energy (E_p) from 22 to 19.2 kJ·mol^{-1}.[77] Infrared spectroscopy indicates a corresponding shift in the position of the carbonyl peak, with the bimodal structure (a second peak occurring at lower wavenumber of about 1700 cm^{-1}) that occurs in the presence of butanol attributed to the BMA carbonyl group interacting with the solvent OH group, reducing electron density at the double bond and increasing k_p.[72,77]

Based on these findings, it is not surprising that solvent choice also influences homopropagation kinetics of hydroxyl-functional monomers. Buback and Kurz[83] report a negligible change for the k_p of HEMA in 50 vol% *n*-butanol. Beuermann and Nelke[78] also found that toluene, benzyl alcohol and even supercritical CO_2 did not significantly affect hydroxypropyl methacrylate (HPMA) propagation. However, in THF, k_p values for HPMA were 40% below the corresponding bulk data, a result explained by disruption of monomer-monomer H-bonding by complexation of the HPMA OH group with THF. IR spectroscopy was used to show that the presence of THF reduces the bimodal nature of the carbonyl peak seen for bulk HPMA (and in

BzOH and toluene systems), as THF reduces the H-bonding of the bulk system.[72,78]

There is significantly less data examining the effect of solvent on copolymerization rate. Fukuda et al.,[79] using the rotating sector technique, found that there is no observable difference in $k_{p,cop}$ values for ST/MMA (a system with a significant penultimate effect) measured in bulk and in toluene, a result also found by Olaj and Schnöll-Bitai[80] using the PLP/SEC technique. These results are not surprising; as discussed above, neither homopropagation values nor *r* values exhibit a strong solvent effect in toluene. For ST/MMA in BzOH with f_{ST}=0.5, however, $k_{p,cop}$ increases by 65% as solvent level is increased from 0 to 75%.[84] This increase is comparable as to what is found for MMA k_p (70%), but larger than that observed for ST k_p (40-50%).[75] The results were interpreted assuming that the solvent complexes with MMA radicals more strongly than with ST radicals; as mentioned previously, the *r* values for the system are almost unchanged.[64] No other studies could be found that simultaneously consider the effect of solvent on both copolymer composition and $k_{p,cop}$.

In addition to solvent effect on methacrylates polymerization systems, it is also very interesting to investigate the polymerization behavior of acrylates in different solvents, and the effect of solvent choice on the backbiting reaction.

2.4 Semibatch Reaction and Kinetic Models

Semibatch reactions can supply good control of copolymer composition by carrying on

starved-feed policy, as well as low MW polymers due to continuous high initiator concentration and low heat emission due to low monomer concentration. Mathematical modeling is an important tool enabling successful production of materials with desired properties, especially when considering the complexities of copolymerization kinetics. Mechanistic models for ST/BMA,[37] ST/DMA,[38] BMA/BA[39] and ST/BA[64] copolymerization as well as ST/BMA/BA[40] terpolymerization have been constructed in Predici by previous researchers in our group, and give relatively good fitting to semibatch experimental results.

2.5 Conclusions

Free radical copolymerization kinetics of hydroxyl functional monomers, such as HEMA and HEA, are not well understood, especially combined with the solvent effect on copolymerization. In this work, solvent effect on ST/HEMA, ST/GMA and ST/BMA copolymerization will be systematically studied via the PLP/SEC/NMR method. Also, semibatch reactions of ST/HEMA will be compared to ST/BMA in different solvents, quantifying the importance of solvent type and level on copolymer composition and molecular weight. In addition, HEA homopolymerization and ST/HEA copolymerization kinetics will be investigated using the PLP/SEC/NMR methodology. Further tests will also be done against solvent effect on acrylate branching levels. With all these mechanism in mind, we will discuss the complexities in BMA/HEMA, BA/HEMA and BMA/BA copolymerization in semibatch reactions.

References

1. O'Driscoll, K. F.; Burczyk, A. F. *Polym. React. Eng.: Emulsion Polym., High Convers. Polym., Polycondens., [Proc. Berlin Int. Workshop], 2nd* **1986**, 229.

2. Buback, M.; Frauendorf, H.; Günzler, F.; Vana, P. *J. Polym. Sci., Part A: Polym. Chem.* **2007**, *45*, 2453.

3. Moad, G.; Solomon, D. H. *The Chemistry of Free Radical Polymerization*; Pergamon, Oxford, **2006**.

4. Griffiths, P. G.; Rizzardo, E.; Solomon, D. H. *J. Macromol. Sci., Chem.* **1982**, *A17*, 45.

5. Wang, W.; Hutchinson, R. A. *Macromolecules* **2009**, *42*, 4910.

6. Mayo, F. R. *J. Am. Chem. Soc.* **1953**, *75*, 6133.

7. Mayo, F. R. *J. Am. Chem. Soc.* **1968**, *90*, 1289.

8. Li, D. *PhD Thesis*, Queen's University, Kingston, ON, **2006**.

9. Stickler, M. In *Comprehensive Polymer Science*; Eastmond, G. C.; Ledwith, A.; Russo, S.; Sigwalt, P., Eds.; Pergamon: London, **1989**, *3*, 59-85.

10. Van Herk, A. M. *J. Macromol. Sci., Rev. Macromol. Chem. Phys.* **1997**, *37*, 633.

11. Beuermann, S.; Buback, M. *Prog. Polym. Sci.* **2002**, *27*, 191.

12. Merz, E.; Alfrey, T.; Goldfinger, G. *J. Polym. Sci*. **1946**, *1*, 75.

13. Fukuda, T.; Ma, Y.; Inagaki, H. *Macromolecules* **1985**, *18*, 26.

14. Li, D. ; Li, N.; Hutchinson, R. A. *Macromolecules* **2006**, *39*, 4366.

15. Wang, W.; Hutchinson, R. A. *Macromolecules* **2008**, *41*, 9011.

16. Brandrup, J.; Immergut, E. H.; Grulke, E. A. (Eds.); *Polymer Handbook 4th Edition*, John Wiley & Sons, Inc., New York, **1999**.

17. Grady, M. C.; Simosick, W. J.; Hutchinson, R. A. *Macromol. Symp*. **2002**, *182*, 149.

18. Hutchinson, R. A. *Free radical polymerization*: *Homogeneous*. Handbook of Polymer Reaction Engineering. Edited by Meyer, T. and Keurentjes, J. Wiley-VCH. **2005**.

19. Fukuda, T.; Ide, N.; Ma, Y. D. *Macromol. Symp.* **1996**, *111*, 305.

20. Buback, M.; Feldermann, A. *Aust. J. Chem.* **2002**, *55*, 475.

21. Wang, W.; Hutchinson, R. A. *Macromol. Symp*. **2008**, *261*, 64.

22. Scott, G. E.; Senogles, E. *J. Macromol. Sci., Chem*. **1974**, *8*, 753.

23. Lovell, P. A.; Shah, T. H.; Heatley, F. *Polym. Communi*. **1991**, *32*, 98.

24. Ahmad, N. M.; Heatley, F.; Lovell, P. A. *Macromolecules* **1998**, *31*, 2822.

25. Plessis, C.; Arzamendi, G.; Leiza, J. R.; Schoonbrood, H. A. S.; Charmot, D.; Asua, J. M. *Macromolecules* **2000**, *33*, 4.

26. Azukizawa, M.; Yamada, B.; Hill, D. J. T.; Pomery, P. *J. Macromol. Chem. Phys.* **2000**, *201*, 774.

27. Plessis, C.; Arzamendi, G.; Alberdi, J. M.; Agnely, M.; Leiza, J. R.; Asua, J. M. *Macromolecules* **2001**, *34*, 6138.

28. Plessis, C.; Arzamendi, G.; Leiza, J. R.; Schoonbrood, H. A. S.; Charmot, D.; Asua, J. M. *Ind. Eng. Che. Res*. **2001**, *40*, 3383.

29. Yamada, B.; Azukizawa, M.; Yamazoe, H.; Hill, D. J. T.; Pomery, P. J. *Polymer* **2000**, *41*, 5611.

30. Peck, A. N. F.; Hutchinson, R. A. *Macromolecules* **2004**, *37*, 5944.

31. Nikitin, A. N.; Hutchinson, R. A. *Macromolecules* **2005**, *38*, 1581.

32. Asua, J. M.; Beuermann, S.; Buback, M.; Castignolles, P.; Charleux, B.; Gilbert, R. G.; Hutchinson, R. A.; Leiza, J. R.; Nikitin, A. N.; Vairon, J. P.; van Herk, A. M. *Macromol. Chem. Phys*. **2004**, *205*, 2151.

33. Plessis, C.; Arzamendi, G.; Alberdi, J. M.; van Herk, A. M.; Leiza, J. R.; Asua, J. M. *Macromol. Rapid Commun.* **2003**, *24*, 173.

34. Nikitin, A. N.; Buback, M.; Hesse, P.; Hutchinson, R. A. *Macromolecules* **2007**, *40*, 8631.

35. Barth, J.; Buback, M.; Hesse, P.; Sergeeva, T. *Macromolecules* **2010**, *43*, 4023.

36. Nikitin, A. N.; Hutchinson, R. A.; Wang, W.; Kalfas, G. A.; Richards, J. R.; Bruni, C. *Macromol. React. Eng.* **2010**, *4*, 691.

37. Chiefari, J.; Jeffery, J.; Mayadunne, R. T. A.; Moad, G.; Rizzardo, E.; Thang, S. H. *Macromolecules* **1999**, *32*, 7700.

38. Wang, W.; Nikitin, A. N.; Hutchinson, R. A. *Macromol. Rapid Commun.* **2009**, *30*, 2022.

39. Hirano, T.; Yamada, B. *Polymer* **2003**, *44*, 347.

40. Busch, M.; Müller, M. *Macromol. Symp.* **2004**, *206*, 399.

41. Li, D.; Grady, M. C.; Hutchinson, R. A. *Ind. Eng. Chem. Res*. **2005**, *44*, 2506.

42. Wang, W.; Hutchinson, R. A. *AIChE J.* **2011, *57***, 227.

43. Junkers, T.; Barner-Kowollik, C. *Macromol. Theory Simul.* **2009,** *18*, 421.

44. Former, C.; Castro, J.; Fellows, C. M.; Tanner, R. I.; Gilbert, R. G. *J. Polym. Sci.: Part A: Polym. Chem.* **2002**, *40*, 3335.

45. Gaborieau, M.; Koo, S. P. S.; Castignolles, P.; Junkers, T.; Barner-Kowollik, C. *Macromolecules* **2010**, *43*, 5492.

46. Buback, M.; Gilbert, R. G.; Hutchinson, R. A.; Klumperman, B.; Kuchta, F.; Manders, B. G.; O'Driscoll, K. F.; Russell, G. T.; Schweer, J. *Macromol. Chem. Phys.* **1995**, *196*, 3267.

47. Lyons, R. A.; Hutovic, J.; Piton, M. C.; Christie, D. I.; Clay, P. A.; Manders, B. G.; Kable, S. H.; Gilbert, R. G.; Shipp, D. A. *Macromolecules* **1996**, *29*, 1918.

48. Beuermann, S.; Paquet, D. A.; Jr., McMinn, J. H.; Hutchinson, R. A. *Macromolecules* **1996**, *29*, 4206.

49. Beuermann, S.; Buback, M.; Davis, T. P.; Garcia, N.; Gilbert, R. G.; Hutchinson, R. A.; Kajiwara, A.; Kamachi, M.; Lacik, I.; Russell, G. T. *Macromol. Chem. Phys.* **2003**, *204*, 1338.

50. Beuermann, S.; Buback, M.; Davis, T. P.; Gillbert, R. G.; Hutchinson, R. A.; Kajiwara, A.; Klumpermann, B.; Russell, G. T. *Macromol. Chem. Phys.* **2000**, *201*, 1355. 134

51. Beuermann, S.; Buback, M.; Davis, T. P.; Gilbert, R. G.; Hutchinson, R. A.; Olaj, O. F.; Russell, G. T.; Schweer, J.; van Herk, A. M. *Macromol. Chem. Phys*. **1997**, *198*, 1545.

52. Genkin, V. N.; Sokolov, V. *Doklady Akademii Nauk SSSR*. **1997**, *234*, 94.

53. Olaj, O. F.; Bitai, T. ; Hinkelmann, F. *Makromolekulare Chemie*. **1987**, *188(7)*, 1689.

54. Gilbert, R. G. ©1999; http://www.kcpc.usyd.edu.au/resources/notes/PLP.pdf.

55. Asua, J. M.; Beuermann, S.; Buback, M.; Castignolles, P.; Charleux, B.; Gilbert, R. G.; Hutchinson, R. A.; Leiza, J. R.; Nikitin, A. N.; Vairon, J. P.; van Herk, A. M. *Macromol. Chem. Phys*. **2004**, *205*, 2151.

56. Barner-Kowollik, C. ; Günzler, F. ; Junkers, T. *Macromolecules* **2008**, *41*, 8971.

57. Davis, T. P.; O'Driscoll, F. K.; Piton, M. C.; Winnik, M. A. *Polymer International*. **1991**, *24*, 65.

58. Lyons, R. A.; Hutovic, J.; Piton, M. C.; Christie, D. I.; Clay, P. A.; Manders, B. G.; Kable, S. H.; Gilbert, R. G. *Macromolecules* **1996**, *29*, 1918.

59. Van Herk, A. M. *Macromol. Rapid Commun.* **2009**, *30*, 1964.

60. Barb, W. G. *J. Polym. Sci*. **1953**, *10*, 49.

61. Barb, W. G. *J. Polym. Sci*. **1953**, *11*, 117.

62. Klumperman, B.; O'Driscoll, K. F. *Polymer* **1993**, *34*, 1032.

63. Klumperman, B.; Kraeger, I. R. *Macromolecules* **1994**, *27*, 1529.

64. O'Driscoll, F. K.; Monteiro, J. M.; Klumperman, B. *J. Polym. Sci. Part A.* **1997**, *35*, 515.

65. Harwood, H. J. *Makromol. Chem., Makromol. Symp*. **1987**, *10/11*, 331.

66. Ito, T; Otsu, T. *J. Macromol. Sci. Part A: Chem.* **1969**, *3*, 197.

67. Fujihara, H; Yamazaki, K; Matsubara, Y; Yoshihara, M; Maeshima, T. *J. Macromol. Sci. Part A: Chem.* **1979**, *13*, 1081.

68. Bontà, G; Gallo, B. M; Russo, S. *Polymer* **1975**, *16*, 429.

69. Lebduška, J.; Šnupárek, J.; Kašpar, K.; Čermák, V. *J. Polym. Sci.: Part A: Polym. Chem*. **1986**, *24*, 777.

70. Schoonbrood, H. A. S.; Aerdts, A. M.; German, A. L.; van der Velden, G. P. M. *Macromolecules* **1995**, *28*, 5518.

71. Sánchez-Chaves, M; Martinez, G; Madruga, E. *J. Polym. Sci.: Part A: Polym. Chem.* **1999**, *37*, 2941.

72. Beuermann, S. *Macromol. Rapid Commun.* **2009**, *30*, 1066.

73. Hutchinson, R. A.; Paquet, Jr. D. A.; Beuermann, S.; McMinn, J. H. *Ind. Eng. Chem. Res*. **1998**, *37*, 3567.

74. Coote, M. L.; Davis, T. P. *Eur. Polym. J*. **2000**, *36*, 2423.

75. Zammit, M. D.; Davis, T. P.; Willett, G. D.; O'Driscoll, K. F. *J. Polym. Sci.: Part A: Polym. Chem.* **1997**, *35*, 2311.

76. Morrison, B. R.; Piton, M. C.; Winnik, M. A.; Gilbert R. G.; Napper D. H. *Macromolecules* **1993**, *26*, 4368.

77. Beuermann, S. *Macromolecules* **2004,** *37*, 1037.

78. Beuermann, S.; Nelke, D. *Macromol. Chem. Phys.* **2003**, *204*, 460.

79. Fukuda, T.; Kubo, K.; Ma, Y-D.; Inagaki, H. *Polym. J. (Tokyo)* **1987**, *19*, 523.

80. Olaj, O. F.; Schnöll-Bitai, I. *Monatshefte für Chemie*. **1999**, *130*, 731.

81. Coote, M. L.; Davis, T. P.; Klumperman, B.; Monteiro, M. J. *Rev. Macromol. Chem. Phys.* **1998**, *38*, 567.

82. Kamachi, M. *Adv. Polym. Sci.* **1981**, *38*, 56.

83. Buback, M.; Kurz, C. *Macromol. Chem. Phys.* **1998,** *199*, 2301.

84. Buback, M.; Müller, E. *Macromol. Chem. Phys.* **2007**, *208*, 581.

Chapter 3 Copolymerization Kinetics of ST/HEMA and Solvent Effect on ST/Methacrylates Systems

Preface

As the starting point of my research, ST/HEMA copolymerization in bulk was firstly studied by the PLP/SEC/NMR technique in order to fill the knowledge gap of kinetic parameters. However, ST/HEMA system demonstrated some unique kinetic behavior compared to ST/alkyl methacrylates systems, which drew my curiosity to explore solvent effect on different ST/methacrylates systems and verify the main cause of the unique behavior of ST/HEMA system. This chapter combines two published works in Macromolecules (2009, Vol. 42, 7736 and 2010, Vol. 43, 6311) that demonstrate the importance of H-bonding effects on copolymerization kinetics.

3.1 Introduction

As discussed in the literature review, we have focused attention on styrene (ST) – methacrylate (xMA) copolymers, studying the effect of methacrylate ester group (denoted by x) and temperature on polymer composition and propagation kinetics for copolymers of butyl methacrylate (BMA) and ST,[1] dodecyl methacrylate (DMA) and ST[2] and glycidyl methacrylate (GMA) and ST.[3] Although following a general family behavior, small differences were found in

the relative reactivity of GMA to ST compared to alkyl methacrylates BMA and DMA. In this work, we extend the study to the copolymerization of ST with 2-hydroxyethyl methacrylate (HEMA), an important functional monomer used in the coatings industry.

Incorporating HEMA into polymer chains has garnered much attention, especially in the biomedical field,[4] because of the monomer's high polarity. Early work demonstrated that the polarity and hydrophilicity of solvents affect copolymer composition and the copolymerization rate of ST/HEMA system.[5,6] More recently, Schoonbrood et al.[7] used proton NMR to determine the monomer reactivity ratios of ST and HEMA in bulk polymerization, and Sánchez-Chaves et al.[8] described the cumulative composition as a function of conversion and the monomer conversion as a function of polymerization time in *N*,*N*-dimethylformamide (DMF) solution. We apply the PLP/SEC technique to the study of ST/HEMA propagation kinetics as a function of monomer composition over a range of temperatures and copolymer composition is determined using proton NMR.

In addition to the study of ST/HEMA in bulk, the solvent effect on ST/HEMA, ST/BMA and ST/GMA copolymerization is also discussed in this chapter. PLP/SEC/NMR technique is also to simultaneously consider the solvent effect on both copolymer composition and $k_{p,cop}$.

3.2 Experimental

3.2.1 Materials

All the chemicals received from Aldrich summarized in Table 3.1 were used as received unless otherwise indicated. The THF for SEC analysis was distilled to remove the impurities and collected for reuse.

Table 3.1 Chemicals used in this work

Chemical Name	**Purity**	**Purpose**
Styrene (ST)	99%	Monomer
2-Hydroxyethyl methacrylate (HEMA)	98%	Monomer
Butyl methacrylate (BMA)	99%	Monomer
Glycidyl methacrylate (GMA)	99%	Monomer
Dimethyl sulfoxide-*d*6	99.9 atom%D	Solvent
Chloroform-*d6*	99.8 atom%D	Solvent
2,2-Dimethoxy-2-phenyl-acetophenone (DMPA)	99%	Photoinitiator

3.2.2 PLP/SEC/NMR

Low conversion polymerizations were conducted in a pulsed laser setup consisting of a Spectra-Physics Quanta-Ray 100 Hz Nd:YAG laser that is capable of producing a 355 nm laser

pulse of duration 7-10 ns and energy of 1-50 mJ per pulse. The laser beam is reflected twice (180°) to shine into a Hellma QS165 0.8 mL cuvette contained in a temperature controlled cell used as the PLP reactor. A digital delay generator (DDG, Stanford Instruments) is attached to the laser in order to regulate the pulse output repetition rate at a value between 10 and 100 Hz. Monomer mixtures in bulk with 5 mmol·L^{-1} DMPA photoinitiator were added to the quartz cell and exposed to laser energy, with temperature controlled by a circulating oil bath. Experiments were run in the temperature range of 50-120 °C, with styrene fraction in the monomer mixture varied between 0 and 100%. Monomer conversions were kept below 5% to avoid significant composition drift, and temperature was controlled to ±1 °C during pulsing.

Polymers produced by PLP were used to determine $k_{p,cop}$ values from analyses of polymer molecular weight distributions (MWD) measured by size exclusion chromatography (SEC). The resulting samples from PLP were precipitated in diethyl ether and the solid polymers were separated from liquid by centrifuge. The polymers were dried in a vacuum oven and then redissolved in THF. Copolymers with greater than 70 mol% HEMA are not THF-soluble, and thus were not analyzed. Molecular weight distributions were measured with a Waters 2960 separation module connected to a Waters 410 differential refractometer (DRI) and a Wyatt Instruments Dawn EOS 690 nm laser photometer multiangle light scattering (LS) detector. Tethahydrofuran (THF) was used to carry polymers at a flow rate of 1 mL·min^{-1} through the four Styragel columns (HR 0.5, 1, 3, 4) maintained at 35 °C. The DRI detector was calibrated by 10 molecular weight polystyrene standards (870-355000 Da) with narrow polydispersities, and the LS detector was calibrated by

toluene as recommended by the manufacturer.

The polymers isolated from the PLP experiments were also used for composition analysis by proton NMR. The polymer was dissolved in dimethyl sulfoxide-*d*6 for proton NMR analysis conducted at room temperature on a 400 MHz Bruker instrument. For example with ST/HEMA copolymer spectrum, the copolymer shows chemical shifts from the aromatic protons in styrene units in the region of 7.4-6.2 ppm, from the methyl protons and hydroxyl protons of main chain HEMA units in the region 1.1-0.1 ppm and 4.9-4.3 ppm.[8] A typical spectrum is shown in Figure 3.1. Copolymer composition (F_{HEMA} = mol fraction HEMA) was estimated from proton NMR via two methods, either ratioing the area from the ST aromatic protons with the peak area from the HEMA methyl protons:

$$F_{\mathrm{HEMA}} = \frac{5A_{H1}}{5A_{H1} + 3A_{A}} \tag{3.1}$$

or with the peak area from the hydroxyl proton:

$$F_{\mathrm{HEMA}} = \frac{5A_{H2}}{5A_{H2} + A_{A}} \tag{3.2}$$

where A_{H1} and A_{H2} are the peak areas of methyl and hydroxyl protons, respectively, and A_A is the peak area of aromatic protons. The polymer compositions estimated by the two methods agreed well, with reported values determined using the more distinct hydroxyl peak. Monomer reactivity ratios, estimated using the non-linear parameter estimation capabilities of the computer package PREDICI by fitting of Mayo-Lewis equation to the experimental mole fraction of HEMA in

copolymer composition (F_{HEMA}) data obtained at each temperature.

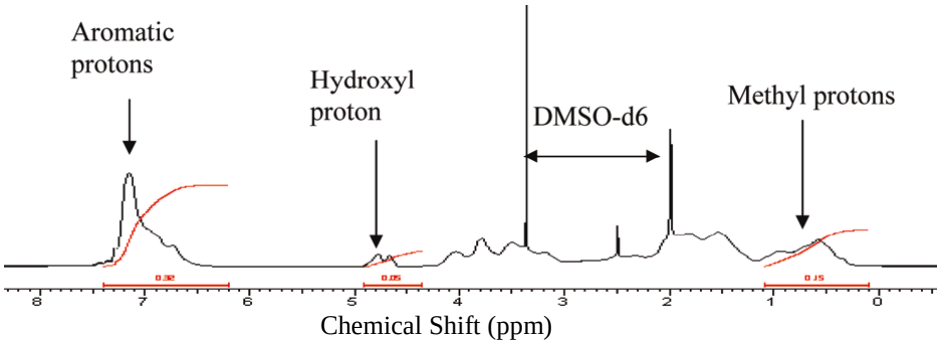

Figure 3.1 NMR spectrum of copolymer produced at 50 °C from a styrene/2-hydroxyethyl methacrylate (HEMA) monomer mixture containing 30 mol% HEMA.

The parameters necessary to estimate $k_{p,cop}$ from SEC data are summarized in Table 3.2, with monomer densities calculated as a function of temperature, the refractive index (d*n*/d*c*) values required for interpretation of LS results and Mark-Houwink parameters required in order to analyze the output from the RI detector. The copolymer MW is calculated as a composition-weighted average of the homopolymer values, a methodology shown valid in previous studies.[1,3,9] Agreement between the two detectors was good (within 10%) over a wide range of MW values, between 5×10^3 and 1×10^5 Da. Reported $k_{p,cop}$ values are calculated using the LS results.

The refractive index (d*n*/d*c*) of the polymer in THF is required to process the data from the LS detector. A Wyatt Optilab DSP refractometer, calibrated with sodium chloride, was used to measure

these values for several ST/HEMA copolymer samples. Six samples of 0.1-20 mg·mL^{-1} were prepared in THF for each polymer and injected sequentially to construct a curve with slope d*n*/d*c*. As homopolymer of HEMA cannot be dissolved in THF, d*n*/d*c* values for ST homopolymer and copolymers of ST/HEMA produced from monomer mixtures containing 0.1-0.7 molar fractions HEMA were measured as shown in Figure 3.2, with the homopolymer value for HEMA estimated as 0.0556 mL·g^{-1} by extrapolation.

Monomer mixtures in bulk and solution were examined using a Nicolet FT-IR spectrometer at room temperature to examine for the effect of H-bonding on the methacrylate carbonyl peak in the range of 1700 to 1720 cm^{-1}.

Table 3.2 Parameters for calculation of $k_{p,cop}$ from SEC analysis of PLP-generated copolymer samples of styrene with methacrylates in solution

			Mark-Houwink parameters		
Species	Density ρ (g·mL^{-1})	d*n*/d*c* (mL·g^{-1})	K×10^4 (dL·g^{-1})	a	ref
styrene	0.9193-0.000665*T*/°C[10]	0.1834	1.14	0.716	17
HEMA	1.0920-0.00098*T*/°C[11]	0.055	2.39	0.537	this work
GMA	1.094728-0.001041*T*/°C[12]	0.09314	2.78	0.537	12
BMA	0.91454-0.000964*T*/°C[13]	0.0834	1.48	0.064	17
toluene	0.88575-0.000941*T*/°C[14]	-	-	-	-
n-butanol	0.8398-0.00119*T*/°C[15]	-	-	-	-
DMF	1.235026-0.000972*T*/°C[16]	-	-	-	-

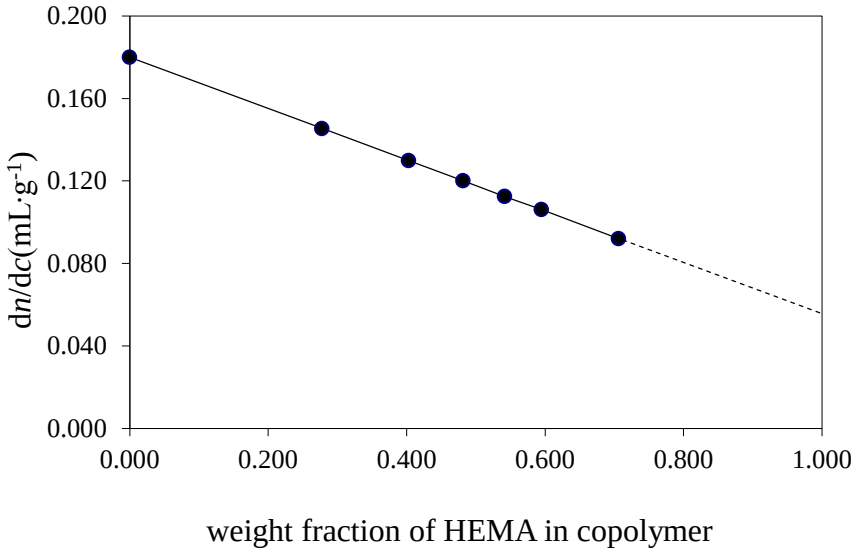

Figure 3.2 Refractive index (d*n*/d*c*) values for styrene/2-hydroxyethyl methacrylate (HEMA) copolymers in THF at 35 °C, plotted as a function of weight fraction HEMA in copolymer.

3.3 Results and Discussion

3.3.1 Bulk Copolymerization of ST/HEMA

An important assumption of both the terminal and penultimate models is that the monomer addition reactions are irreversible. For methacrylate systems, depropagation can occur at appreciable rates at higher temperatures (>120 °C), depending on monomer concentrations.[18,19] However, our previous work[1,3] has shown that depropagation does not affect low conversion bulk ST/xMA copolymerization at temperatures below 130 °C; thus depropagation does not need to be considered for this study.

Monomer Reactivity Ratios As only a single ST/HEMA bulk copolymerization study was found in literature, it is necessary to verify the monomer reactivity ratios reported for 50 °C. In addition, it is important to examine whether the values vary with temperature. Low conversion PLP experiments were carried out from 50-120 °C and the resulting polymers composition was analyzed by NMR. The full set of experimental conditions and results is summarized in Appendix A.1.1, with a plot of HEMA mole fraction in the copolymer plotted against monomer composition in Figure 3.3. The copolymer composition curve has the shape commonly observed for ST-xMA systems, and the data are well-represented by the Mayo-Lewis terminal model using the literature monomer reactivity ratios of r_{HEMA}=0.49 and r_{ST}=0.27.[7] In addition, the data indicate that there is no significant effect of temperature on copolymer composition, with data up to 120 °C well represented by the same set of *r* values.

It is interesting to compare these results to other ST/xMA systems. Table 3.3 summarizes monomer reactivity ratios for ST copolymerized with MMA, BMA, DMA, GMA and HEMA, and Figure 3.4 presents the corresponding Mayo-Lewis curves for these systems. The curves for ST/HEMA and ST/GMA are very similar, and differ significantly from the curves for the three alkyl methacrylates. With GMA and HEMA, methacrylate-enriched copolymer is produced in styrene-rich monomer mixtures relative to the alkyl methacrylates, a difference captured by the lower r_{ST} value. A full computational study has been done to explore these reactivity differences, in cooperation with the group of Prof. Moscatelli (Politecnico di Milano, Italy), as documented in a journal publication.[20] GMA and HEMA are more reactive toward ST radicals compared to alkyl

methacrylates, and the difference in reactivity is correlated to the shift of carbonyl group peak in the IR spectrum.

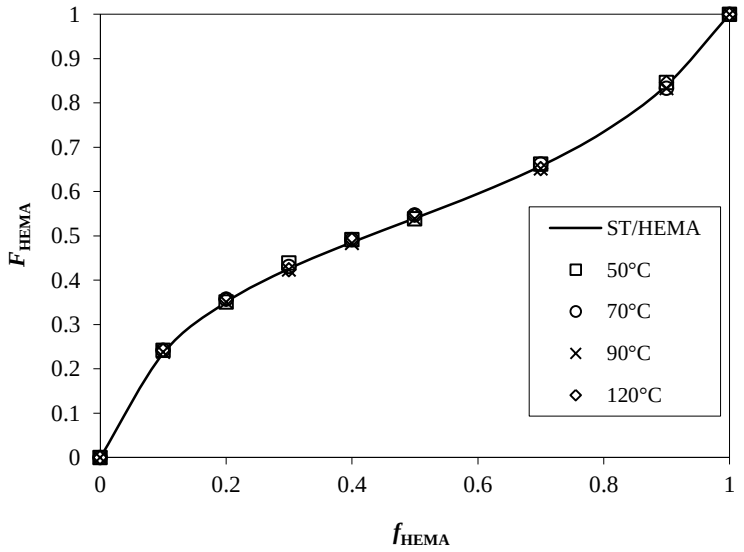

Figure 3.3 Copolymer composition data for low-conversion styrene/2-hydroxyethyl methacrylate (HEMA) bulk copolymerization at varying temperatures, plotting mole fraction HEMA in copolymer (F_{HEMA}) as a function of HEMA mole fraction in the monomer phase (f_{HEMA}). The solid curve is the prediction of the terminal copolymerization model with literature[2,6] monomer reactivity ratios r_{HEMA}=0.49 and r_{ST}=0.27.

Table 3.3 Monomer reactivity ratios for copolymerization of styrene (ST) with various methacrylates[a]

	ST/HEMA	ST/GMA[3]	ST/BMA[1]	ST/DMA[2]	ST/MMA[9]
r_{ST}	0.27	0.31	0.61	0.57	0.49
r_{xMA}	0.49	0.51	0.42	0.45	0.49

[a] 2-hydroxyethyl methacrylate (HEMA), glycidyl methacrylate (GMA), butyl methacrylate (BMA), dodecyl methacrylate (DMA), methyl methacrylate (MMA)

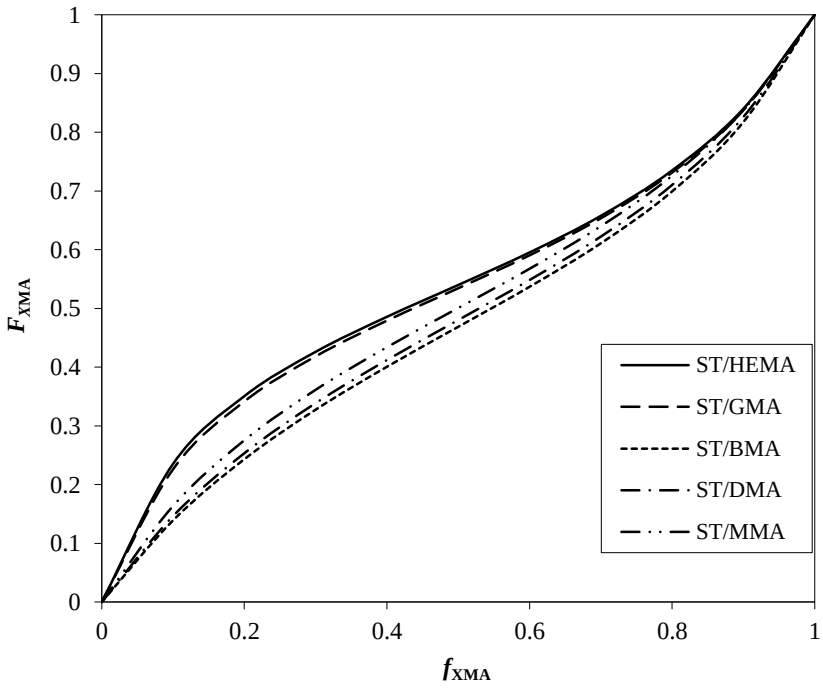

Figure 3.4 Mole fraction methacrylate in copolymer (F_{xMA}) vs. mole fraction in monomer mixture (f_{xMA}) for ST/HEMA, ST/GMA, ST/BMA, ST/DMA, and ST/MMA, calculated using the monomer reactivity ratios in Table 3.3.

Copolymerization Propagation Kinetics The PLP/SEC technique has proven to be an efficient and accurate method to investigate $k_{p,cop}$, based on careful analysis of polymer MWDs. In PLP experiments, each laser flash initiates new radicals from photoinitiator, with these radicals propagating and, in some cases, terminating in the time period between two flashes. Those radicals that survive the dark period between pulses are likely to be terminated by the next laser flash, forming a significant population of dead chains with length L_0,

$$L_0 = k_{p,cop}[M]t_0 \tag{3.3}$$

Given the total monomer concentration [M] and flash interval t_0, the copolymer-averaged

propagation rate coefficient $k_{p,cop}$ can be deduced. There is a probability that some radicals survive the next laser flash and terminate with a later flash, such that signals corresponding to chains of length $2L_0$, $3L_0$, can also be observed. If well-structured MWDs are formed, like those shown in Figure 3.3, $k_{p,cop}$ values can be calculated from the first inflection point of the MWD according to

$$k_{p,cop}/\mathrm{L}\cdot\mathrm{mol}^{-1}\mathrm{s}^{-1} = \frac{\mathrm{MW}_0}{1000\rho t_0} \tag{3.4}$$

where MW_0 is the polymer molecular weight at the first inflection point and ρ ($g{\cdot}mL^{-1}$) is the density of monomer mixture calculated assuming volume additivity. In addition, the MW value at the second inflection point should occur at a value of twice that of MW_0, providing an important check for PLP consistency.

The parameters necessary to estimate $k_{p,cop}$ from SEC data are summarized in Table 3.2, with monomer densities calculated as a function of temperature, and the refractive index (dn/dc) for interpretation of LS results measured as discussed previously. However, Mark-Houwink parameters for HEMA homopolymer are required in order to analyze the output from the RI detector, with the copolymer MW calculated as a composition-weighted average of the homopolymer values. As the homopolymer of HEMA cannot be dissolved in THF, these values have been estimated. The '*a*' exponent value was set to the value reported for GMA,[3] and the '*K*' was adjusted to achieve agreement between LS and RI MW results for ST/HEMA produced with $f_{HEMA} \leq 0.7$, according to the following relations:

$$\log(\mathrm{MW})_{\mathrm{HEMA}} = \frac{1+a_{\mathrm{S}}}{1+a_{\mathrm{HEMA}}}\log(\mathrm{MW})_{\mathrm{S}} + \frac{1}{1+a_{\mathrm{HEMA}}}\log\left(\frac{K_{\mathrm{S}}}{K_{\mathrm{HEMA}}}\right) \tag{3.5}$$

$$\log(\mathrm{MW})_{\mathrm{cop}} = (1-w_{\mathrm{HEMA}})\log(\mathrm{MW})_{\mathrm{S}} + w_{\mathrm{HEMA}}\log(\mathrm{MW})_{\mathrm{HEMA}} \tag{3.6}$$

where w_{HEMA} is the weight fraction of HEMA in the copolymer. This methodology to establish calibration for the RI detector is not ideal, as it depends upon the accuracy of the LS results. However, as the LS results are processed using experimentally determined d*n*/d*c* values for the copolymers, the RI results are used only as a check on SEC operation. Agreement between the two detectors was good, within 10%, over a wide range of MW_0 values, between 5×10^3 and 1×10^5 Da (see Appendix A.1.1).

A systematic PLP/SEC study with experiments from 50 to 120 °C has been carried out, with complete experimental conditions and results summarized in Appendix A.1.1. Most experiments were conducted at 50 Hz; a few experiments were run with a pulse repetition rate of 33 Hz, with the $k_{\mathrm{p,cop}}$ values obtained in good agreement with 50 Hz results. Above 120 °C, no meaningful PLP structure was obtained, possibly due to styrene thermal polymerization and/or crosslinking involving HEMA impurities. Typical results are shown in Figure 3.5, a plot of copolymer MWDs measured by the two detectors for comonomer mixtures of varying composition pulsed at 90 °C with a laser repetition rate of 50 Hz, and the corresponding first-derivative plots used to identify inflection points. The MWDs shift to the right and the corresponding MW_0 values increase as the mole fraction of HEMA in the comonomer mixture increases from 0 to 0.7. This shift is not surprising, as the propagation rate coefficient for HEMA is seven times greater than that of ST at

90 °C, as calculated according to the Arrhenius equations determined from previous PLP/SEC homopolymerization studies:[11,22]

$$k_{p,HEMA}/L \cdot mol^{-1} \cdot s^{-1} = 10^{6.954} \exp(-2634/(T/K)) \quad (3.7)$$

$$k_{p,ST}/L \cdot mol^{-1} \cdot s^{-1} = 10^{7.630} \exp(-3910/(T/K)) \quad (3.8)$$

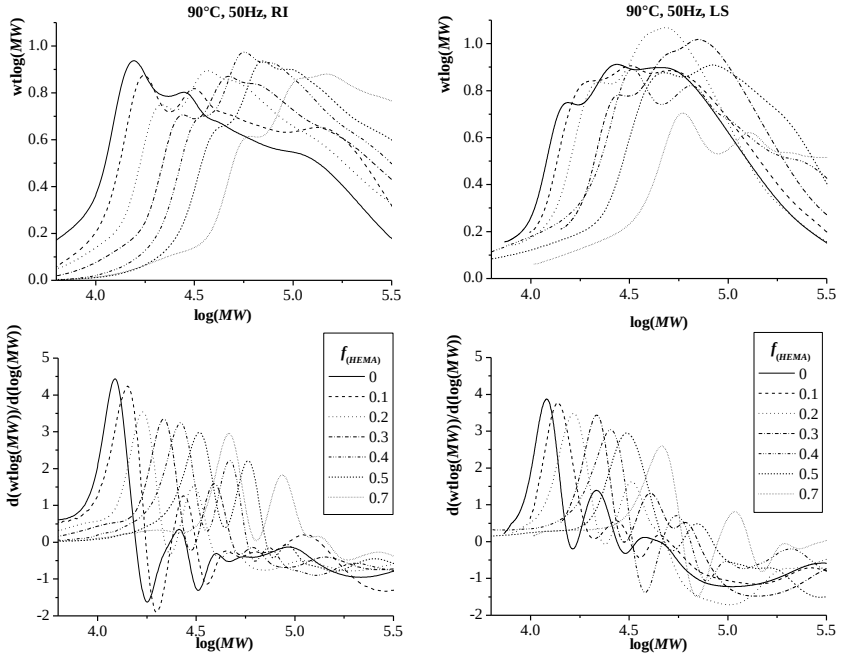

Figure 3.5 MWDs (top) and corresponding first derivative (bottom) plots obtained for styrene/2-hydroxyethyl methacrylate (HEMA) copolymer produced by PLP at 90 °C and 50 Hz, as measured by RI (left) and LS (right) detectors. Monomer compositions are given as mole fraction HEMA (f_{HEMA}).

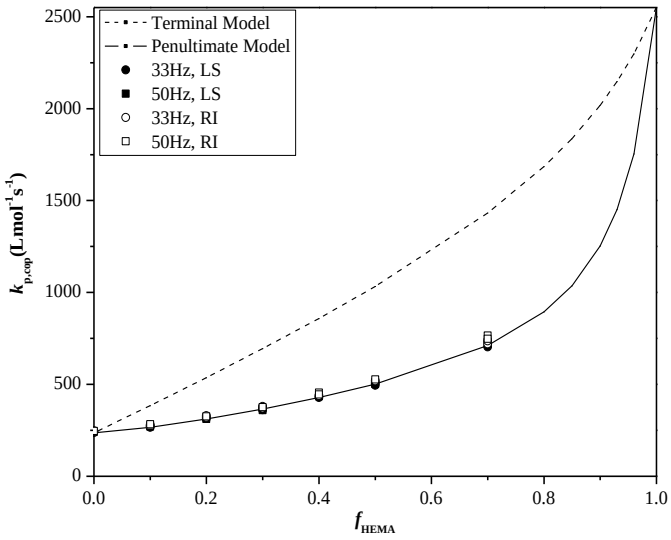

Figure 3.6 Copolymer propagation rate coefficients ($k_{p,cop}$) data vs 2-hydroxyethyl methacrylate (HEMA) monomer mole fraction, as measured by PLP/SEC at 50 °C. Terminal model predictions are indicated by dashed line and penultimate model fit, calculated with s_{ST}=0.38 and s_{HEMA}=1.34, by the solid line.

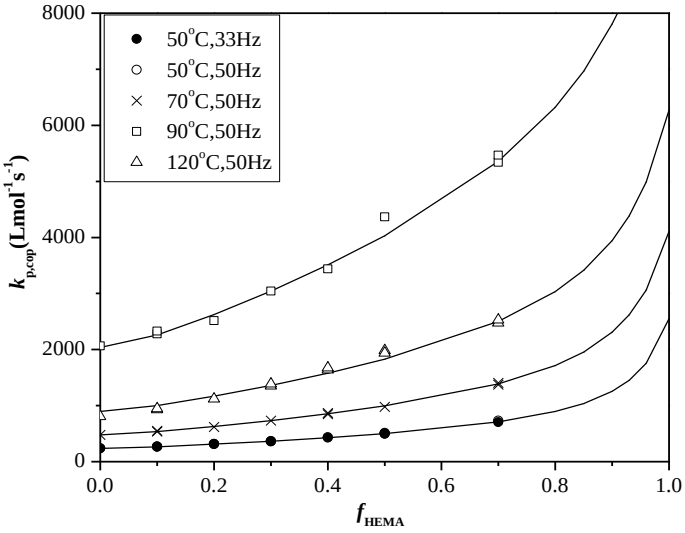

Figure 3.7 Experimental $k_{p,cop}$ (L·mol^{-1}·s^{-1}) values determined by SEC analysis of styrene/2-hydroxyethyl methacrylate (HEMA) copolymers produced via PLP experiments, plotted as a function of HEMA monomer mole fraction. Lines indicate data fits using the implicit penultimate unit effect model, with s_{ST}=0.38 and s_{HEMA}=1.34.

The $k_{p,cop}$ data obtained at 50 °C is plotted in Figure 3.6 as a function of monomer composition. The value increases from the ST homopolymer value of 240 $L \cdot mol^{-1} \cdot s^{-1}$ to 700 $L \cdot mol^{-1} \cdot s^{-1}$ with f_{HEMA}=0.7. As mentioned before, the agreement between the $k_{p,cop}$ estimated from LS and RI detectors is excellent, as is the agreement between experiments run at 33 and 50 Hz. Also shown in Figure 3.6 is the prediction of the terminal model, calculated using the monomer reactivity ratios that describe the copolymer composition data in bulk, r_{HEMA}=0.49 and r_{ST}=0.27, and the homopolymer k_p values calculated according to Eq 3.5 and 3.6. The deviation between experiment and the terminal model prediction is significant, with the terminal model overpredicting $k_{p,cop}$ by as much as factor of two. It is clear that the terminal model cannot simultaneously describe copolymer composition and reaction rate for the ST/HEMA system, as observed previously for ST copolymerized with alkyl methacrylates[1,9,23,24] and with the functional monomer GMA.[3] As for these other systems, the IPUE model provides a good fit to the experimental data. Radical reactivity ratios, s_{ST}=0.38±0.01 and s_{HEMA}=1.34±0.71, estimated by non-linear regression, are able to fit the entire set of $k_{p,cop}$ data between 50 and 120 °C, as determined by LS analysis and shown in Figure 3.7. While enthalpic contributions cannot be ruled out, a single pair of temperature-independent *s* values is sufficient to represent the data, as found previously for the ST/BMA[1] and ST/GMA[3] systems.

Table 3.4 summarizes the kinetic coefficients for these three ST/methacrylate systems. (The reactivity ratios of ST/MMA and ST/DMA are very similar to ST/BMA.) It is difficult to determine whether the difference in the *s* values reflects real kinetic differences, or is a reflection of the higher

uncertainty in estimating these coefficients.[1] Despite the difference in absolute k_p values for the three methacrylates, the relative addition of styrene to methacrylate radicals is similar (r_{xMA} between 0.4 and 0.5). However, the functional monomers GMA and HEMA add onto a styrene radical significantly faster than does BMA, as reflected in the lower r_{ST} values.

Table 3.4 Values of copolymerization reactivity ratios and homopropagation rate coefficients (k_p, in $L \cdot mol^{-1} \cdot s^{-1}$, at 90 °C) for bulk copolymerization of styrene (ST) with 2-hydroxyethyl methacrylate (HEMA), glycidyl methacrylate (GMA) and *n*-butyl methacrylate (BMA)

	ST/HEMA	ST/GMA[3]	ST/BMA[1]
r_{ST}	0.27±0.01	0.31±0.01	0.61±0.03
r_{xMA}	0.49±0.03	0.51±0.02	0.42±0.03
s_{ST}	0.38±0.01	0.28±0.01	0.44±0.05
s_{xMA}	1.34±0.71	1.05±0.23	0.62±0.2
$k_{p,ST}$	895	895	895
$k_{p,xMA}$	6272	2550	1926

3.3.2 Solvent Effect on Copolymerization of ST and Methacrylates

A series of PLP/SEC experiments were performed at 90 °C for the ST/HEMA, ST/GMA, and ST/BMA systems in *n*-butanol (polar with hydroxyl group), DMF (polar without hydroxyl group) and toluene (non-polar) solvents, with solvent levels at 25 and 50 vol%. Most experiments were conducted at a laser repetition rate of 50 Hz, with a few at 25 and 33 Hz. Except for the solvent

presence, the experimental conditions are identical to those used in the recent PLP/SEC studies of bulk copolymerization,[1,3] including the ST/HEMA results discussed in the previous section. Proton NMR was used to determine composition of the low conversion samples. The complete set of experimental results, both copolymer composition and $k_{p,cop}$ data, is available in Appendix A.1.2.

The solution polymerization results presented here build on the bulk studies of ST/BMA, ST/GMA and ST/HEMA propagation kinetics summarized in Figure 3.3 and 3.7, with corresponding IPUE coefficients at 90 °C summarized in Table 3.4. For reasons that will become apparent, the effect of solvent on copolymer composition and on $k_{p,cop}$ will be discussed separately before considering the implications that the combined set of measurements have on our understanding of copolymerization propagation kinetics.

Copolymer Composition. Figure 3.8 plots copolymer composition as a function of monomer composition, as determined in low conversion ST/xMA experiments at 90 °C conducted with 25 or 50 vol% solvent present. The solid line in each plot is calculated assuming terminal kinetics and using the reactivity ratios determined from analysis of the corresponding bulk systems summarized in Table 3.4.

For ST/HEMA (Figure 3.8a), the presence of butanol and DMF leads to the formation of copolymer enriched in ST relative to the bulk case for copolymerizations conducted with low

HEMA content (f_{HEMA}<0.6); the copolymer composition converges as that found for copolymerizations in bulk with higher HEMA content (f_{HEMA}>0.6). The opposite trend is observed for copolymerizations performed in toluene: HEMA-rich copolymer is formed (relative to the bulk system) for mixtures with medium and high HEMA content (f_{HEMA}>0.2), with the copolymer composition the same as found for bulk mixtures with low HEMA content. The data set at each solvent level has been fit to the Mayo-Lewis equation via non-linear parameter estimation, with results (including 95% confidence intervals) summarized in Table 3.5. The observed shifts in copolymer composition for copolymerization in butanol and DMF are best fit by keeping r_{HEMA} constant at the bulk value and increasing r_{ST}, while the results obtained for polymerization in toluene are best fit with r_{ST} relatively constant and increasing r_{HEMA}.

Table 3.5 Monomer reactivity ratios of ST/HEMA in solution, determined by fit of the terminal model to experimental data shown in Figure 3.8a.

	Bulk	Toluene		DMF		Butanol
		25 vol%	50 vol%	25 vol%	50 vol%	50 vol%
r_{ST}	0.27±0.01	0.26±0.02	0.23±0.02	0.35±0.01	0.45±0.03	0.44±0.03
r_{HEMA}	0.49±0.03	0.66±0.08	1.09±0.18	0.49±0.04	0.53±0.10	0.54±0.10

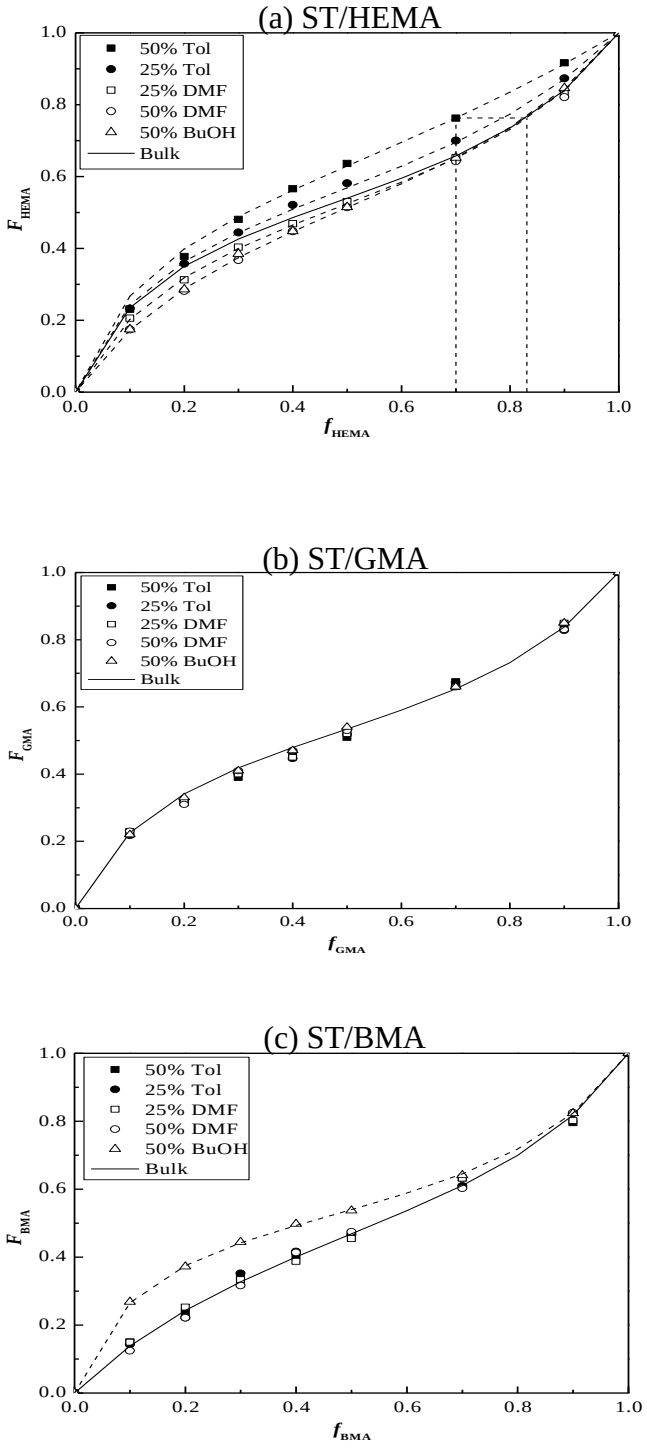

Figure 3.8 Copolymer composition data for low-conversion styrene/xMA copolymerization in solvents at varying concentrations, plotting mole fraction xMA in copolymer (F_{xMA}) as a function of xMA mole fraction in the monomer phase (f_{xMA}). The solid curve in each plot is the prediction of the terminal copolymerization model with monomer reactivity ratios in bulk.

In contrast to the ST/HEMA results and despite the polarity of GMA, the copolymer composition of ST/GMA is not affected by solvent choice to any significant effect (Figure 3.8b). ST/BMA composition (Figure 3.8c) is unchanged by DMF or toluene solvent, but is significantly affected by the addition of BuOH, a result captured by a significant change in r_{ST} (r_{ST}=0.21±0.02, r_{BMA}=0.38±0.04 in BuOH compared to r_{ST}=0.61±0.03 and r_{BMA}=0.42±0.03 in bulk). The results summarized in Figure 3.8 are in good agreement with the ST/HEMA and ST/MMA literature discussed in Ch 2: with the exception of alcohols, solvent has, at most, a minor effect on reactivity ratios for copolymerization of ST with alkyl methacrylates (MMA, BMA), but has a startling effect on the copolymerization of ST with HEMA. Supplemental to the previous literature, we find that ST/GMA copolymer composition (and thus reactivity ratios) is rather insensitive to solvent choice, and that the variation in reactivity ratios for the ST/HEMA system changes systematically with solvent level, a result not reported in previous studies.

Previous ST/xMA copolymer composition studies have been explained using both reactivity (H-bonding affecting the relative reactivity of radicals to monomer) and physical (the ratio of monomer concentrations at the reactive site are different than in the bulk mixture) arguments. First consider the physical bootstrap effect by examining Figure 3.8a at a specific f_{HEMA} value of 0.70, as marked on the plot. The corresponding HEMA fraction in the copolymer HEMA in BuOH and DMF is the same as measured in bulk, with F_{HEMA}=0.62. However, the experimentally determined F_{HEMA} value is 0.75 in 50 vol% toluene solution. Assuming that this difference in composition can be attributed solely to the bootstrap effect (HEMA monomer is preferentially partitioned around

the HEMA-rich copolymer chains in the non-polar toluene solvent) and that the bulk reactivity ratios are true values, the plot indicates that the fraction of HEMA in the monomer mixture found locally around the radicals must be enriched to 0.82. Meanwhile, in the polar solvents butanol and DMF, ST monomer preferentially partitions to the ST-rich copolymer chains, an effect that diminishes as the HEMA fraction is increased in the monomer mixture (and in the copolymer that is formed). While often used to explain copolymer composition in polar systems, however, it is difficult to simply use only the bootstrap effect to explain these ST/HEMA results. One reason is that it is inconsistent with the $k_{p,cop}$ results (presented later). In addition, no similar solvent effect on copolymer composition is observed for the relatively polar ST/GMA systems, from which it can be concluded that it is an effect specific to H-bonding.

Thus, let us consider solvent effects on the monomer relative reactivity. As discussed by Beuermann[26] and Ito and Otsu,[27,28] IR spectroscopy can be used as a probe to study monomer and solvent interactions. From the FT-IR spectra shown as Figure 3.9, a shoulder at 1708 cm^{-1} for the methacrylate carbonyl region is observed in bulk ST/HEMA that is not present for ST/GMA or ST/BMA. The shoulder results from hydrogen bonding between the monomer OH group and carbonyl O atom, strengthening the positive partial charges at the carbonyl C atom and at the double bond as shown schematically in Figure 3.10, leading to a significant charge transfer in the transition state of propagation. When toluene is added to the system, the HEMA H-bonding is still distinct but diluted, such that the monomer reactivity towards a ST radical remains unchanged from bulk (see r_{ST} values in Table 3.5). However, the r_{HEMA} value changes significantly, to the point

where HEMA monomer addition to a HEMA radical is favoured over ST addition (r_{HEMA}>1). Generally speaking, when charge transfer in the transition state is significant, the stability of the charge transfer species is affected by the polarity of the solvent,[29] which can explain why toluene has an effect on the ST/HEMA reactivity ratios, but no influence on the ST/GMA system.

The shoulder for HEMA at 1708 cm^{-1} disappears in the presence of DMF for the ST/HEMA mixture (see Figure 3.9), similar to what was reported by for 2-hydroxypropyl methacrylate (HPMA) in THF.[30] As shown schematically in Figure 3.10, this disappearance indicates that the HEMA-HEMA interactions are disrupted and replaced by hydrogen bonding between the DMF carbonyl oxygen and the HEMA hydroxyl group. The 1708 cm^{-1} peak for HEMA remains unchanged when *n*-butanol is added to the system; however, a significant amount of the HEMA-HEMA H-bonding is replaced by HEMA-BuOH H-bonding (see Figure 3.10). In both cases, the disruption of hydrogen bonding between HEMA molecules leads to a decreased rate of monomer addition to ST radicals compared to bulk copolymerization. These spectra suggest that BuOH and DMF affect ST/HEMA copolymer composition through specific interactions with HEMA, while toluene works through a polarity effect.

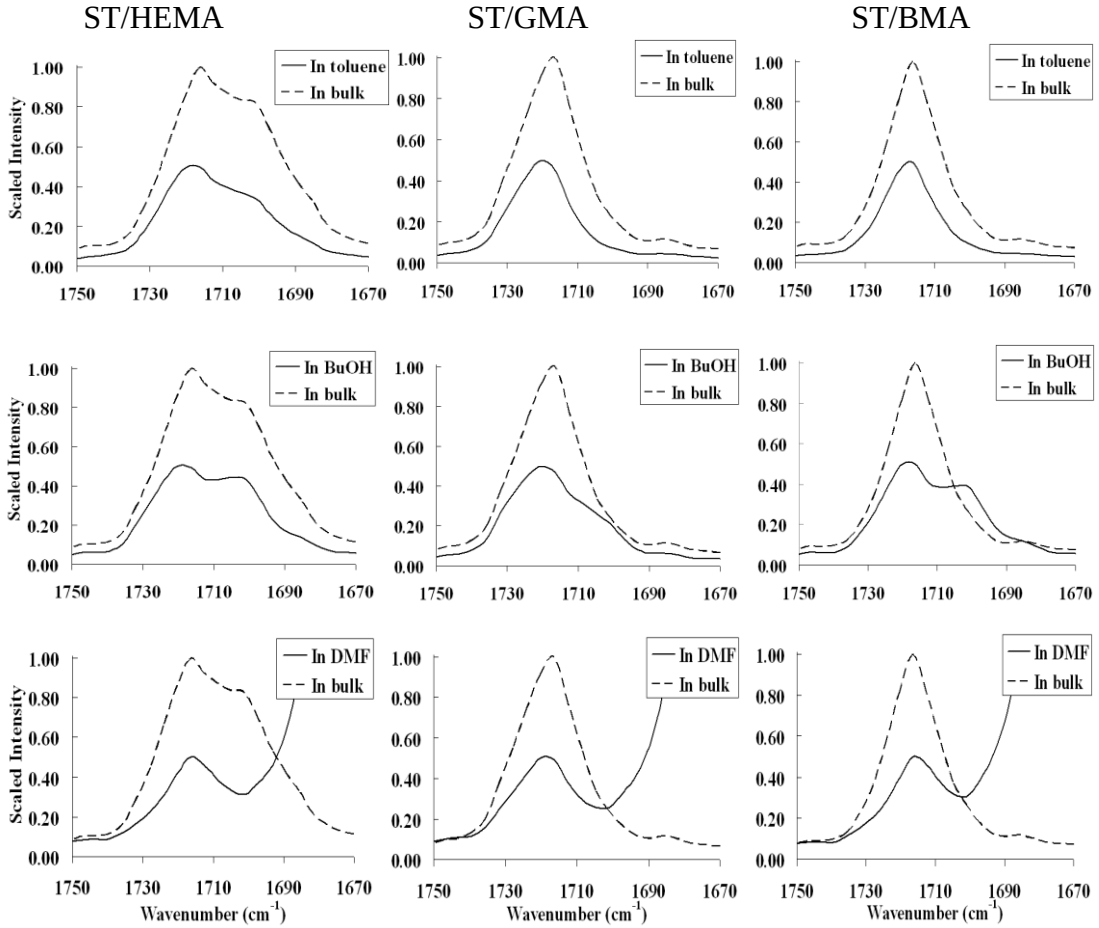

Figure 3.9 FT-IR spectra comparison of comonomer mixtures (1:1 mole ratio) of ST/HEMA (left column), ST/GMA (middle column) and ST/BMA (right column) at room temperature in bulk and in: 50 vol% toluene (top row), butanol (middle row) and DMF (bottom row) solutions.

The addition of BuOH to the ST/BMA system leads to the formation of the same shoulder in the IR peak observed for ST/HEMA in bulk, an indication of H-bonding in the system. As discussed by Fujihara et al.[31] for ST/MMA in ethanol, this bonding reduces the electron density of the BMA double bond, making it more reactive towards ST radicals compared to bulk and other solvents. Following similar logic, Beuermann proposed that disruption of monomer-monomer H-bonding causes HPMA to assume homopropagation kinetics in polar solution that are similar to those of alkyl methacrylates in bulk.[26] This hypothesis is consistent with the ST-HEMA

copolymerization behaviour found in DMF; the value of r_{ST} required to fit the data (see Figure 3.8 and Table 3.5) increases to 0.45, a value that is more typical for ST with alkyl methacrylates.[1] Meanwhile, addition of butanol to ST/BMA causes the value of r_{ST} required to fit the data to decrease to 0.21, similar to the value measured for ST/HEMA. DMF and BuOH may have some polarity effects on the ST/HEMA system, but the effect of solvent on H-bonding is what controls the monomer reactivity ratios.

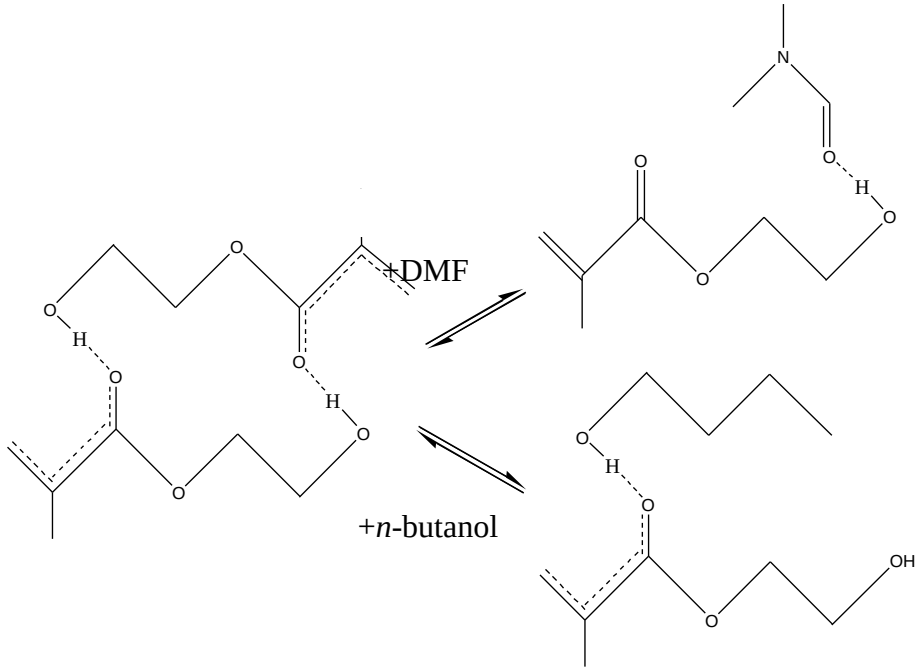

Figure 3.10 Schematic representation of H-bonding between two HEMA monomer molecules in bulk (left), compared to between DMF and HEMA or between *n*-butanol and HEMA in solution.

Copolymerization Propagation Coefficient Figure 3.11 plots the values of $k_{p,cop}$ at 90 °C as a function of monomer composition, determined from low conversion ST/xMA experiments in 25

and 50 vol% toluene, 25 and 50 vol% DMF, and 50 vol% BuOH. The solid lines drawn in Figure 3.11 are calculated assuming implicit penultimate kinetics and using the monomer and radical reactivity ratios and homopropagation rate coefficients determined from analysis of the corresponding bulk systems summarized in Table 3.4. What can be immediately observed is that the $k_{p,cop}$ values measured in toluene are in very good agreement with those for the bulk ST/xMA systems for all three methacrylates, in agreement with the previous ST/MMA studies.[32,33]

The $k_{p,cop}$ values measured in DMF are lower than the bulk values throughout most of the composition range. This difference is clearly observed for ST homopolymerization (f_{xMA}=0); in agreement with previous literature,[34] our PLP results indicate that k_p values for ST is reduced by 20% in DMF compared with bulk. This result can be explained by a reversible complexation between DMF and the aromatic group of styrene, similar to the arguments used by Kamachi et al.[35] to explain the aromatic solvent effect on polymerization of vinyl acetate. The decrease in $k_{p,cop}$ values in DMF relative to bulk becomes smaller as the methacrylate fraction in the ST/BMA and ST/GMA systems increase, with no solvent effect observed for homopolymerization of BMA or GMA values in DMF. For ST/HEMA, however, the difference between $k_{p,cop}$ and the bulk system increases in magnitude with increasing HEMA fraction in the monomer phase. This trend strongly suggests that the HEMA k_p value is significantly reduced in DMF, as would be expected based upon the 40% decrease of HPMA k_p in THF reported in literature.[30] As shown by the FT-IR spectra in Figure 3.9 and schematically in Figure 3.10, DMF disrupts H-bonding between HEMA molecules, increasing the electron density at the double bond and decreasing the k_p value.

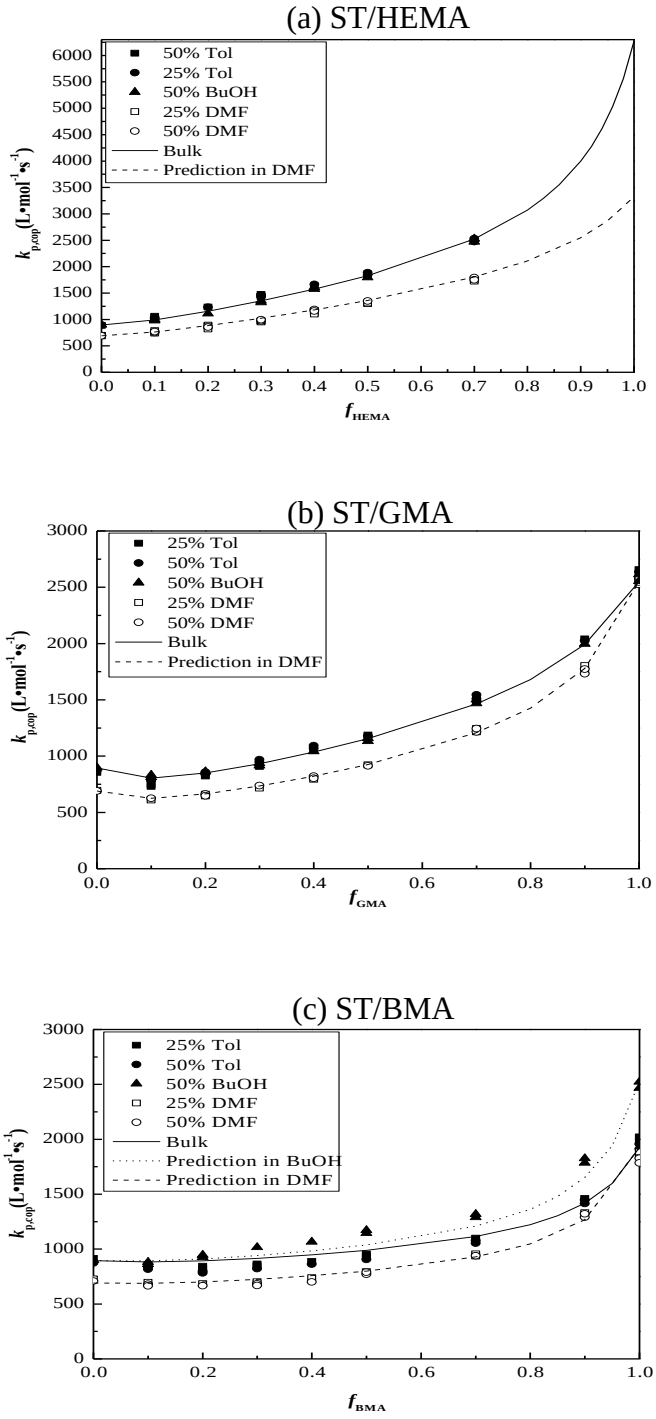

Figure 3.11 Experimental $k_{p,cop}$ (L·mol^{-1}·s^{-1}) values determined by SEC analysis of ST/xMA copolymers produced via PLP experiments, plotted as a function of monomer mole fraction. Lines indicate predictions according to the implicit penultimate unit effect model with *r* and *s* values taken from bulk studies (Table 3.4). Values for $k_{p,ST}$ in DMF, $k_{p,HEMA}$ in DMF and $k_{p,BMA}$ in BuOH adjusted according to experimental data (see text).

The immediate question that arises is whether or not the penultimate model will provide a fit to the ST/xMA $k_{p,cop}$ data in DMF using the *r* and *s* values (for bulk polymerization) from Table 3.4, after adjusting the endpoint k_p values to account for solvent effects. The dashed lines in each figure indicate that this is indeed the case; in all cases the IPUE provides a good representation of the data. Thus, $k_{p,cop}$ values can be predicted for solution polymerization using bulk *r* and *s* copolymerization results not only for systems that exhibit no solvent effects (ST/xMA in toluene), but also for solvents that influence homopropagation behaviour. The result is surprising since, as shown in Figure 3.8a, H-bonding has a significant effect on ST/HEMA copolymer composition in both toluene and DMF solution.

n-Butanol is not only a polar solvent but also carries an active hydroxyl group. Thus, it is interesting to look into its effect on ST/xMA copolymerization. For ST/GMA (Figure 3.11b), the $k_{p,cop}$ curve is in good agreement with the bulk and toluene solution systems, and well represented using the bulk values for homopropagation kinetics and IPUE reactivity ratios summarized in Table 3.4. (In agreement with the study of ST homopolymerization in EtOH and methanol,[36] BuOH has no effect on ST homopolymerization kinetics.) Figure 3.11a also indicates that ST/HEMA $k_{p,cop}$ is the same in BuOH as in bulk and toluene for monomer mixtures containing up to 70 mol% HEMA; this result suggests that HEMA homopolymerization k_p values are the same in BuOH as in bulk, in agreement with previous results for HPMA in BzOH[30] and for HEMA in ethanol.[11]

For ST/BMA (Figure 3.11c), BuOH enhances the homopropagation of BMA by 30% at 90 °C,

in agreement with the results presented by Beuermann.[15] As shown in the spectrum in Figure 3.9, the addition of BuOH to the system leads to H-bonding between the BuOH and BMA, making $k_{p,cop}$ act in a fashion similar to homopropagation. The line plotted in Figure 3.11c makes this adjustment, but keeps the *r* and *s* values set to bulk values. The experiment data are close to the IPUE predictions using the *r* and *s* values determined in bulk. A small adjustment (to s_{ST}=0.49 and s_{BMA}=0.80) within the uncertainty range reported in Table 3.4, provides an excellent fit to the data (curve not shown). As for the ST/HEMA data, this good representation is surprising, as BuOH significantly affects copolymer composition and corresponding *r* estimates (Figure 3.8c).

Combined Data Sets. We now turn back to the full set of composition and $k_{p,cop}$ results summarized in Figure 3.8 and 3.11. For ST/BMA and ST/GMA, the curves calculated using the Table 3.4 IPUE parameter values from bulk copolymerization provide a good representation of the $k_{p,cop}$ values measured in toluene as well as copolymer composition data. The same can be said for the ST/GMA results measured in BuOH. Bulk *r* and *s* values also provide a good fit to the copolymer composition and $k_{p,cop}$ values measured in DMF for ST/BMA and ST/GMA, after decreasing the $k_{p,ST}$ value at 90 °C by 20% (to 691 $L \cdot mol^{-1} \cdot s^{-1}$) to match the homopolymerization PLP/SEC results. Thus, 5 out of the 9 systems are easily understood and represented by the IPUE model of copolymerization kinetics. The same, however, cannot be said for ST/BMA polymerized in BuOH and for the complete set of ST/HEMA solution results.

Figure 3.12 replots both the copolymer composition and $k_{p,cop}$ results for ST/BMA in BuOH. The composition data (Figure 3.12a) can be fit by the terminal model, but using a different set of monomer reactivity ratios (r_{ST}=0.21, r_{BMA}=0.38) compared to the values for the bulk system (r_{ST}=0.61 and r_{BMA}=0.42). Also shown is the copolymer composition curve plotted using *r* values estimated for ST/HEMA bulk (r_{ST}=0.27, r_{HEMA}=0.48). The copolymer composition curves (and reactivity ratio estimates) for ST/BMA in BuOH and ST/HEMA in bulk are quite similar, suggesting that the effect of H-bonding is also similar. This result is consistent with the 30% increase observed for $k_{p,BMA}$ in BuOH compared to the bulk value; addition of BuOH to the BMA system causes the alkyl methacrylate to shift in reactivity towards the behaviour of HEMA.[26]

The ST/BMA $k_{p,cop}$ experimental data measured in BuOH are reasonably well represented by the IPUE model using the *r* and *s* values determined in bulk. Of course, one would consider that the *r* values fit to the ST/BMA composition data in BuOH should be used in Eq 2.29 and 2.30 to calculate $k_{p,cop}$ for this system. As shown in Figure 3.12b, however, this adjustment causes significant deviation between the experimental data and the IPUE predictions. It is possible to refit the IPUE model to the data using the new *r* values and with s_{ST}=0.32±0.02 and s_{BMA}=0.27±0.03 (compared to the Table 3.4 values of 0.44±0.05 and 0.62±0.2). However, the shape of the best-fit IPUE line does not match the data particularly well, suggesting that an explicit consideration of H-bonding effects is needed.

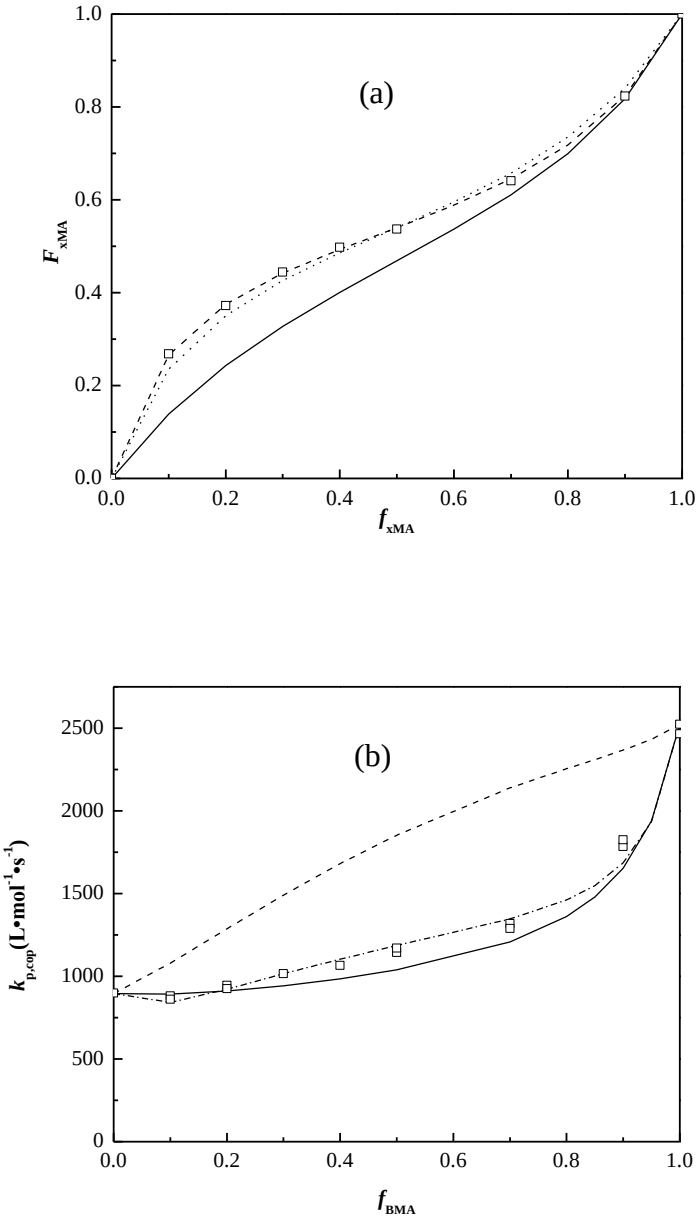

Figure 3.12 (a) Copolymer composition (F_{xMA}) and (b) $k_{p,cop}$ results for ST/BMA copolymerization in 50 vol% BuOH solution (symbols) compared to predictions calculated using: IPUE reactivity ratios determined in bulk (——); *s* values from bulk and *r* values fit to copolymer composition data in BuOH (- - -); and *s* values fit to BuOH $k_{p,cop}$ data with *r* values fit to copolymer composition data in BuOH (-·-). All lines calculated with $k_{p,BMA}$=2523 L·mol^{-1}·s^{-1}, as measured in BuOH solution. The dotted line in a) represents copolymer composition obtained in the bulk ST/HEMA system.

It is also difficult to come up with a cohesive description of the ST/HEMA copolymerization propagation kinetics. As found for ST/BMA in BuOH, the ST/HEMA *r* values measured in bulk provide a reasonable match to $k_{p,cop}$ data according to the IPUE model (Figure 3.11a) but not copolymer composition data (Figure 3.8a). To examine this result further, we calculate $k_{p,cop}$ curves using the *r* values from Table 3.5 (estimated from the terminal model fit to copolymer composition for each solvent system) with *s* values estimated from bulk copolymerization; as discussed earlier, the $k_{p,ST}$ and $k_{p,HEMA}$ values in DMF are decreased by 20% and 40% compared to bulk, respectively,. The resulting curves are shown as Figure 3.13a. The change in *r* values has a quite significant effect in the $k_{p,cop}$ curves calculated for ST/HEMA copolymerization in all the solvents, moving the IPUE predictions in toluene above the experimental values, the predictions in DMF below the data, and the predictions in BuOH well below the experimental results. The IPUE can be forced to match the experimental $k_{p,cop}$ data by adjusting the *s* values for each solvent system, as shown in Figure 3.13b with the best-fit values summarized in Table 3.6. While providing a good fit to the data, the need to have solvent-specific radical and monomer reactivity ratios to describe ST/HEMA copolymer composition and $k_{p,cop}$ data is disappointing.

It is interesting to note that the parameter that controls the shape of the ST/HEMA $k_{p,cop}$ curve is different for toluene than the polar solvents. It is possible to achieve a reasonable fit to the 50 vol% toluene data with s_{ST} fixed at the bulk value of 0.38 and s_{HEMA} decreased to 0.35; the data cannot be well-represented keeping s_{HEMA} fixed and varying s_{ST}. The corresponding copolymer composition data measured in toluene were also fit by keeping r_{ST} fixed and changing r_{HEMA}. The opposite is

true for the ST/HEMA $k_{p,cop}$ data in DMF and BuOH, which are fit by increasing s_{ST} values compared to bulk; similarly, the r_{ST} values were varied to fit the ST/HEMA copolymer composition data in DMF and BuOH. For these latter fits, the s_{HEMA} values are indeterminate, and thus could be kept at the bulk value of 1.34 without significantly affecting the shape of the curve. Perhaps these systematic variations will provide a means to modify the IPUE to account for specific H-bonding interactions.

Table 3.6 Values of IPUE reactivity ratios and homopropagation rate coefficients (k_p, in $L \cdot mol^{-1} \cdot s^{-1}$) at 90 °C for copolymerization of styrene (ST) with 2-hydroxyethyl methacrylate (HEMA) in solution and in bulk

	Bulk[20]	Toluene		DMF		Butanol
		25 vol%	50 vol%	25 vol%	50 vol%	50 vol%
r_{ST}	0.27±0.01	0.26±0.02	0.23±0.02	0.35±0.01	0.45±0.03	0.44±0.03
r_{HEMA}	0.49±0.03	0.66±0.08	1.09±0.18	0.49±0.04	0.53±0.10	0.54±0.10
s_{ST}	0.38±0.01	0.47±0.02	0.64±0.08	0.45±0.02	0.47±0.02	0.47±0.13
s_{HEMA}	1.34±0.71	0.35±0.05	0.19±0.02	0.65±0.22	*n.d.*	*n.d.*
$k_{p,ST}$	895	895	895	691	691	895
$k_{p,HEMA}$	6272	6272	6272	3763	3763	6272

n.d.= not determined

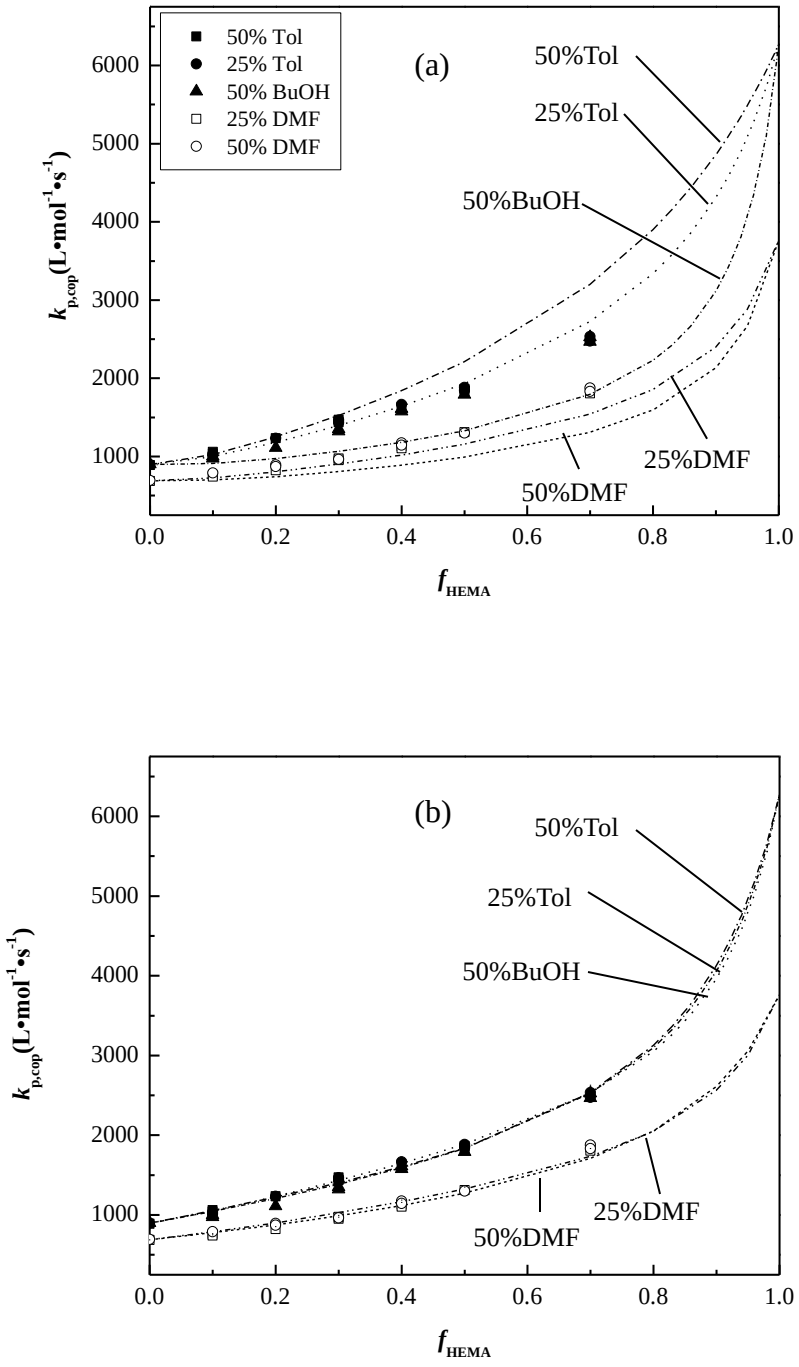

Figure 3.13 IPUE model representation of ST/HEMA solution $k_{p,cop}$ data (symbols as in Figure 3.6a) obtained by PLP/SEC at 90 °C: (a) Curves calculated using *r* values fit to composition data (Table 3.5) and estimates for *s* from bulk copolymerization (s_{ST}=0.38 and s_{HEMA}=1.34); (b) Curves calculated using *r* values fit to composition data (Table 3.5) and *s* values fit to each individual data set (Table 3.5).

3.4 Conclusions

The PLP technique has been employed to systematically investigate free radical bulk copolymerization of ST and HEMA in the temperature range of 50-120 °C and solution copolymerization of ST with BMA, GMA, and HEMA at 90 °C. Copolymer composition data, determined via proton NMR, illustrate that HEMA exhibits higher reactivity to ST radicals than do alkyl methacrylates and the solvent effects comonomer reactivity ratios. DMF and *n*-butanol both decrease the reactivity of ST radicals with HEMA, most likely due to the disruption of monomer-monomer hydrogen bonding, while nonpolar toluene increases the reactivity of HEMA radicals toward HEMA compared to ST. Addition of *n*-butanol to the ST/BMA system also significantly affects copolymer composition, increasing the relative addition rate of BMA to a ST radical. However, addition of toluene or DMF to ST/BMA has little or no effect on copolymer composition, a result also seen for ST/GMA copolymerization in all three solvents. From this study it is clear that H-bonding solvents or monomers cause copolymer composition to vary greatly compared to bulk. The terminal model can still be used to represent these composition data, with a systematic variation in monomer reactivity ratios with solvent choice and concentration.

Despite the variation in copolymer composition with solvent choice, the variation of the composition-averaged copolymer propagation rate coefficients, $k_{p,cop}$, with monomer composition is well-described by the implicit penultimate unit effect (IPUE) model using reactivity ratios

estimated in bulk, provided that homopropagation end point values are adjusted for solvent effects. (DMF decreases the value of $k_{p,ST}$ and $k_{p,HEMA}$; *n*-butanol increases the value of $k_{p,BMA}$.) The fact that *s* and *r* values determined in bulk provide a good representation of $k_{p,cop}$ curves for H-bonding systems but not copolymer composition is surprising, and will be further explored with a study of copolymerization propagation kinetics and solvent effects of hydroxyl functional monomers in mixed acrylate/methacrylate systems. In addition to kinetic studies, a series of semibatch reactions will be carried on to examine solvent effects on the complete free radical copolymerization process.

References

1. Li, D. Li, N.; Hutchinson, R. A. *Macromolecules* **2006**, *39*, 4366.
2. Wang, W.; Hutchinson, R. A. *Macromol. React. Eng.* **2008**, *2*, 199.
3. Wang, W.; Hutchinson, R. A. *Macromolecules* **2008**, *41*, 9011.
4. Wichterle. *Encyclopedia of Polymer Technology, Wiley, New York.* **1971,** *15*, 275.
5. Okano, T.; Aoyagi, J.; Shinohara, J. *Nippon Kagaku Kaishi*. **1976**, *1*, 161.
6. Lebduška, J.; Šnupárek Jr., J.; Kašpar, K.; Čermák, V. *J. Polym. Sci.: Part A: Polym. Chem*. **1986**, *24*, 777.
7. Schoonbrood, H. A. S.; Aerdts, A. M.; German, A. L.; van der Velden, G. P. M. *Macromolecules* **1995**, *28*, 5518.
8. Sánchez-Chaves, M; Martinez, G; Madruga, E. L. *J. Polym. Sci.: Part A: Polym. Chem.* **1999**, *37*, 2941.
9. Coote, M. L.; Zammit, M. D.; Davis, T. P.; Willett, G. D. *Macromolecules* **1997**, *30*, 8182.
10. Zhang, M.; Ray, W. H. *J. Appl. Polym. Sci.* **2002**, *86*, 1630.
11. Buback, M.; Kurz, C. *Macromol. Chem. Phys.* **1998,** *199*, 2301.
12. Hutchinson, R. A.; Beuermann, S.; Paquet. D. A., Jr.; McMinn, J. H.; Jackson, C.

Macromolecules **1998**, *31*, 1542.

13. Hutchinson, R. A.; Beuermann, S.; Paquet. D. A., Jr.; McMinn, J. H.; Jackson, C. *Macromolecules* **1997**, *30*, 3490.
14. Couvreur, L.; Piteau, G.; Castignolles, P. ; Tonge, M. ; Coutin, B. ; Charleux, B. ; Vairon, J-P. *Macromol. Symp.* **2001**, *174*, 197.
15. Beuermann, S. *Macromolecules* **2004,** *37*, 1037.
16. Corradini, F.; Marchetti, A.; Tagliazucchi, M.; Tassi, L.; Tosi, G. *Can. J. Chem. Eng.* **1993**, *71*, 124.
17. Hutchinson, R. A.; Paquet, D. A., Jr. ; McMinn, J. H. ; Beuermann, S. ; Fuller, R. E.; Jackson, C. *5th International Workshop on Polymer Reaction Engineering*; DECHEMA Monographs 131; VCH Publishers: Weinheim, Germany, 1995; pp 467.
18. Hutchinson, R. A.; Paquet, Jr. D. A.; Beuermann, S.; McMinn, J. H. *Ind. Eng. Chem. Res*. **1998**, *37*, 3567.
19. Bywater, S. *Trans. Faraday Soc*. **1955**, *51*, 1267.
20. Liang, K; Dossi, M; Moscatelli, D; Hutchinson, R. A. *Macromolecules.* **2009**, *42*, 7736.
21. Barb, W. G. *J. Polym. Sci*. **1953**, *11*, 117.
22. Buback, M.; Gilbert, R. G.; Hutchinson, R. A.; Klumperman, B.; Kuchta, F.; Manders, B. G.; O'Driscoll, K. F.; Russell, G. T.; Schweer, J. *Macromol. Chem. Phys.* **1995**, *196*, 3267.
23. Davis, T. P.; O'Driscoll, K. F.; Piton, M. C.; Winnik, M. A. *J. Polym. Sci., Part C: Polym. Lett.* **1989**, *27*, 181.
24. Davis, T. P.; O'Driscoll, K. F.; Piton, M. C.; Winnik, M. A. *Macromolecules* **1990**, *23*, 2113.
25. Liang, K.; Hutchinson, R. A. *Macromolecules* **2010**, *43*, 6311.
26. Beuermann, S. *Macromol. Rapid Commun.* **2009**, *30*, 1066.
27. Ito, T; Otsu, T. *J. Macromol. Sci. Part A: Chem.* **1969**, *3*, 197.
28. Otsu, T; Ito, T; Imoto, M. *J. Polym. Sci. A*. **1966**, *4*, 733.
29. Coote, M. L.; Davis, T. P.; Klumperman, B.; Monteiro, M. J. *Rev. Macromol. Chem. Phys.* **1998**, *38*, 567.
30. Beuermann, S.; Nelke, D. *Macromol. Chem. Phys.* **2003**, *204*, 460.
31. Fujihara, H; Yamazaki, K; Matsubara, Y; Yoshihara, M; Maeshima, T. *J. Macromol. Sci. Part A: Chem.* **1979**, *13*, 1081.
32. Fukuda, T.; Kubo, K.; Ma, Y-D.; Inagaki, H. *Polym. J. (Tokyo)* **1987**, *19*, 523.
33. Olaj, O. F.; Schnöll-Bitai, I. *Monatshefte für Chemie*. **1999**, *130*, 731.

34. Coote, M. L.; Davis, T. P. *Eur. Polym. J.* **2000**, *36*, 2423.

35. Kamachi, M.; Liaw, D. J.; Nozakura, S. *Polym. J.* **1979**, *12*, 921.

36. Morrison, B. R.; Piton, M. C.; Winnik, M. A.; Gilbert R. G.; Napper D. H. *Macromolecules.* **1993**, *26*, 4368.

Chapter 4 Solvent Effect on Semibatch Free Radical Copolymerization of ST/HEMA at High Temperatures

Preface

The effects of H-bonding on ST/HEMA copolymerization kinetics have been examined in Ch 3 by the PLP/SEC/NMR technique, focusing on chain propagation only. In order to have a picture of solvent effect on the overall process of copolymerization, high temperature semibatch free radical copolymerizations of HEMA and styrene were carried out in xylene and DMF solution. The detailed comparison between the experimental profiles with different temperatures and solvent concentrations indicates that the solvent effect through H-bonding can be suppressed by increased temperature. In addition the influence of crosslinking reactions, the main cause of high molecular weights in HEMA copolymers, are decreased substantially. The work in this chapter has been accepted for publication in Macromolecular Symposia.

4.1 Introduction

Acrylic copolymers used as binder resins in solvent-borne automotive coatings are produced at high temperature (usually >120 °C) and low solvent levels via free-radical polymerization in a semibatch process.[1] Two streams, one a mixture of monomers and the second an initiator solution,

are fed at a constant rate over a period of several hours into a jacketed reactor initially charged with solvent. The mixture at the end of the batch typically contains ~70 wt% of low molecular weight (MW) copolymer (number average MW < 5000 g/mol) in solution. Instantaneous conversion in the reactor is high at all times, with temperature control achieved through operation at the reflux temperature of the solvent. Good reactor control is required to ensure that the copolymer composition and distribution of reactive functional groups is uniform among the copolymer chains produced over the course of the batch. This uniformity is required, as the functional groups on the low molecular weight (MW) chains react on the surface of the vehicle, crosslinking to form the final high MW coating. Thus, a good understanding of solvent effect on copolymerization kinetics in semibatch reactions under these higher temperature conditions is required.

Previous studies have successfully described the kinetic complexities of polymerization of acrylates, methacrylates and styrene at high temperatures, including variable initiator efficiency,[2-4] penultimate propagation and termination for multimonomer systems,[2,3,5] depropagation of methacrylates,[1,2,5-7] acrylate backbiting and slow propagation or scission of the resulting midchain radical,[8-10] and reaction of the macromonomers formed by scission.[10] Consideration of all of these effects are necessary to provide a good representation of terpolymerization, as shown in a study of styrene (ST), butyl methacrylate (BMA), and butyl acrylate (BA) over a broad range of polymer compositions.[11]

Most of these detailed studies were carried out using alkyl (meth)acrylates, whereas functional ester groups provided by monomers such as glycidyl methacrylate (GMA) or

2-hydroxyethyl methacrylate (HEMA) are required for crosslinking. While acrylic monomers follow family-type behavior (all methacrylate monomers depropagate, all acrylate monomers backbite), there are some differences in reactivity that can influence their polymerization behavior. Kinetic studies utilizing the pulsed-laser polymerization (PLP) technique combined with size exclusion chromatography (SEC) measurement of the resulting polymer molecular weight distribution (MWD) and NMR determination of copolymer composition yield simultaneous information about copolymerization reactivity ratios as well as overall propagation rate.[4] It was found that GMA and HEMA produce methacrylate-enriched copolymer in styrene-rich bulk monomer mixtures relative to alkyl methacrylates such as BMA.[12] More recently, PLP-SEC-NMR studies revealed that the reactivity of the hydroxyl functional monomer (HEMA or HEA) is also significantly influenced by intermolecular hydrogen bonding between monomer units or between monomer and solvent, affecting copolymer composition and propagation rate[13] and even the acrylate backbiting mechanism,[14,15] as discussed later in this thesis.

Thus, it is necessary to explore how choice of solvent affects the starved-feed semibatch process used to produce acrylic copolymers for automotive coatings. This work will compare the high temperature semibatch free radical copolymerization of ST and HEMA in xylene (a nonpolar solvent) and dimethyl formamide (DMF, a polar solvent which disrupts HEMA hydrogen bonding[13]) to copolymerization of butyl methacrylate (BMA) and ST at identical conditions. In particular, the effect of solvent choice on polymer MW will be examined. It will

also be shown that the presence of ethylene glycol dimethacrylate (EGDMA), an impurity arising from esterification between HEMA and ethylene glycol during monomer preparation,[16] has a significant impact on polymer MW. Due to the difficulty in separating EGDMA from HEMA[16] no purification is undertaken in industry; in this work we have chosen to mimic this industrial practice.

4.2 Experimental

HEMA (97% purity containing 200-220 ppm monomethyl ether hydroquinone, and ethylene glycol dimethacrylate (EGDMA) as impurity arising from esterification between methacrylic acid or HEMA and ethylene glycol[16]), and styrene (99% purity inhibited with 10-15 ppm of 4-*tert*-butylcatechol) were purchased from Sigma Aldrich and used as received. Dibenzoyl peroxide (BPO), and *tert*-butyl peroxyacetate (TBPA), serving as initiator at 110 and 138 °C respectively, were obtained from Arkema. A xylene isomeric mixture with boiling point range between 136 and 140 ºC and DMF (99.8% purity) was obtained from Sigma-Aldrich and used as received. Semibatch reactions were performed in a 1 L LabMax reactor system with an agitator and reflux condenser, and with initiator and monomer feed rates and reaction temperature automatically controlled. The reactor was charged with 215 g solvent and brought up to the reaction temperature of 110 or 138 °C. Monomer mixtures and initiator solution were continuously fed at a fixed rate over 6 hours with initiator fed for an extra 15 minutes; the total initiator charge was 1.5 mol% of the monomer charge. Samples of approximately 2 mL were drawn from the

reactor at specified times into ice-cold 4-methoxyphenol (1 g/L) solution to terminate the reaction.

The residual monomer concentration in the samples was determined using a Varian CP-3800 gas chromatograph (GC) setup, as detailed before.[5] Calibration standards were constructed by mixing measured quantities of styrene and HEMA (or BMA) monomers into a known mass of acetone, and a linear calibration curve was constructed by plotting peak area versus monomer concentration. Size-exclusion chromatography (SEC) analyses of the polymer samples were performed using a Waters 2960 separation module with a Waters 410 differential refractometer (RI detector) and a Wyatt Technology Light Scattering detector (LS detector). Calibration for the RI detector was established using 8 linear narrow PDI polystyrene standards over a large range of molecular weight, from 890 to 3.55×10^5 g/mol, and the MW of the copolymers and poly(HEMA) (or poly(BMA)) are obtained by universal calibration using known Mark-Houwink parameters.[13] The output signal of LS detector provides the absolute molar mass without the need for calibration standards but with knowledge of the dn/dc value ($(dn/dc)_{ST} = 0.180$, $(dn/dc)_{HEMA} = 0.0556$, $(dn/dc)_{BMA} = 0.080$ [13]). In all cases MW averages from the two detectors were within 15% of each other; averages calculated from the RI detector are reported, due to better reproducibility.

4.3 Results and Discussion

4.3.1 ST/HEMA vs. ST/BMA at 110 °C

ST/BMA and ST/HEMA semibatch experiments were first conducted at 110 °C in DMF and

xylene, to examine the influence of solvent choice on polymerization rate and polymer molecular weights in the starved feed process used to produce acrylic resin for coatings. All experiments had a fixed polymer/monomer content of 65 wt% in solution at the end of the batch, with monomer and BPO initiator added at a constant rate over 6 hours. The fraction of ST in the comonomer mixture was kept constant at 75 wt%, to prevent solubility issues during the production of high conversion ST/HEMA copolymers. Figures 4.1 and 4.2 show the monomer concentration and copolymer molecular weight profiles for ST/BMA and ST/HEMA reactions at 110 °C, respectively. The general shapes of the curves are similar to those measured for ST/BMA[5] and ST/dodecyl methacrylate[2] at 138 °C. From Figure 4.1, it is obvious that solvent choice has no effect on the copolymerization rate (monomer concentration profiles) of ST/BMA, and also does not influence polymer MW. This result is in agreement with previous kinetic experiments, which found that solvent polarity had no influence on ST/BMA copolymer composition or the copolymer-averaged propagation kinetic coefficient ($k_{p,cop}$).[13]

However, significant variation in the level of HEMA free monomer and copolymer molecular weight with solvent choice can be seen for the ST/HEMA system (Figure 4.2). The finding that HEMA concentrations in DMF are always higher than those in xylene is consistent with kinetic studies; under pseudo steady-state semibatch operating conditions monomer concentrations should be inversely proportional to propagation rate, and $k_{p,cop}$ values for ST/HEMA in DMF have been found to be lower than those in toluene (a solvent very similar to xylene).[13] However, it is surprising to find that the weight-average MWs of copolymer

synthesized in xylene are almost double those produced in DMF, with the absolute value reaching as high as 40 kg/mol. This finding suggests that, just as DMF disrupts H-bonding between HEMA molecules, it also disrupts branching reactions (perhaps involving EGDMA impurity) that occur in the absence of DMF.

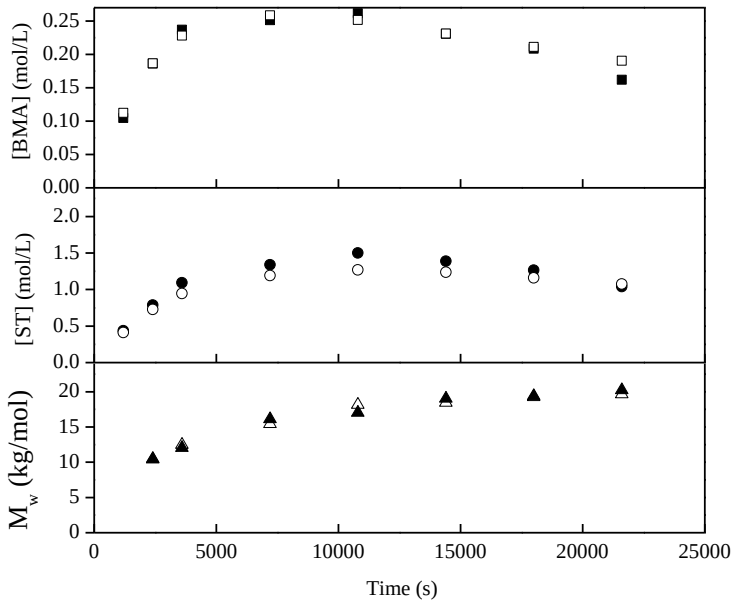

Figure 4.1 Monomer concentration ([BMA] and [ST]) and polymer MW experimental profiles for ST/BMA semibatch copolymerizations at 110 °C with ST/BMA mass ratio of 75/25. Specified monomer mass ratio in the feed is with 65 wt% final polymer content and 1.5 mol% initiator relative to monomer. The solid symbols are from polymerization in DMF, while the open symbols are from polymerization in xylene.

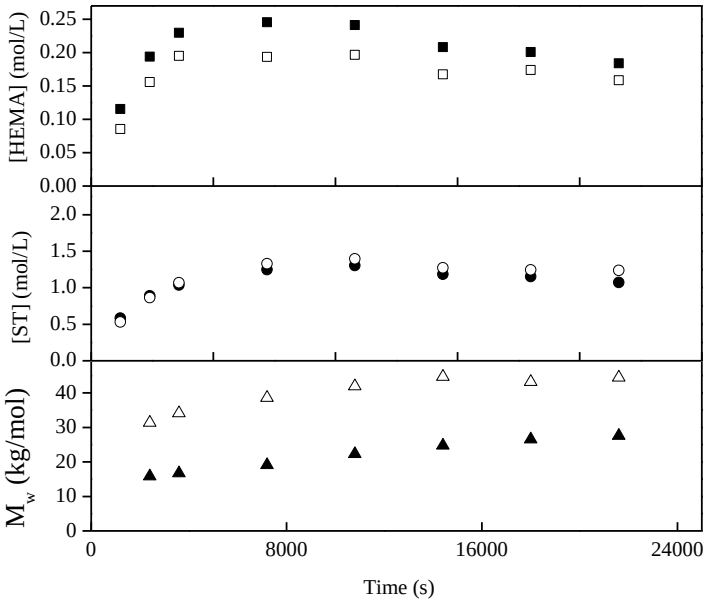

Figure 4.2 Monomer concentration ([HEMA] and [ST]) and polymer MW experimental profiles for ST/HEMA semi-batch copolymerizations at 110 °C with ST/HEMA mass ratio of 75/25. Specified monomer mass ratio in the feed is with 65 wt% final polymer content and 1.5 mol% initiator relative to monomer. The solid symbols are from polymerization in DMF, while the open symbols are from polymerization in xylene.

Comonomer composition (f_{BMA} or f_{HEMA}, in mole fraction) and cumulative copolymer composition (F_{BMA} or F_{HEMA}) for this set of semibatch reactions are compared in Figure 4.3; the comonomer composition is calculated directly from GC measurement of monomer concentrations, while the copolymer composition is estimated from monomer material balances. Similar trends are seen in both systems: copolymer composition is controlled by monomer feed ratio in both solvents (an essential feature of starved-feed systems), with the pseudo steady-state value reached after the first hour of operation. Using the reactivity ratios measured at 90 °C from the PLP/NMR study, we can estimate the theoretical monomer composition that corresponds to this copolymer

composition, as indicated in the Mayo-Lewis plot shown as Figure 4.4. These values are indicated by dashed horizontal lines in Figure 4.3, and can be compared to the experimentally determined comonomer composition. For ST/BMA, solvent choice has negligible effect on the pseudo steady-state value of f_{BMA}, which agrees with the expected value very well. For ST/HEMA, however, there are offsets between the expected values (as determined from the Mayo-Lewis curves shown in Figure 4.4) and the experimentally measured values. While f_{HEMA} in DMF is higher than the value in xylene, as expected, both sets of experimental values are significantly higher than the expected values from the PLP/SEC/NMR data taken from Ch 3. As the PLP study was conducted at 90 °C, this result may indicate that temperature has a significant influence on the solvent effect on copolymer composition for ST/HEMA. In order to explore this possibility, another set of PLP/NMR experiments were conducted with ST/HEMA at 110 °C in toluene and DMF, with the results shown in Figure 4.5. It is seen that the copolymer composition in toluene at 110 °C moves downward towards the curve for ST/HEMA in bulk, while that in DMF at 110 °C moves downward towards the curve for ST/BMA. Thus, temperature is found to have a significant effect on the influence of solvent on the ST/HEMA reactivity ratios that control free monomer levels during semibatch operation.

As explained in our previous work (Ch 3),[13] it is the competition of HEMA-HEMA *vs.* HEMA-solvent H-bonding that affects relative monomer reactivity and thus copolymer composition. The data in Figure 4.5 indicates that temperature affects this competition, with H-bonding between HEMA molecules suppressed when temperature increases from 90 °C to

110 °C. Thus, the polarity effect of toluene is reduced, leading to behavior similar to ST/HEMA in bulk. Meanwhile, DMF can more easily disrupt HEMA H-bonding at 110 °C, leading to HEMA polymerization behavior that approaches that of BMA. It should also be noted that with starved feed operation, overall monomer concentrations are lower (and polymer concentrations higher) than the levels used in the kinetic experiments, a difference that may also affect the extent of H-bonding.

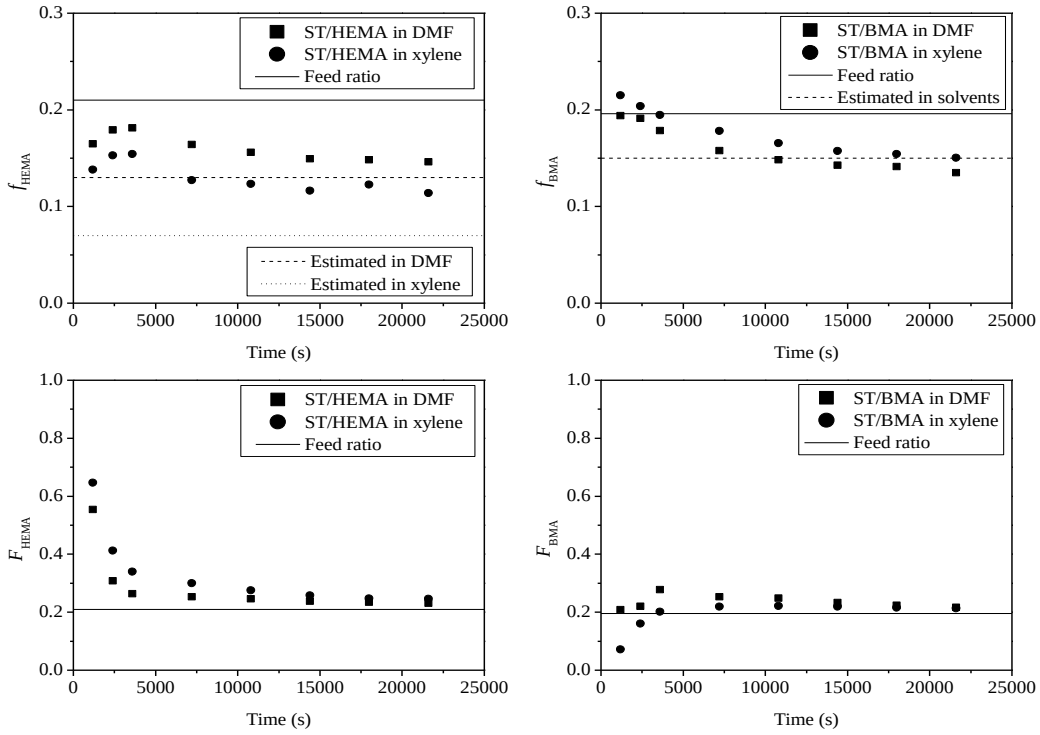

Figure 4.3 Monomer composition (top two plots, f_{HEMA} and f_{BMA}) and cumulative copolymer composition (bottom two plots, F_{HEMA} and F_{BMA}) in the semibatch reactions, as determined from GC measurement of residual monomer and calculated by mass balance. Solid horizontal lines indicate the monomer feed ratio converted to a molar basis; dashed horizontal lines indicate the expected value of *f* based upon copolymer composition.

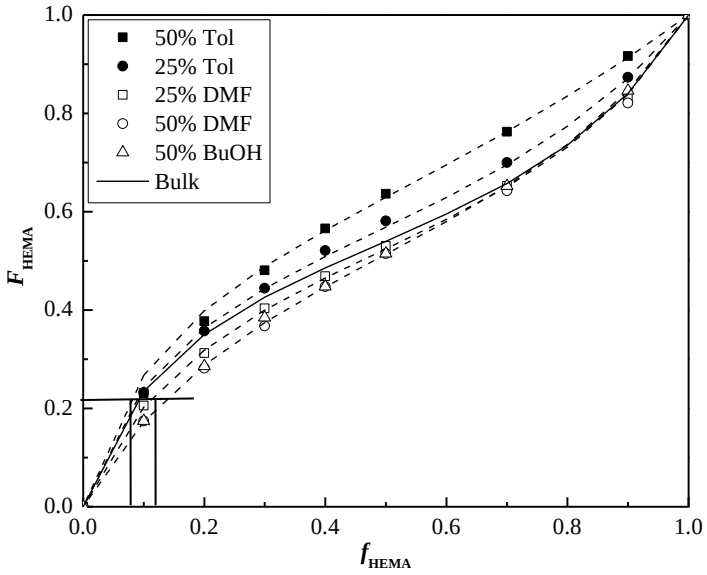

Figure 4.4 HEMA mole fraction (F_{HEMA}) in ST/HEMA copolymer determined as a function of comonomer mole composition (f_{HEMA}) from kinetic experiments conducted in different solvents at 90 °C (adapted from Ref. 13).

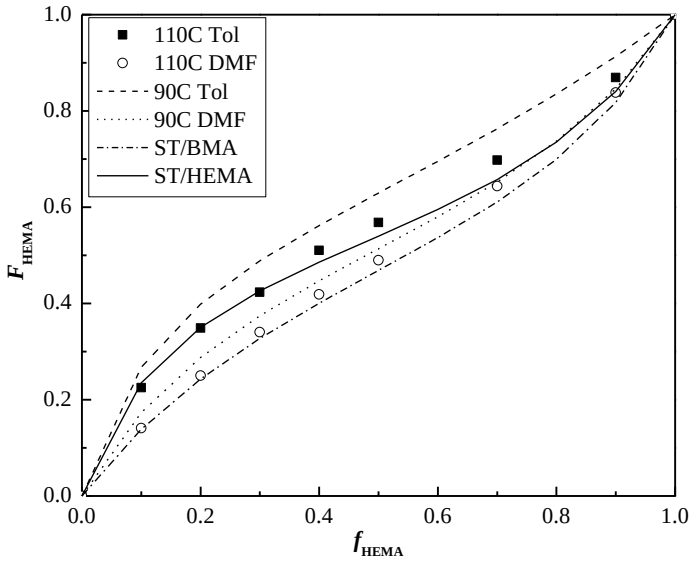

Figure 4.5 Composition of ST/HEMA (or ST/BMA) copolymer as a function of comonomer mole composition from kinetic experiments conducted in 50 vol% solvents at 90 and 110 °C.

4.3.2 ST/BMA and ST/HEMA at 138 °C

In order to further examine the solvent effect, ST/BMA and ST/HEMA semibatch experiments were run at 138 °C in DMF and xylene, with TBPA as initiator. The first set of experiments had a fixed ST level of 75 wt% relative to total monomer (as at 110 °C), with final solvent level at either 35 or 65 wt%. Other conditions remain the same as at 110 °C. Figure 4.6 compares the influence of solvent content and type (DMF or xylene) on ST/HEMA and ST/BMA semibatch polymerizations. For ST/BMA, lower solvent content leads to higher free monomer concentrations and polymer MWs, in agreement with previous semibatch studies;[1-4] however, as observed at 110 °C, solvent type has no effect.

With ST/HEMA the general trends observed for ST/BMA (lower solvent content leads to higher free monomer concentrations and MWs) are also seen. In addition, the general influence of solvent type is the same as at 110 °C, with one notable difference: copolymer MW at 138 °C is higher in DMF than in xylene. The absolute weight-average MW values in 35% xylene at the two temperatures are very similar (40 kg/mol), suggesting that H-bonding for this system does not change significantly. On the other hand, the weight-average MW value in DMF at 138 °C is close to 60 kg/mol, much higher than the 25 kg/mol measured at 110 °C. This important difference has been verified by repeat experimentation as shown in Appendix A.2. We hypothesize H-bonding between DMF and HEMA is suppressed at higher temperature, leading to increased crosslinking. However, the support for this hypothesis must be collected both experimentally and theoretically.

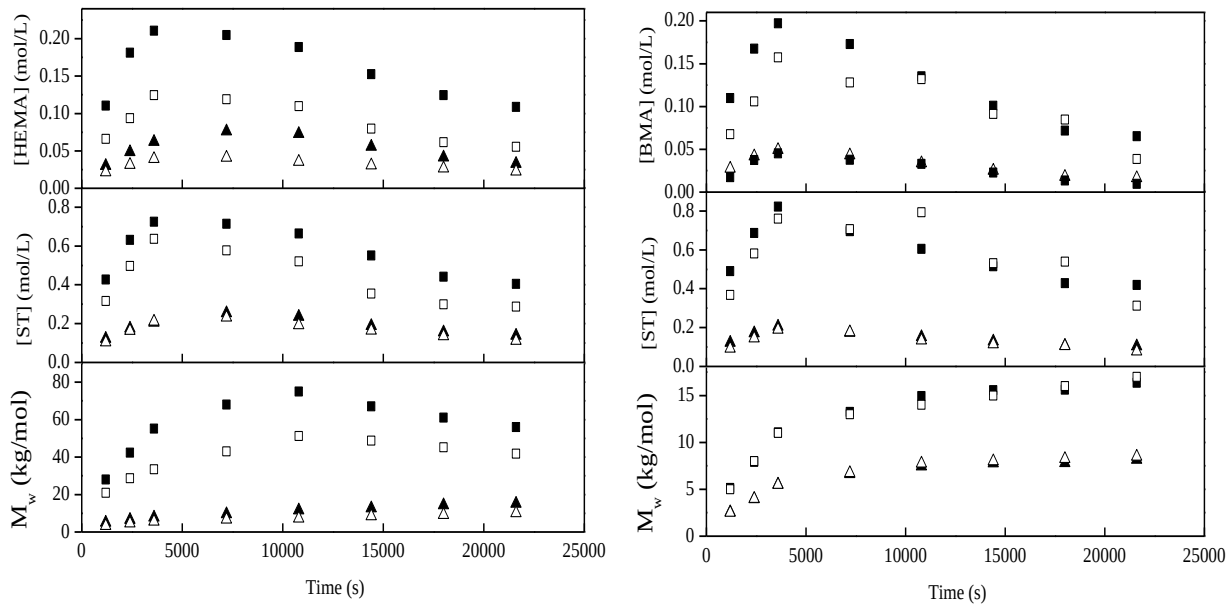

Figure 4.6 A comparison of the influence of solvent content on monomer concentration and polymer MW experimental profiles for ST/HEMA (left) and ST/BMA (right) semibatch polymerizations at 138 °C to produce copolymer containing 75 wt% ST. Solid symbols indicate reactions in DMF with 35 wt% (■) and 65 wt% (▲) solvent. Open symbols indicate reactions in xylene with 35 wt% (□) and 65 wt% (△) solvent.

Also of interest for the ST/HEMA copolymerization results in Figure 4.6 is the very large difference in MW values seen with 65 wt% solvent compared to 35 wt%. Not only is the solvent difference much less pronounced at lower polymer content (65 wt% solvent), but the absolute values (8-10 kg/mol) are similar to those observed for the ST/BMA system. Thus, there is a synergetic effect of polymer content with the solvent choice on polymer MWs. To further explore the relationship between HEMA level and polymer MW, semibatch experiments with a lower fraction of HEMA comonomer (12.5 instead of 25 wt%) were also run at 138 °C in both DMF and xylene, with 35 wt% solvent. As shown in Figure 4.7, while the reaction (free monomer)

profiles with 12.5 wt% HEMA show the same trends as those with 25 wt% HEMA, polymer weight-average MWs are much smaller with the lower HEMA level. In addition, the relative MW difference between reaction in DMF and xylene becomes negligible when switching from 25 wt% to 12.5 wt% HEMA, indicating that the importance of branching is dependent on HEMA concentration.

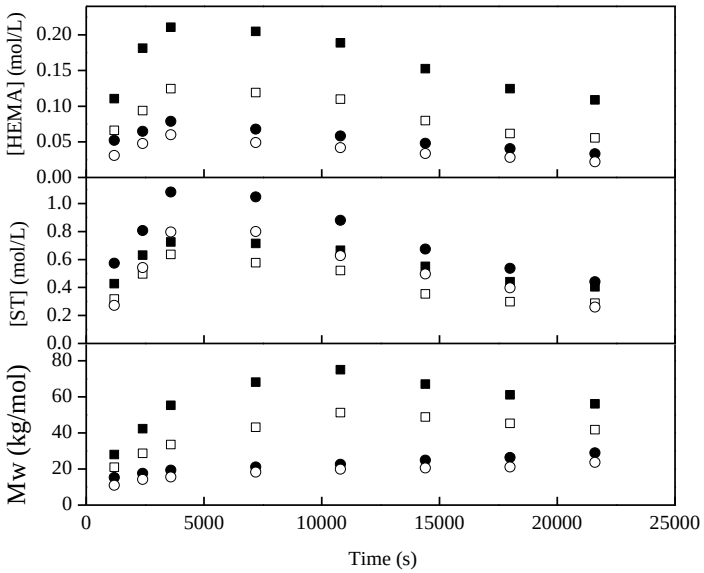

Figure 4.7 Monomer concentration ([HEMA] and [ST]) and polymer weight-average MWs for ST/HEMA semibatch copolymerizations at 138 °C with 65wt% final polymer content and 1.5 mol% initiator relative to monomer. Solid symbols indicate reactions in DMF with 25 wt% (■) and 12.5 wt% (●) HEMA in the monomer mixture. Open symbols indicate reactions in xylene with 25 wt% (□) and 12.5 wt% (○) HEMA in the monomer mixture.

4.3.3 BMA Homopolymerization at 138 °C

The experiments described above demonstrate the combined influence of higher HEMA fraction and total polymer content on the formation of high polymer weight-average MWs (>40 kg/mol).

The proportional increase of MWs with HEMA monomer level suggests that this long-chain branching is associated with the HEMA monomer. A possible branching agent in those systems is ethylene glycol dimethacrylate (EGDMA), which is present in ppm levels in commercial HEMA monomers as an impurity formed during HEMA synthesis. In order to verify the effect of EGDMA in polymerization, the homopolymerization of BMA with 100 ppm EGDMA has been carried out at 138 °C with 35 wt% xylene. The polymer weight-average MW is compared in Figure 4.8 to that formed in BMA homopolymerization without EGDMA under the same conditions, with the MW values more than doubled due to the introduction of EGDMA. As well as the increased average MW values, the polymer MWD formed with added EGDMA has a significant tail at higher MWs, another indicator of long chain branching. This result demonstrates the important effect of EGDMA impurity on polymer MWs under starved-feed operation.

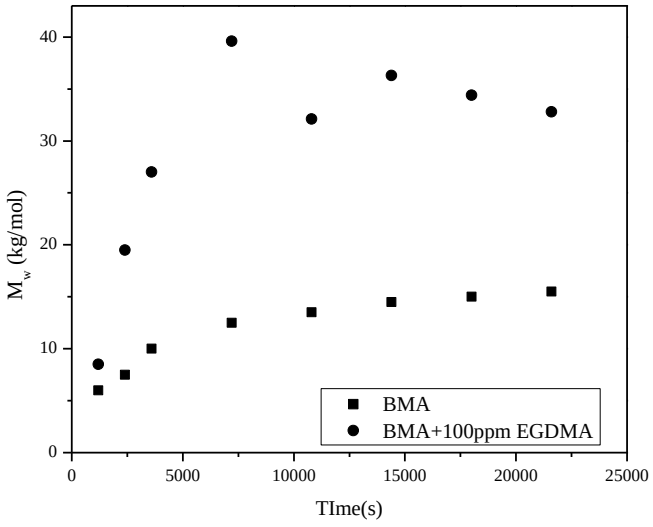

Figure 4.8 Homopolymerization of BMA with or without EGDMA at 138 °C with 35 wt% xylene.

4.4 Conclusion

High temperature semibatch ST/HEMA free radical copolymerization was investigated in DMF and xylene solution at 110 and 138 °C. Copolymer MWs formed by ST/HEMA semibatch polymerization increase with: (1) increasing reaction temperature in DMF solvent, despite the opposite trend observed for ST/BMA; (2) increasing polymer content, also observed for ST/BMA but not to the same extent; (3) increasing HEMA fraction in the copolymer; (4) DMF solvent instead of xylene, especially in combination with higher HEMA levels and lower solvent fractions.

The effect of solvent choice on ST/HEMA copolymerization is very distinctive compared to the ST/BMA system under similar starved-feed operating conditions. The coupled variation of monomer composition in the reactor with temperature and solvent is in good agreement with low-conversion kinetic studies of copolymer vs. comonomer composition, and is attributed to competitive hydrogen bonding of HEMA with itself and with solvent. The surprising increase in ST/HEMA copolymer MW values (compared to ST/BMA) is caused by branching reactions involving dimethacrylate impurity found in HEMA commercial monomers, with the extent of branching also influenced by the combination of solvent choice and temperature. In the following chapter, we will perform BMA/HEMA semibatch copolymerizations to examine the direct effect of changing methacrylate type on polymer MW.

References

1. Grady, M. C.; Simonsick, W. J.; Hutchinson, R. A. *Macromol. Symp*. **2002**, *182*, 149.

2. Wang, W.; Hutchinson, R. A. *Macromol. Symp.* **2008**, *261*, 64.

3. Wang, W.; Hutchinson, R. A. *Macromol. React. Eng.* **2008**, *2*, 199.

4. Wang, W.; Hutchinson, R. A. *Macromolecules* **2009**, *42*, 4910.

5. Li, D.; Hutchinson, R. A. *Macromol. Symp.* **2006**, *243*, 24.

6. Li, D.; Grady, M. C.; Hutchinson, R. A. *Ind. Eng. Chem. Res.* **2005**, *44*, 2506.

7. Wang, W. ; Hutchinson, R. A.; Grady, M. C. *Ind. Eng. Chem. Res.* **2009**, *48*, 4810.

8. Peck, A. N. F.; Hutchinson, R. A. *Macromolecules* **2004**, *37*, 5944.

9. Wang, W.; Hutchinson, R. A. *Macromol. Symp.* **2010**, *289*, 33.

10. Wang, W.; Hutchinson, R. A. *Macromol. Rapid Commun.* **2009,** *30*, 2022.

11. Wang, W.; Hutchinson, R. A. *AIChE J.* **2011,** *57*, 227.

12. Liang, K.; Dossi, M.; Moscatelli, M.; Hutchinson, R. A. *Macromolecules* **2009**, *42*, 7763.

13. Liang, K.; Hutchinson, R. A. *Macromolecules* **2010**, *43*, 6311.

14. Liang, K.; Hutchinson, R. A. *Macromol. Rapid Commun.* **2011**, *32*, 1090.

15. Liang, K.; Hutchinson, R. A.; Barth, J.; Samrock, S.; Buback, M. *Macromolecules* **2011**, *44*, 5843.

16. Montheard, J.-P.; Chatzopoulos, M.; Chappard, D. *J. Macromol. Sci., Part C: Poly. Rev.* **1992**. *32*, 1.

Chapter 5 Solvent Effect on BMA/HEMA Copolymerization

Preface

The previous two chapters describe the kinetic behavior of ST/methacrylate copolymerization, and the effect of H-bonding on polymerization kinetics. As the primary solvent effect is attributed to H-bonding involving the methacrylate ester group, it is of interest to study the effects of both a H-bonding solvent (*n*-butanol) and a polar solvent (DMF) on BMA/HEMA copolymerization. This chapter investigates the kinetic behavior of BMA/HEMA in solution using both PLP-SEC-NMR and semibatch polymerization at higher temperature. As the relevant literature reviews and experimental techniques have already been presented in the previous chapters, the experimental results will be discussed directly.

Results and Discussion

5.1 Kinetic Studis on BMA/HEMA Copolymerization

As discussed in Ch 3, HEMA monomers form intermolecular H-bonding which can be disrupted by DMF. Also, BMA interacts with *n*-butanol, increasing the reactivity of the BMA double bond to radical addition. Thus, in this section, PLP studies of BMA/HEMA copolymerization are carried out in BuOH and DMF at 90 and 100 °C, and the combined solvent effect on copolymer

composition and propagation rate coefficient will be examined. The detailed PLP-SEC-NMR results are listed in Appendix A.3.

As indicated in Figure 5.1a, the plot of BMA/HEMA copolymer composition, HEMA-rich copolymer is formed in bulk, due to the increased reactivity of HEMA monomer to radical addition. The monomer reactvitity ratios in bulk are estimated as r_{BMA}=0.35±0.28 and r_{HEMA}=1.49±0.67. As expected, the introduction of DMF decreases the HEMA reactivity to that of BMA, such that the copolymer composition lies close to the diagonal, with no preferential HEMA incorporation ($r_{HEMA} \cong r_{BMA} \cong 1$). Use of BuOH as a solvent, on the other hand, increases the BMA reactivity towards that of HEMA, again forcing the copolymer composition data towards the diagonal line ($r_{HEMA} \cong r_{BMA} \cong 1$).

The corresponding $k_{p,cop}$ data are presented in Figure 5.1b. DMF is seen to decrease the propagation rate coefficient significantly with $k_{p,cop}$ staying relatively constant close to the BMA bulk value with changing composition. As discussed previously, DMF reduces $k_{p,HEMA}$ by disrupting intermolecular H-bonding, such that HEMA reactivity becomes similar to that of BMA. The data plotted in Figure 5.1b, with $k_{p,cop} \approx k_{p,BMA}$, are consistent with this explanation. Meanwile, BuOH increases the propagation rate coefficient of BMA by roughly 25% (from 2000 to 2500 $L \cdot mol^{-1} \cdot s^{-1}$), in agreement with results from Ch 3 (Figure 3.11). As BuOH has no effect on the HEMA propagation rate coefficient, the $k_{p,cop}$ values quickly converge to the values measured for the bulk system. These results can also be well-explained by H-bonding effects as presented in

Ch 3. The bulk $k_{p,cop}$ data, collected at both 90 and 100 °C, are well-represented by the curves generated using the terminal model. As the terminal model fits both copolymer composition and $k_{p,cop}$ data well for the bulk BMA/HEMA system, it can be inferred that the radical reactivity in methacrylate/methacrylate copolymerization is only dependent on the type of terminal unit, with negligible influence from the identity of the methacrylate unit in the penultimate position.

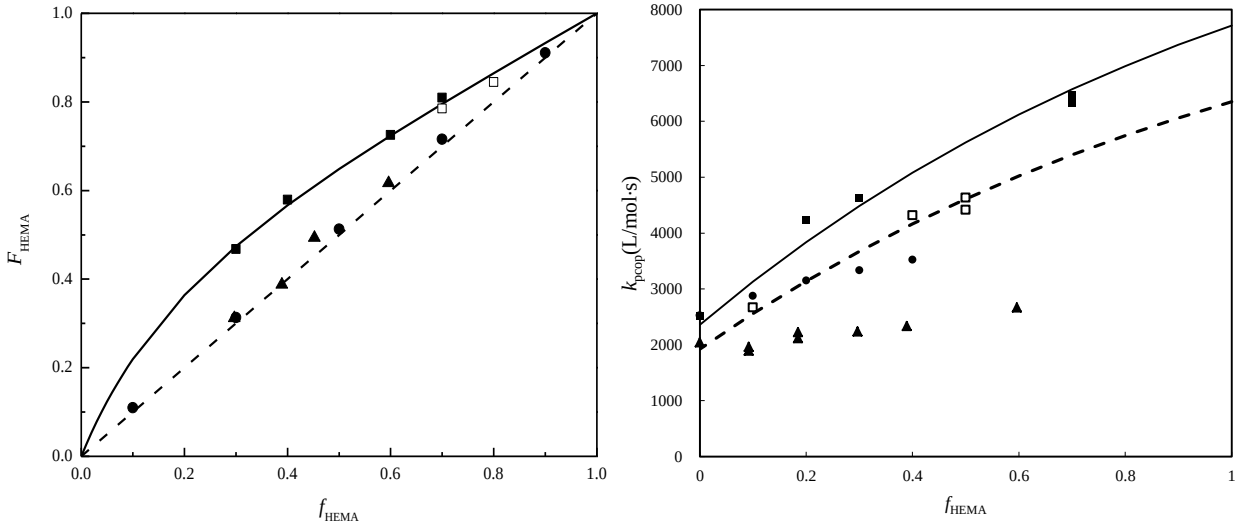

(a) (b)

Figure 5.1 PLP/SEC/NMR results for BMA/HEMA copolymerization in different solvents at 90 and 100 °C. (■, 100 °C in bulk; □, 90 °C in bulk; ●, 90 °C in BuOH; ▲, 90 °C in DMF) (a) Mole fraction of HEMA in copolymer (F_{HEMA}) as a function of HEMA mole fraction in the monomer phase (f_{HEMA}). The solid curve is the prediction of the terminal copolymerization model in bulk while the dashed curve represents the diagonal line. (b) Copolymer propagation rate coefficients ($k_{p,cop}$) data vs 2-hydroxyethyl methacrylate (HEMA) monomer mole fraction. Terminal model predictions at 100 °C and 90 °C are indicated by the solid line and dashed line, respectively.

5.2 BMA/HEMA Semibatch Copolymerization

Semibatch experiments of BMA/HEMA with 25 wt% HEMA were carried out in 35 wt% xylene or DMF at 138 °C. It is seen from the free monomer and MW profiles in Figure 5.2 that the reaction conducted in DMF leads to significant higher free monomer concentrations and polymer MWs than values measured in xylene. As decreasing the HEMA fraction in the feed was found to significantly affect MWs for ST/HEMA copolymerizations (Ch 4), semibatch experiments with 12.5 wt% HEMA were also run. As shown in Figure 5.2, the free HEMA concentration for this mixture is reduced relative to the 25% HEMA recipe, but is still significantly higher in DMF compared to xylene. MWs are also affected by HEMA ratios in the same fashion as observed in the ST/HEMA system (Ch 4): increasing HEMA fraction in BMA/HEMA copolymer leads to an increase in M_w values, with the increase greater in DMF than in xylene.

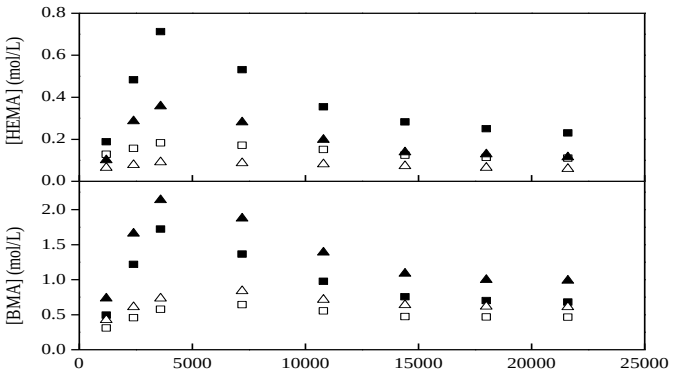

Figure 5.2 Monomer concentration ([HEMA] and [BMA]) for BMA/HEMA semibatch copolymerizations at 138 °C with BMA/HEMA mass ratio of 75/25 (■,□) and 87.5/12.5 (▲,△). Specified monomer mass ratio in the feed is with 65 wt% final polymer content and 1.5 mol% initiator relative to monomer. Solid symbols indicate reactions in DMF, and empty symbols indicate reactions in xylene.

In order to analyze these results further, Figure 5.3 compares total monomer concentrations, HEMA monomer fractions and polymer MWs for BMA homopolymerization and BMA/HEMA copolymerization with different HEMA feed ratios. Free monomer levels measured in BMA homopolymerization in xylene are similar to those measured for BMA/HEMA copolymerization in the same solvent. However, the total monomer concentrations in DMF are always higher than those in xylene, which is in agreement with the results in Figure 5.1b showing that $k_{p,cop}$ values in DMF are much lower than those in xylene. On the other hand, HEMA monomer fractions in DMF are also higher than those in xylene, which can also be connected to the kinetic studies in Figure 5.1a that indicate that a higher HEMA monomer ratio in DMF is required compared to that in xylene to achieve the same level of HEMA incorporation in the copolymer. Note that the copolymer composition produced by the semibatch process always match the monomer feed ratios (represented by the solid and dash lines), due to the starved-feed policy. Thus, the findings from the kinetic studies in Figure 5.1 can be applied to explain the effect of solvent on semibatch BMA/HEMA copolymerization.

The MW profiles in Figure 5.3 present the highest M_w with 25 % HEMA feed ratio in DMF, which is very similar to ST/HEMA copolymerization under the same condition in Ch 4. It suggests the same mechanism leads to high M_w (up to 80 kg/mol) in BMA/HEMA and ST/HEMA systems. Also included in the MW plot are results for BMA homopolymer produced under identical semibatch conditions; the values are much lower and similar to M_w values obtained with 12.5 wt% HEMA in the mixture. Table 5.1 summarizes the M_w results of the final

sample from ST/BMA, ST/HEMA and BMA/HEMA copolymerizations at 138 °C. It can be found that the addition of HEMA leads to higher polymer MWs and the MW difference in different solvents lessens as the HEMA content is lowered.

Table 5.1 M_w results for semibatch copolymerization of ST/BMA, ST/HEMA and BMA/HEMA at 138 °C with 65 wt% polymer.

M_w values (kg/mol)	ST/BMA	ST/HEMA		BMA/HEMA	
in xylene		12.5%HEMA	25%HEMA	12.5%HEMA	25%HEMA
in DMF	16.8	23.5	41.7	15.2	25.5
	16.3	28.9	55.6	18.0	35.9

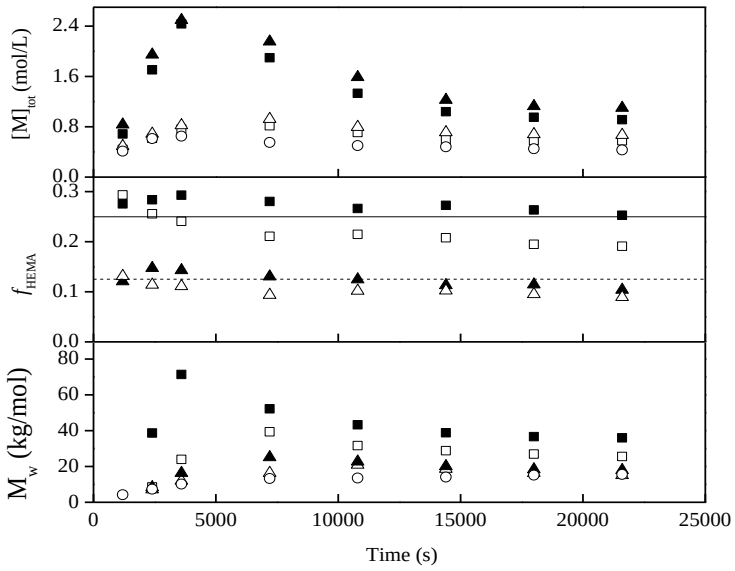

Figure 5.3 Total monomer concentration, HEMA monomer ratio and polymer molecular weight experimental profiles for BMA/HEMA semibatch copolymerizations at 138 °C with BMA/HEMA mass ratio of 75/25 (■,□), 87.5/12.5 (▲,△) and 100/0 (○). Specified monomer mass ratio in the feed is with 65 wt% final polymer content and 1.5 mol% initiator relative to monomer. Solid symbols indicate reactions in DMF, and empty symbols indicate reactions in xylene. Lines represent HEMA feed ratio for 25 % (solid) and 12.5 % (dash).

Ch 4 discusses some potential causes of the shift in MW with HEMA content and solvent choice. However, the detailed mechanism for ST/HEMA semibatch reactions was not clear, as the reactions at 110 °C and 138 °C had reversed results: at 110 °C the MW values of ST/HEMA copolymer formed in xylene were higher than those produced in DMF, while polymers produced in DMF had higher MWs at 138 °C. To further explore the combined effect of temperature and solvent on polymer MWs, semibatch homopolymerizations of BMA with 100 ppm added EGDMA were carried out in xylene and DMF at 110 and 138 °C. At 110 °C (Figure 5.4a), the MWs of polymer produced in both solvents are the same while Figure 5.4b indicates significantly higher polymer MWs produced in DMF than in xylene at 138 °C. This result suggests that DMF enhances the branching reaction caused by EGDMA at higher temperatures. Combined with previous conclusions from ST/HEMA and BMA/HEMA copolymerization, the influence of solvent on copolymer MWs can be summarized as follows: DMF disrupts HEMA intermolecular H-bonding, but at higher temperatures (138 °C), DMF enhances the branching reaction involving EGDMA and increases copolymer MWs.

The interactions between branching reactions and solvent choice are not obvious. Matsumoto et al.[1] have proposed that H-bonding involving monomer units incorporated into the polymer is significant and may lead to increased polymer MW through gelation. In order to examine if H-bonding involving polymers may play a role in our system, ST/HEMA and BMA/HEMA copolymers produced by semibatch reactions were tested by FT-IR in solvents, with the results shown in Figure 5.5. All the tests are made at room temperature with copolymer produced in

semibatch reaction redissolved in solvents, with 50 wt% polymer in the mixture. As discussed in the presentation of the FT-IR analysis method in Ch 3, the focus is put on the effect of H-bonding on the carbonyl group of methacrylates, whose signal is around 1708 cm^{-1}. However, the H-bonding signal does not show up in either ST/HEMA or BMA/HEMA copolymers for either solvent. While this examination is conducted in the absence of monomer, it shows that there is no significant solvent/polymer interaction involving the incorporated HEMA units. However, the influence of solvent on incorporated EGDMA units, present in ppm levels, cannot be directly studied.

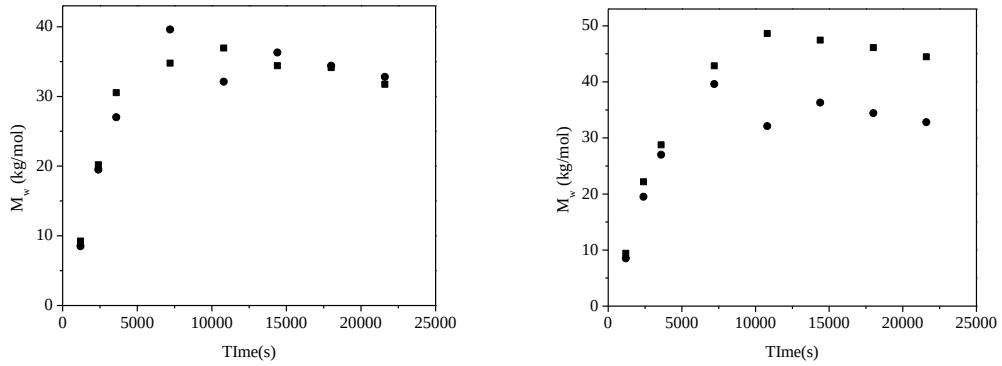

(a) (b)

Figure 5.4 BMA homopolymerization with 100ppm EGDMA in xylene (●) and DMF (■) at (a) 110 °C and (b) 138 °C.

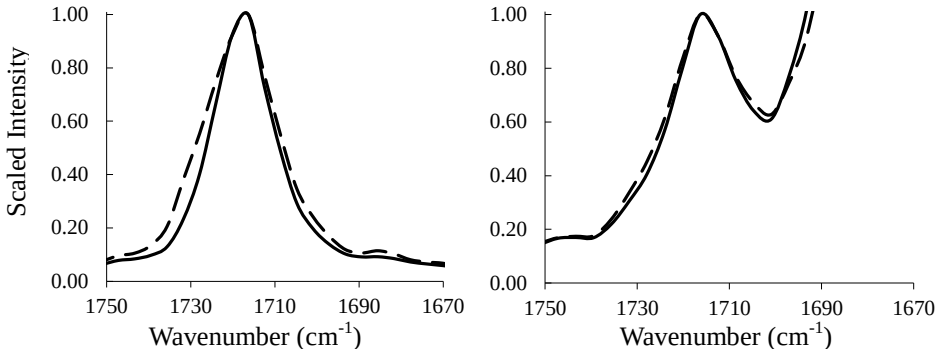

Figure 5.5 FT-IR spectra for ST/HEMA (solid) and BMA/HEMA (dashed) 75/25 copolymers in xylene (a) and DMF (b).

Conclusions

Solvent effects on BMA/HEMA copolymerization have been studied using both the PLP technique as well as by conducting semibatch experiments. In the kinetic study, it was found that HEMA preferentially incorporates into copolymers in bulk due to the effect of intermolecular H-bonding on HEMA monomer reactivity, with the $k_{p,cop}$ values well fit by terminal model. BuOH and DMF influence H-bonding such that BMA and HEMA demonstrate similar reactivity in both solvents; $k_{p,cop}$ values in DMF are reduced closer to $k_{p,BMA}$ value while those in BuOH are increased closer to $k_{p,HEMA}$. These results are used to explain the concentration and composition of free monomer level measured during BMA/HEMA copolymerization.

High MWs caused by EGDMA are still observed, with DMF found to enhance the branching reaction at 138 °C but not at 110 °C. The BMA/HEMA semibatch reaction profiles generally follow the trends observed with ST/HEMA copolymerization under the same

conditions, with H-bonding effects influencing copolymer MWs at lower temperature while solvent polarity increasing the extent of branching at higher temperature.

References

1. Matsumoto, A.; Ueda, A.; Aota, H.; Ikeda, J. *Euro. Polym. J.* **2002**, *38*, 177

Chapter 6 H-bonding Effects on Acrylate (Co)polymerization Kinetics

Preface

Free radical polymerization kinetics of acrylates, including short chain branching or backbiting, has been discussed in Ch 2. Due to the disruption between chain-length and radical lifetime caused by short chain branching, it is difficult to utilize the PLP technique to study acrylate propagation behavior above 20 °C. This chapter will show the successful application of PLP to the homopolymerization of 2-hydroxyethyl acrylate (HEA) between 20 and 60 °C using pulse repetition rates of 50 and 100 Hz, an indication that HEA is not subjected to the intramolecular chain transfer to polymer (backbiting) reactions dominant for other acrylates, and will examine how the extent of backbiting can be influenced by solvent choice. The copolymerization of ST/HEA is also investigated by PLP-SEC, and compared to the previous ST/HEMA results. Monomer reactivity ratios and propagation rate coefficients are estimated at 50 °C, with Arrhenius parameters for bulk HEA chain-end homopropagation deducted based on experiments conducted between 20 and 60 °C. This chapter combines three published works in Macromolecular Chemistry and Physics (2012, Vol. 213, 1706), Macromolecular Rapid Communication (2011, Vol. 32, 1090) and Macromolecules (2011, Vol. 44, 5843) that demonstrate the importance of H-bonding effects on short chain branching of poly(acrylates).

6.1 Introduction

Hydroxyl-functional monomers such as 2-hydroxyethyl methacrylate (HEMA) and 2-hydroxyethyl acrylate (HEA) are important components in acrylic copolymer coatings, serving

as a crosslinking base group.[1] In addition, HEA is also widely used in polymer hydrogels, with applications in biomedical materials such as contact lenses, implanted devices and artificial tissues.[2-7] As pHEA exhibits high biocompatibility and low thrombogenicity, biomedical material research has been focused primarily on the development of pHEA-based hydrogels.[6] Controlled radical polymerization has been used to synthesize homopolymers and block copolymers based on HEA with well-defined structures for drug deliveries.[8-10]

In order to produce these specialty polymer materials with desired composition and molar mass, it is necessary to have a good understanding of the polymerization kinetic behavior. However, there are significant difficulties in obtaining k_p values for acrylates by PLP; rather than producing well-structured distributions, the PLP-generated polyacrylate MMDs are broad and indistinct. For *n*-butyl acrylate (BA), the most widely studied acrylate, it was only possible to measure chain-end k_p values up to a temperature of 20 °C with a pulse-repetition rate of 100 Hz;[11] recently, this temperature range has been extended to 70 °C using a laser repetition rate of 500 Hz.[12] Overwhelming evidence has emerged that the loss of PLP structure is due to the effect of intramolecular chain transfer to polymer (backbiting), as summarized in a 2004 IUPAC benchmark paper for butyl acrylate,[9] and more recently reviewed by van Herk.[13] The propagating chain-end radical abstracts a hydrogen atom from a CH unit on its own backbone, favored through the formation of a six-membered ring, with the resulting mid-chain radical capable of undergoing propagation or termination. As addition to the mid-chain radical is much slower than to the chain-end radical, the relationship between chain length and chain lifetime is disrupted, causing the loss of the typical PLP structure.

The acrylate intramolecular chain-transfer mechanism has a dramatic effect on polymerization rate and apparent reaction-order, as has been documented in numerous studies for

BA (e.g., [14-16]) as well as for methyl acrylate (MA)[17] and *n*-dodecyl acrylate (DA).[18] In addition, the presence of midchain radicals has been directly detected using EPR spectroscopy for BA,[19-21] DA,[22] cyclohexyl acrylate,[23] phenyl acrylate,[24] *tert*-butyl acrylate,[25] and also acrylic acid (AA) in water.[26] Monomer addition to the midchain radical leads to the formation of a quaternary carbon branchpoint on the polymer chain which is directly observable by ^{13}C NMR; indeed, it was the high level of branching detected by NMR that led to the discovery of this important mechanism for BA.[27]

The ^{13}C NMR detection of branchpoints in polymer has been used to confirm intramolecular hydrogen transfer to a range of acrylates, including BA (e.g, [14,27-30]), ethyl acrylate (EA),[29-30] MA,[30] hexyl acrylate,[30] and 2-ethylhexyl acrylate (EHA).[31] Indirect evidence of branching, by the loss of PLP-structure in polymer MMDs, is documented for a wide range of alkyl acrylates[11-13,32-36] as well as AA.[37-38] Application of a 500 Hz laser extends the temperature range over which chain-end propagation may be measured using the PLP-SEC technique;[12] however, the loss of PLP structure in the polymer MMDs at 70-80 °C is still attributed to the effect of backbiting not only for BA,[12] but also for isobornyl acrylate, *tert*-butyl acrylate and 1-ethoxyethyl acrylate[39] and a series of carbamate acrylates.[40]

While the above survey is not exhaustive, it indicates that the intramolecular chain-transfer reaction is a general feature of acrylate monomers, regardless of the size or functionality of the ester group. Thus, it was surprising to find that this mechanism is greatly suppressed (or even completely eliminated) for the polymerization of 2-hydroxyethyl acrylate (HEA), a functional monomer whose copolymers have variety of commercial applications as adhesives, biomaterials and coatings.[41-43] As well as providing evidence to support this finding, the results are also correlated to intermolecular H-bonding in the system.

As the PLP study on HEA homopolymerization is successful, it is easier to investigate copolymerization systems involving HEA. However, relative to the literature available for functional methacrylates, there are very few copolymerization studies that involve HEA. When taken to high conversions, the presence of HEA monomer in a copolymerization leads to high molecular weight products through cross-linking and transfer to polymer reactions. Yocum and Nyquist determined that the high polymer molar mass (and sometimes gelation) is caused by divinyl crosslinking agents which are side products of monomer synthesis.[44] McManus et al.[45] and Chow et al.[46] conducted copolymerizations of HEA with styrene (ST) in bulk and in benzene solvent, respectively, using low conversion experiments to determine reactivity ratios for the monomers. Catala et al. studied the copolymerization of HEA with methyl acrylate (MA), ethyl acrylate and butyl acrylate (BA) at 60 °C, and concluded that an increase in the size of the ester alkyl group favors introduction of HEA into the copolymer.[47]

Pertinent to the current ST/HEA study, it was found that ST/HEMA produced methacrylate-enriched copolymer relative to alkyl methacrylates such as methyl methacrylate (MMA), butyl methacrylate (BMA), and dodecyl methacrylate (DMA), as presented in Ch 3. The difference in copolymer composition was reflected in the increased reactivity of HEMA towards a styrene radical (r_{ST} of 0.27-0.31) compared to the alkyl methacrylates towards a styrene radical (r_{ST} of 0.5-0.6), and was explained by an accompanying computational study that demonstrated that the increased polarity of the HEMA ester group reduced the electron density at the double bond and thus increased the addition rate of HEMA to a styrene radical relative to BMA.[48] Subsequent experimental work showed that solvent choice can influence this behavior by affecting the intermolecular H-bonding in the system.[49]

In this work, the PLP-SEC technique has been applied to the study of bulk copolymerization

of ST/HEA. As well as reporting the values of $k_{p,cop}$ for this system, SEC calibration is established for poly(HEA). In addition to the PLP-SEC study on how solvent choice can influence backbiting with BA and HEA, semibatch BA homopolymerization experiments in different solvents have been carried out. For both the kinetic and semibatch experiments, the branching level of the polymers is measured using ^{13}C NMR.

6.2 Experimental

HEA (96% purity, containing 200-650 ppm monomethyl ether hydroquinone as inhibitor), BA (99% purity, containing 10-60 ppm monomethyl ether hydroquinone as inhibitor), styrene (99% purity, containing 10-15 ppm of 4-tert-butylcatechol), photoinitiator DMPA (2,2-dimethoxy-2-phenylacetophenone, 99% purity) and anhydrous DMSO-d_6 (dimethyl sulfoxide-d_6, containing 99.9 atom % D) were all obtained from Sigma Aldrich and used as received. The details of semibatch experiments and other chemicals mentioned in this chapter can be found in Ch 4. Low conversion polymerizations were conducted in the pulsed laser setup described in Ch 3.

Polymers produced by PLP were used to determine $k_{p,cop}$ values from analyses of polymer molar mass distributions (MMDs) measured by SEC using a Viscotek 270max separation module with a refractive index (RI), viscosity (IV) and light scattering (low angle LALS and right angle RALS) triple detector setup. A set of two porous PolyAnalytik columns with an exclusion limit molecular weight of 20×10^6 g·mol^{-1} were used in series at 40 ℃. Distilled THF was used as the eluent at a flow rate of 1 mL·min^{-1}. The MMDs were calculated using two different methodologies. First, the principle of universal calibration was applied to analyze data from the

RI detector, using a calibration curve constructed with narrow molecular weight polystyrene standards ranging from 6910 to 3,300,000 g·mol^{-1}. The Mark-Houwink parameters for poly(HEA) and copolymers were estimated directly from the curve generated by the output from the viscosity and LS detectors. The multiple-detector calibration method was also used to obtain the absolute values of polymer molar mass with the refractive index (d*n*/d*c*) of pST and pHEA in THF as 0.185[51] and 0.0662,[52] respectively. In order to check the consistency of these methodologies with previous results from a Waters 2960 separation module coupled with RI and a Wyatt LS detector (for details of this setup see Chapter 3), PLP-generated pMMA samples have been run on both SEC setups. The calculated k_p values are compared to literature value in Table 6.1. The comparison indicates a good agreement between two SEC setups with different calibration methods, as also shown in Appendix A.4.1 for a ST/HEA copolymer sample.

Table 6.1 k_p values for MMA homopolymerization at 50°C as measured by PLP at 50 Hz

	Literature value[53]	**Viscotek**		**Waters**	
		Multiple Detector	Universal Calibration	RI	LS
$\boldsymbol{k_p}$**/L·mol^{-1}·s^{-1}**	648	658	587	658	628

The acrylate homopolymers isolated from the PLP experiments were also subjected to ^{13}C NMR analysis at room temperature on a Bruker DRX-500MHz spectrometer operating at 125.8 MHz. The pHEA and pBA samples were dissolved in DMSO-d_6 and chloroform-*d*, respectively, with a minimum concentration of 100 mg·mL^{-1}. Chemical shifts were referenced to the solvent resonance at 40 ppm for DMSO-d_6 and 77 ppm for chloroform-*d*. Spectra were run with continuous proton decoupling using a pulse interval of 0.5 s and a flip angle of 45° to maximize the signal-to-noise ratio. In order to check the quantitative accuracy of these fast pulse spectra, some

samples were analysed with NOE suppression by inverse gated decoupling and with relaxation time of 10 s to allow complete recovery of all carbons between pulses.[54] A critical peak in this work is the quaternary carbon at 48 ppm arising from the branchpoint generated by backbiting.[14,27,30-31] The DEPT technique is also applied to identify different carbon resonances.

The ST/HEA copolymers isolated from the PLP experiments were also used for composition analysis by proton NMR. The polymer was dissolved in dimethyl sulfoxide for proton NMR analysis conducted at room temperature on a 400 MHz Bruker instrument. Copolymer composition is calculated using the chemical shifts from the aromatic protons in styrene units in the region of 7.4-6.2 ppm and from the hydroxyl protons of main chain HEA units in the region 4.9-4.3 ppm.[48,55]

6.3 Results and Discussion

6.3.1 HEA Homopolymerization

PLP experiments with HEA were done as a larger effort to study the copolymerization behavior of hydroxyl-functional monomers, following previous work with 2-hydroxyethyl methacrylate (HEMA).[48,49] Surprisingly it was found that PLP-structured MMDs were produced with repetition rates of 50 and 100 Hz at temperatures to 60 °C. Figure 6.1 compares PLP-generated MMDs of pHEA with those for pBA. The pHEA distributions and first-derivative plots shows distinct PLP structure not seen for pBA, even though the k_p values for HEA at 50 °C (estimated as 34.5×10^3 L·mol^{-1}·s^{-1}), is of similar magnitude to that of BA (28.5×10^3 L·mol^{-1}·s^{-1}). As discussed in the introduction, the BA value was obtained by extrapolation of lower temperature PLP results measured at 100 Hz,[11] or as measured using a 500 Hz repetition rate.[12] That a k_p value for HEA

could be estimated directly from 50 and 100 Hz PLP experiments at 50 °C is a strong indication that the intramolecular transfer reaction must be strongly suppressed for the HEA system.

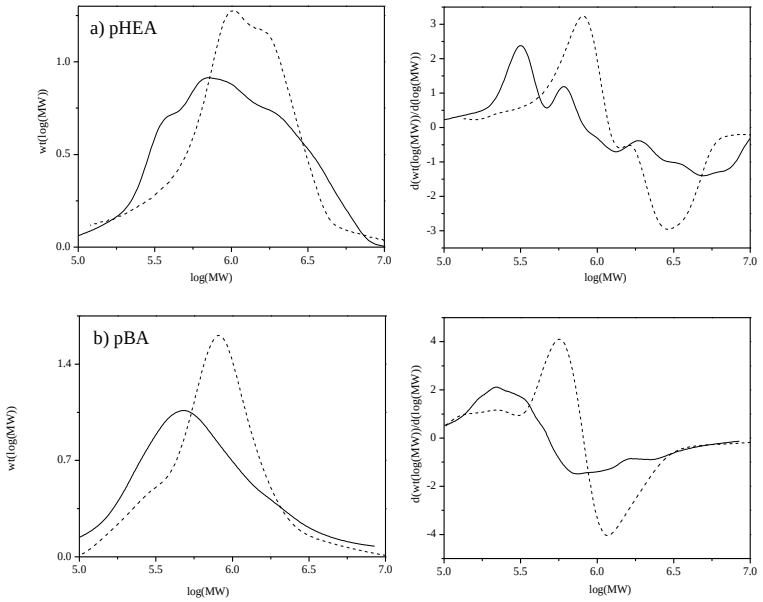

Figure 6.1 Polymer MMDs and corresponding first-derivative plots for PLP-generated (a) pHEA and (b) pBA by bulk polymerization at 50 °C, 50 (- - -) and 100 (—) Hz.

Figure 6.2 compares ^{13}C NMR spectra of the pBA and pHEA PLP-generated samples. The quaternary carbon peak at 48 ppm is clearly seen for pBA, with the estimated branching level of 0.2-0.3% in good agreement with previous literature,[54] but is not found in the pHEA sample. (Details regarding peak assignments and integrations are provided in Appendix A.4.2) To the best of our knowledge, HEA is the first acrylate without this branching, a result that may be related to the strong intramolecular H-bonding in the system.

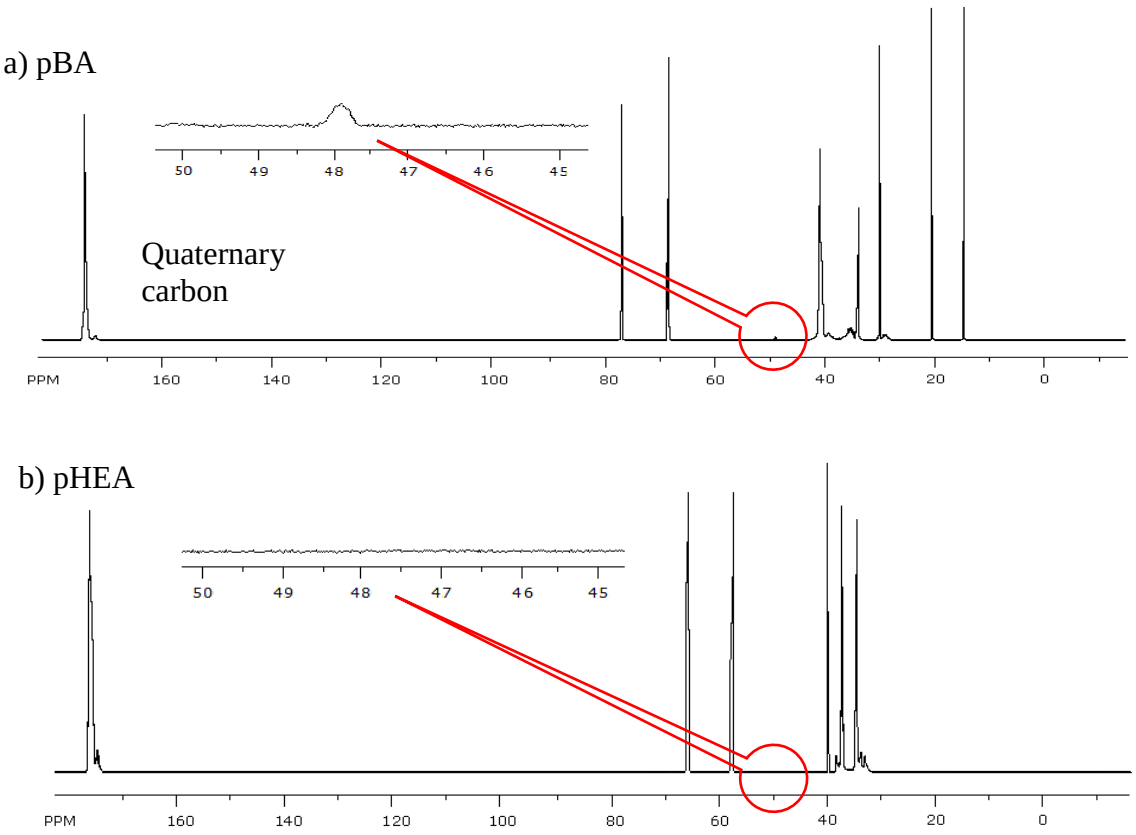

Figure 6.2 ^{13}C NMR spectra of pBA and pHEA generated by PLP of bulk monomer at 50 °C.

In previous studies of HEMA copolymerization behavior[48,49] (see Ch 3) we have found, in accord with the work of Beuermann,[56,57] that the addition of *N*,*N*-dimethylformamide (DMF) as a solvent decreases HEMA k_p values by 40% due to the disruption of HEMA-HEMA intermolecular H-bonding. In contrast, the introduction of H-bonding to an alkyl methacrylate leads to a higher k_p value, with an increase of 30% observed by addition of *n*-butanol (BuOH) to *n*-butyl methacrylate (BMA).[49,56,58] Thus, we decided to investigate the effect of adding DMF (as a H-bond disrupter) to HEA and adding BuOH (as a H-bond inducer) to BA PLP experiments. The resulting polymer MMDs and first-derivative plots are shown as Figure 6.3. Comparing with Figure 6.1, it is seen that pHEA starts to lose PLP structure (including loss of a clear secondary inflection point) when DMF is introduced to the system, while the pBA MMD exhibits PLP structure when produced in the

presence of BuOH solvent. As summarized in Table 6.2, the apparent k_p values for HEA in DMF is about 30% lower than that in bulk while the k_p value measured for BA in BuOH is roughly 20% higher than in bulk, in good agreement with solvent effects observed for the corresponding methacrylate systems.[49,56-58]

Table 6.2 Experimental conditions and results for solution pulsed-laser polymerization of 2-hydroxyethyl acrylate in dimethylformamide and *n*-butyl acrylate in *n*-butanol at 50 °C and 100 Hz with [DMPA]=5mmol·L^{-1}.

Sample (50v/50v)	Conversion %	SEC Result		
		M_1 ($g \cdot mol^{-1}$)	M_2/M_1	k_p from M_1 ($L \cdot mol^{-1} \cdot s^{-1}$)
HEA in DMF	2.3	122076	3.16	24086
	2.5	122374	3.20	24178
BA in BuOH	2.0	158489	2.00	35456
	2.1	158489	1.95	35456

The structures of the PLP-generated MMDs in Figures 6.1 and 6.3 suggest that the H-bonding in the system has an influence on the backbiting mechanism. The ^{13}C NMR analyses shown in Figure 6.4 support this conclusion. The quaternary carbon peak, not observed in bulk HEA polymerization (Figure 6.2b) is seen for the pHEA sample produced in DMF solution (Figure 6.4b). Meanwhile, the quaternary carbon peak observed in the pBA sample generated in bulk (Figure 6.2a) is lost among the baseline noise when BA is polymerized in BuOH (Figure 6.4a).

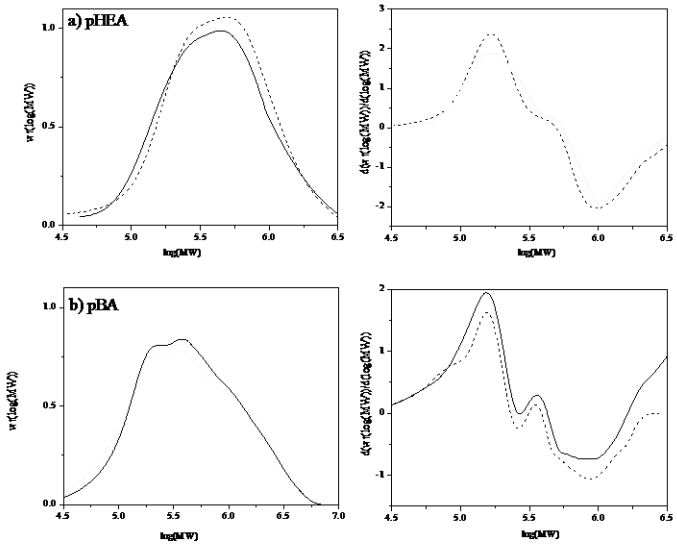

Figure 6.3 Polymer MMDs and corresponding first-derivative plots for PLP-generated by solution polymerization of (a) 50 vol% HEA in DMF, and (b) 50 vol% BA in BuOH at 50 °C and 100 Hz. (Two replicate experiments at each condition.)

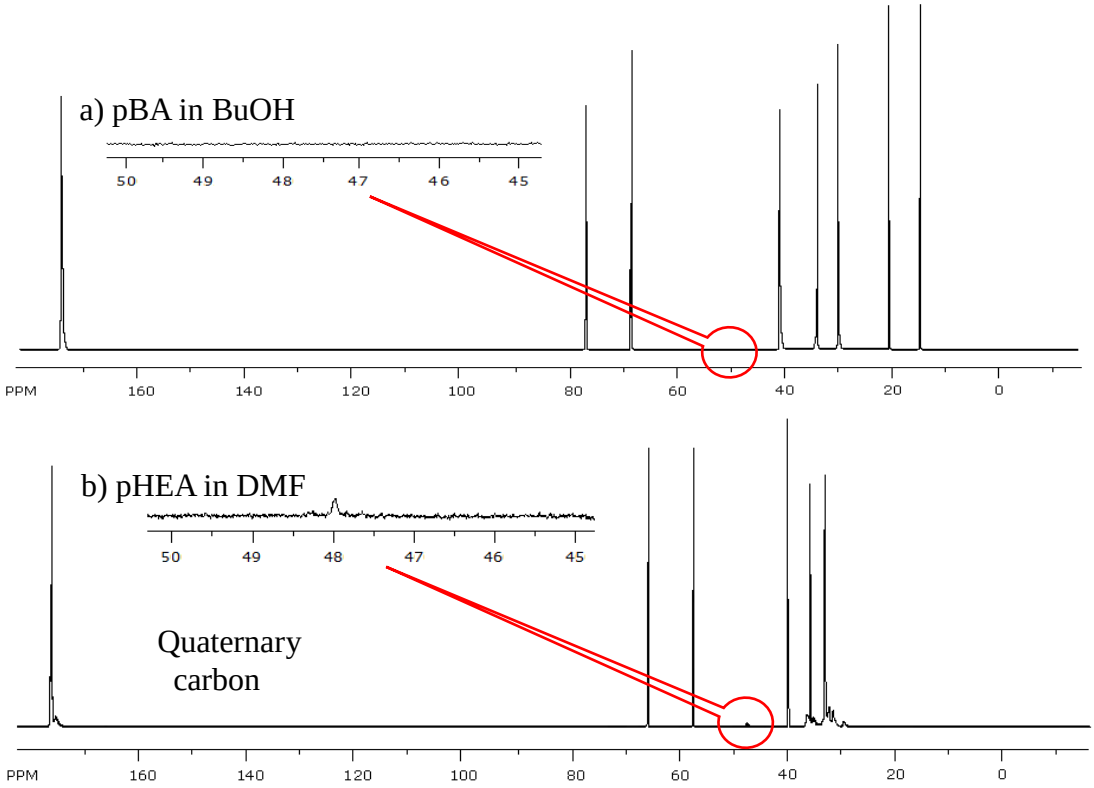

Figure 6.4 ^{13}C NMR spectra of pBA generated by PLP of BA in BuOH and pHEA generated by PLP of HEA in DMF at 50 °C.

While we cannot conclude that the intramolecular chain transfer reaction does not occur, it is clear that H-bonding greatly disrupts the mechanism. Good PLP structure was observed for bulk HEA polymerizations conducted at 50 and 100 Hz in the temperature range of 20-60 °C (see Appendix A.4.3). Figure 6.5 shows the resulting Arrhenius plot for HEA k_p values, which are analyzed using the newly-determined Mark-Houwink parameters for pHEA presented later in Table 6.2. The k_p values for HEA are 25% higher than those for BA, with the Arrhenius parameter A=1.72±0.08×10^7 L·mol^{-1}·s^{-1} and activation energy E_a=16.78±0.14 kJ·mol^{-1}, in the range found for other acrylates.[43,48,49,54,56] These values were obtained by linear fitting of ln(k_p) vs. inverse temperature data, implicitly assuming that values in ln(k_p) have a constant absolute error. This assumption is equivalent to a constant relative error in k_p, an error structure that arises from estimation of the inflection points by differentiation of the log(MW) curves.[28] The difference between HEA and BA k_p values, while significant, is much smaller than the three-fold increase found for HEMA compared to BMA.[23]

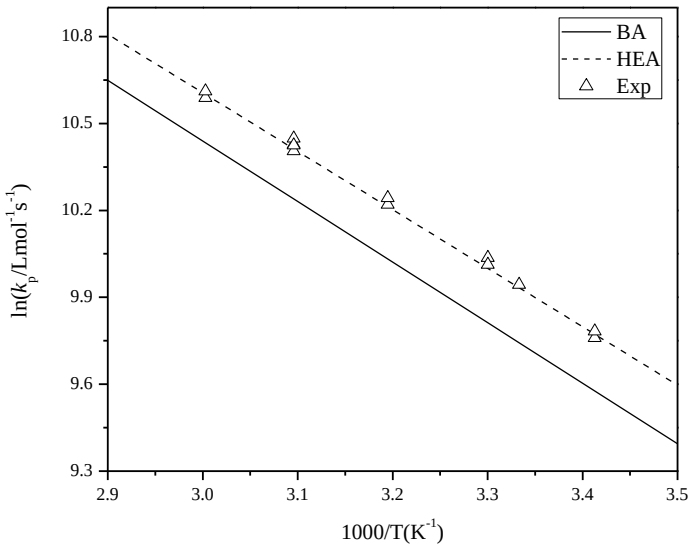

Figure 6.5 Arrhenius plot for homopropagation rate coefficient (L·mol^{-1}·s^{-1}) of HEA, as measured by the PLP-SEC technique, with BA Arrhenius relationship taken from [41].

6.3.2 ST/HEA Copolymerization in Bulk

Copolymer Composition. The reported literature values of terminal model monomer reactivity ratios for bulk ST/HEA show some scatter, as summarized previously.[59] The most comprehensive study, that by McManus et al.,[45] presents a statistical evaluation and reports monomer reactivity ratios with relatively small confidence intervals. The current study, while focusing on $k_{p,cop}$ for the system, provides new composition data for the system. Proton NMR was used to measure the mole fraction of HEA in the poly(ST/HEA) samples generated at 50 °C, with results shown in Figure 6.6 and summarized in Appendix A.4.1. The data are well-represented by the Mayo-Lewis terminal model using the monomer reactivity ratios of r_{ST}=0.44±0.03 and r_{HEA}=0.18±0.04, and are in very good agreement with the composition curve generated using the experimental estimates of reactivity ratios from McManus et al.[45] The TM reactivity ratios estimated computationally by Dossi et al.[59] also provide a good description of the system.

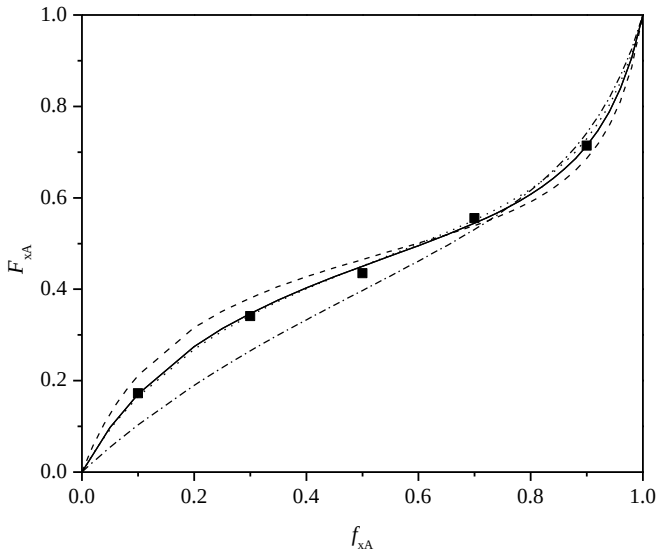

Figure 6.6 Copolymer composition (■, mole fraction of HEA incorporated) from bulk ST/HEA copolymerization at 50 °C. Best fit curve (——) calculated with r_{ST}=0.44 and r_{HEA}=0.18 according to the terminal model, compared with literature estimates from McManus et al.[45] (· · ·) and Dossi et al.[59] (– –). Also plotted is the copolymer composition curve for ST/BA[63] (· – · –).

It is also interesting to compare the copolymer composition curve of ST/HEA with that of ST/BA. The curves have similar shape but, like found for the ST/HEMA vs. ST/BMA comparison,[48] HEA is incorporated into the copolymer at a higher level than the alkyl (meth)acrylate. As found for the corresponding methacrylate/ST systems, the increased incorporation of hydroxy-functional monomer is captured by a decreased r_{ST} value (0.44 for ST/HEA compared to 0.88 for ST/BA), with no appreciable difference in the other monomer reactivity ratio (r_{HEA}=0.18±0.04 compared to r_{BA}=0.24). Thus, the H-bonding effect of HEA in its copolymerization with ST is similar in magnitude to that found for HEMA.

Propagation Rate Coefficient. The PLP/SEC technique has proven to be an efficient and accurate method to investigate $k_{p,cop}$, based on careful analysis of polymer MMDs, as described in Ch 2.

The ST/HEA copolymer samples were analyzed using both SEC setups, with the detailed comparison summarized in Appendix A.4.1. Mark-Houwink parameters of ST/HEA copolymers determined from triple-detection analysis are listed in Table 6.3. As shown in Figure 6.7, there is a systematic decrease in intrinsic viscosity as the HEA content in the copolymer increases, with the experimental values in excellent agreement with values calculated using a weighted composition average of the homopolymer values. The Mark-Houwink parameters were used to estimate MMDs using the principle of Universal Calibration and the RI detector output from both the Waters and the Viscotek setups. Finally, the Wyatt LS output was analyzed using a composition weighted-average of the two homopolymer refractive indices (d*n*/d*c*). Agreement between the two instruments and the various calculation methods is within 10% over MW_o values ranging between 8×10^3 and 6×10^5 Da (Appendix A.4.1).

The $k_{p,cop}$ data for bulk copolymerization of HEA with ST at 50 °C are plotted in Figure 6.8

as a function of monomer composition, increasing with HEA content from the ST homopolymer value of 240 $L \cdot mol^{-1} \cdot s^{-1}$ to the HEA homopolymer of 35000 $L \cdot mol^{-1} \cdot s^{-1}$. Much of the increase occurs for very high HEA content, with an experimental value of 4384 $L \cdot mol^{-1} \cdot s^{-1}$ for f_{HEA}=0.9. Also shown in Figure 6.8 is the prediction of the terminal model, calculated using the monomer reactivity ratios that describe the copolymer composition data (r_{ST}=0.44 and r_{HEA}=0.18) and the homopolymer k_p values. The deviation between experiment and the terminal model prediction is significant, with the terminal model underpredicting $k_{p,cop}$ values by roughly a factor of two. This result contrasts that of ST copolymerization with alkyl acrylates, for which the terminal model overpredicts $k_{p,cop}$ experimental values by as much as factor of two.[61] It is clear that the terminal model cannot simultaneously describe copolymer composition and polymerization rate. The IPUE model has been used to provide an improved fit to the experimental data; despite the good fit shown in Figure 6.8, the uncertainty in the radical reactivity ratios (s_{ST}=3.0±4.5 and s_{HEA}=0.9±63.9), as estimated by non-linear regression, is unacceptably large. Because of its larger confidence interval, s_{HEA} was set to a fixed value and the value of s_{ST} was re-estimated. With s_{HEA} fixed at unity (equivalent to the terminal model), the value of s_{ST} is estimated as 3.9±1.5. Another approach is to set s_{HEA} to 0.11, the value determined for ST/MA[64] and ST/BA[60] under this assumption, the corresponding s_{ST} value is estimated as 5.4±2.3. It is difficult to obtain precise estimates for the radical reactivity values for this system, partially due to the large difference in the two homopropagation rate coefficients, and partially due to the small experimental data set. It is clear, however, that the terminal model cannot provide a good representation of the $k_{p,cop}$ data.

Table 6.3 Mark-Houwink parameters for ST/HEA copolymers in THF measured by triple detector SEC ("Experiment") and as estimated using a composition weighted average ("Calculated")

Monomer molar Composition		pHEA	pST [51]	0.1HEA	0.3HEA	0.5HEA	0.7HEA	0.9HEA
Experiment	Log(*K*/dL·g^{-1})	–3.492		–3.873	–3.799	–3.714	–3.664	–3.544
	a	0.602		0.699	0.679	0.657	0.643	0.618
Calculated	Log(*K*/dL·g^{-1})		–3.943	–3.895	–3.801	–3.709	–3.620	–3.534
	a		0.716	0.704	0.680	0.657	0.635	0.613

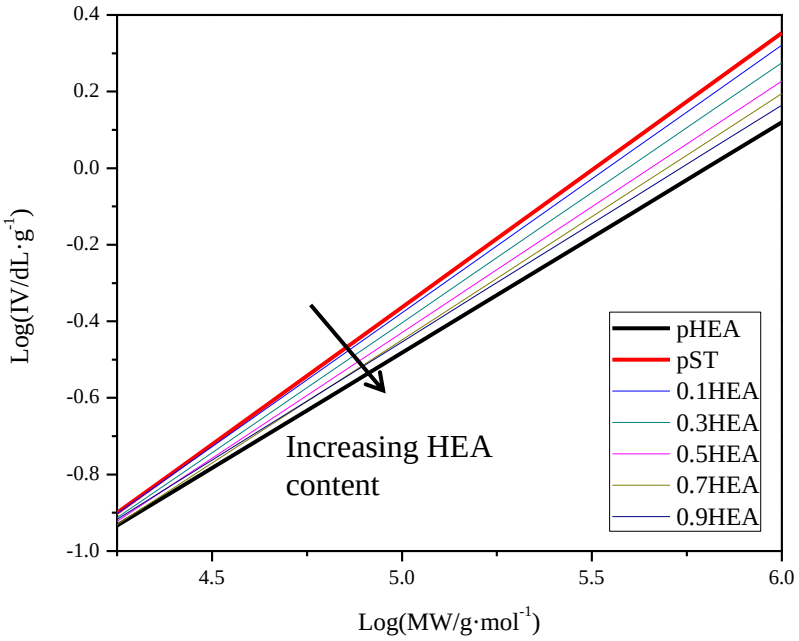

Figure 6.7 Intrinsic viscosity profiles of ST/HEA copolymers in THF (see Table 6.2).

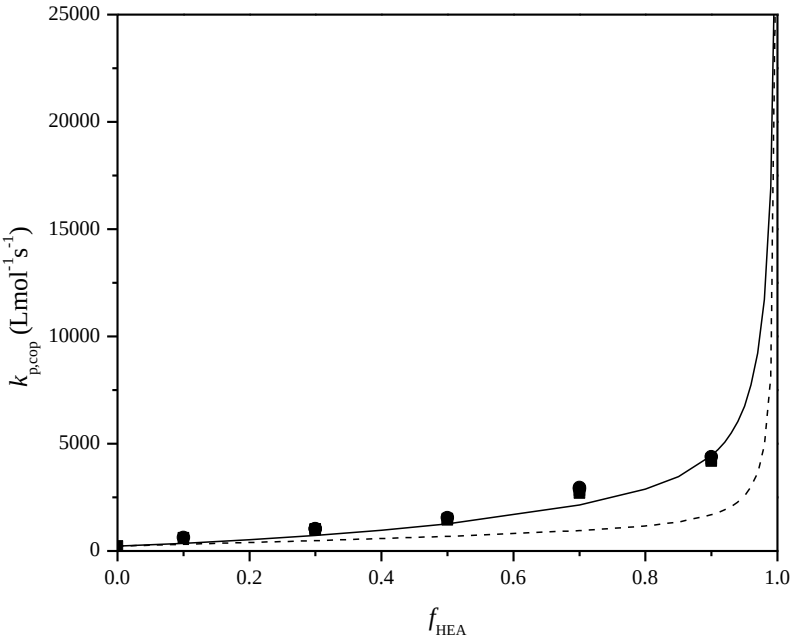

Figure 6.8 Copolymer propagation rate coefficients ($k_{p,cop}$) data (■ from LS analysis and ♦ from triple detection) vs. 2-hydroxyethyl acrylate (HEA) monomer mole fraction, as measured by PLP/SEC at 50 °C. Terminal model predictions are indicated by dashed line and penultimate model fit, calculated with s_{ST}=3.0 and s_{HEA}=0.91, by the solid line.

Table 6.4 Propagation rate coefficients and reactivity ratios for ST/HEA, ST/BA and ST/MA bulk copolymerization

	ST/HEA	**ST/BA** [60]	**ST/MA** [61]
$\boldsymbol{r_{ST}}$	0.44	0.88	0.95
$\boldsymbol{r_{xA}}$	0.18	0.24	0.19
$\boldsymbol{s_{ST}}$	3.0	0.90	0.94
$\boldsymbol{s_{xA}}$	0.91	0.11	0.11
$\boldsymbol{k_{p,xA}}^{a}$	34500	27800	22800

[a] in L·mol^{-1}·s^{-1} calculated at 50 °C

Table 6.4 summarizes the kinetic coefficients for three ST/acrylate systems, ST/HEA, ST/BA and ST/MA. Despite the difference in absolute k_p values for the three acrylates, the relative addition of styrene to acrylate radicals (r_{xA}) is the same. As discussed previously, the functional monomer HEA adds onto a styrene radical significantly faster than does BA or MA, as reflected in the lower r_{ST} values. Although it is difficult to quantify penultimate unit effects from *s* values due to their higher uncertainty, it can be concluded that an HEA unit in the penultimate position increases the reaction rate (s_{xA} >1).

6.3.3 Semibatch BA Homopolymerization

The experimental conditions and operating procedure chosen at 110 °C are similar to those used in an extensive study of high temperature BA semibatch solution polymerization,[65] with the following differences: xylene was used instead of a mixed xylene/ethylbenzene solvent; benzoyl peroxide (BPO, halflife of 8.1 min at 110 °C) was used as initiator instead of *tert*-butyl peroxyoctoate (halflife of 11.8 min); BA and initiator were fed over 3 h instead of a 1 h feed period followed by 1 h hold. Despite these operational differences, the properties – MW averages, MM% and BL% – of the poly(BA) produced with xylene in this study are very similar to those reported in ref. 65 for the same solvent and initiator levels, as summarized in Table 6.5.

Figure 6.9 plots the free monomer levels and MW averages over the course of the experiment. Monomer concentrations remain low (< 0.3 mol/L) throughout the course of both experiments, a general feature of the starved-feed semibatch process,[65-67] and one that promotes SCB formation. Despite the lower [M] in BuOH relative to xylene, however, the MW of the poly(BA) formed in BuOH is significantly higher. The data summarized in Table 6.5 indicate that

replacing the xylene solvent with BuOH has a remarkable effect on polymer properties: BL and MM levels decrease by a factor of 5, and the polymer weight-average MW increases by a similar factor. In addition, the polydispersity index of the polymer decreases from 2.4 (produced in xylene) to 2.1 (in BuOH).

Table 6.5 Properties of poly(butyl acrylate) produced by semibatch solution polymerization at 110 °C [a]

	M_n ($g \cdot mol^{-1}$)	M_w ($g \cdot mol^{-1}$)	MM%	BL%
BA in xylene[65]	4960	10700	0.60	6.55
BA in xylene	4750	11300	0.65	6.02
BA in BuOH	26900	55700	0.13	1.14

[a] Properties of final polymer sample (t=3 h). M_n: number-average MW; M_w: weight-average MW; MM%: number of terminal unsaturations per 100 BA repeat units; BL%: number of branchpoints per 100 BA repeat units.

Eqs 2.34 and 2.35 provide a rough measure of the dramatic effect that H-bonding has on the values of k_{bb} and k_p^{av}. Using the values for k_p (80,200 $L \cdot mol^{-1} \cdot s^{-1}$) and k_p^{MCR} (150 $L \cdot mol^{-1} \cdot s^{-1}$) at 110 °C taken from literature as summarized in the previous modeling study,[10] and using a rough estimate for [M] of 0.28 mol/L in xylene and 0.18 mol/L in BuOH (approximate average over last 2 h of reaction, see Figure 6.9), the estimated value for k_{bb} in BuOH is a factor of 8 lower than the value estimated for the experiment in xylene; the actual difference may be smaller, as there are indications that the value of k_p for BA in BuOH is higher than in bulk.[50] With reduced backbiting, the formation of macromonomer is also lowered, and the polymer

chain-length is dramatically increased as the estimated value of k_p^{av} (from Eq 2.34) increases by a factor of 4-5 in BuOH compared to xylene.

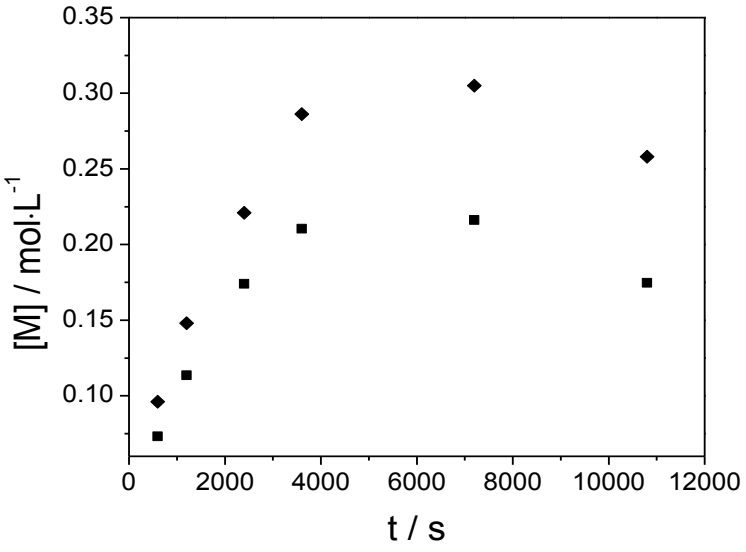

(a)

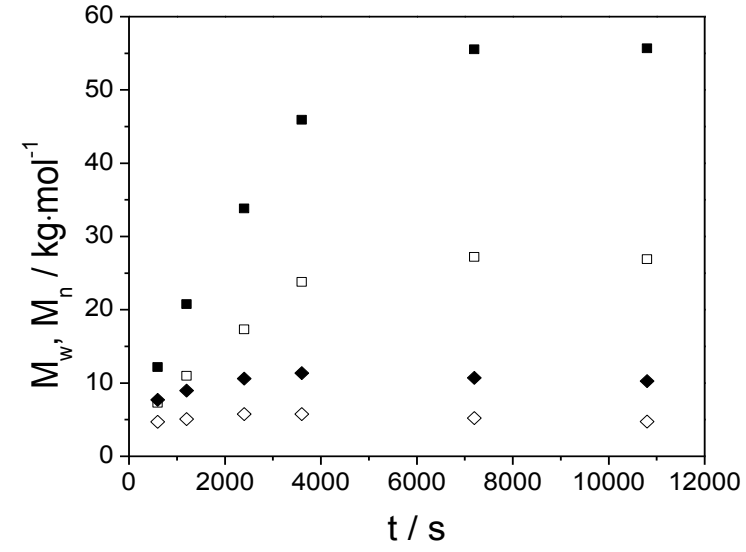

(b)

Figure 6.9 (a) Butyl acrylate concentration ([M]) and (b) polymer number-average (M_n, open symbols) and weight-average (M_w, closed symbols) molecular weight profiles for semibatch starved-feed solution polymerizations at 110 °C in xylene (♦) and *n*-butanol (■).

In support of our semibatch study, the Buback group has applied the SP-PLP-EPR (single-pulse pulsed-laser-polymerization electron-paramagnetic-resonance spectroscopy) technique to directly measure how the concentrations of BA chain-end and midchain radicals differ in a non-polar solvent (toluene) to the H-bonding solvent BuOH.[69] The technique, which consists of highly time-resolved online monitoring of radical concentration after production of an intense burst of radicals by pulsed-laser-induced decomposition of a photoinitiator, was used to estimate that the backbiting rate coefficient of BA is reduced, by about a factor of three, in passing from BA polymerization in toluene (or in bulk) to polymerization in BuOH.[69] While consistent with the lower branching levels of poly(BA) produced by semibatch polymerization in BuOH, the decrease in the backbiting rate coefficient is less pronounced. This difference may result from the lower monomer concentration of 0.18 mol/L in the semi-batch experiments as compared to 1.5 mol/L in the SP-PLP-EPR measurement. These results verify that BuOH inhibits the intramolecular chain transfer to polymer reaction that causes a reduced reaction rate and the formation of branchpoints along the polymer backbone, in agreement with the conclusions inferred from the previous PLP study (Ch 6.3.1).[50] While the exact nature of the H-bonding interaction is yet to be determined, it is shown that the reduced backbiting leads to a significant decrease in poly(butyl acrylate) branching levels for solution polymerization in BuOH compared to xylene at higher-temperature industrially-relevant conditions. An important result of the reduced branching levels in BuOH is the production of higher-MW polymer at identical synthesis conditions.

FT-IR tests have been conducted with monomers in different solvents in Ch 3 and the peak representing H-bonding with carbonyl group of methacrylate monomer is observed at 1708 cm^{-1}. For homopolymerization of BA, BuOH demonstrates strong effect on polymer branching level. Since backbiting reaction happens to the growing radical chains, it is necessary to check whether

H-bonding forms with polymer chains. FT-IR spetra of pBA produced by semibatch reaction at 110 °C and re-dissolved in xylene and BuOH by 50 wt% are shown in Figure 6.10. The H-bonding peak shows up in BuOH at the similar region as found with monomer and it is confirmed that H-bonding formats between polymer chains and BuOH. Thus the solvent effect on backbiting can be explained by the hypothesis that H-bonding with the radical chain end prevents formation of the six-membered ring necessary for branching.

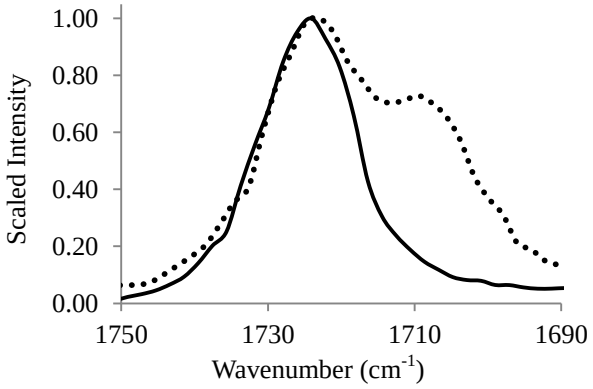

Figure 6.10 FT-IR spectra of pBA in xylene (solid curve) and BuOH (dashed curve).

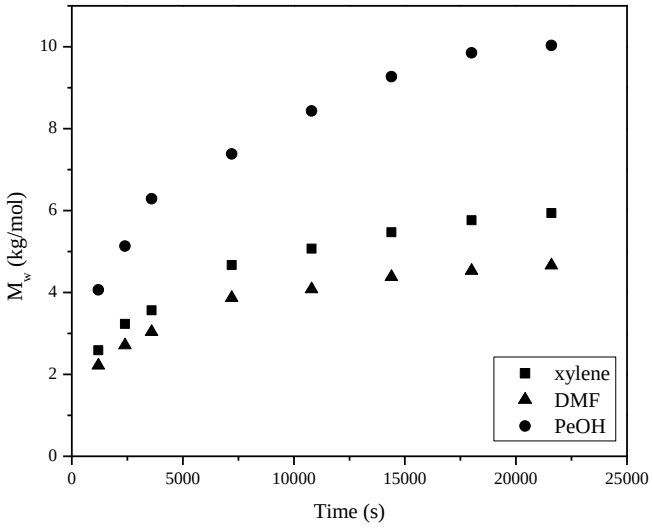

Figure 6.11 Polymer weight-average (M_w) molecular weight profiles for BA semibatch starved-feed solution polymerizations at 138 °C in xylene (■), DMF (▲) and *n*-pentanol (●).

In order to verify the H-bonding effect on branching level, semibatch BA homopolymerizations in 35 wt% xylene, DMF and *n*-pentanol (PeOH) were also carried out at 138 °C with TBPA initiator; the comparison of the weight-average molecular weight profiles is shown in Figure 6.11. Similarly to the results obtained at 110 °C, the MWs of poly(BA) in PeOH are significantly higher than those in DMF or xylene; DMF results in a small decrease in polymer MWs, perhaps due to increased chain-transfer to solvent. Table 6.6 summarizes the properties of the final polymers in the three solvents. The M_w in PeOH almost doubles that of pBA produced in xylene or DMF, while the branching level and macromonomer level are almost cut by half. While in agreement with the results obtained at 110 °C, the factor by which M_w increases and the branching level decreases is smaller. This weakened effect is consistent with the concept that H-bonding effects decrease with increased temperature, as discussed in Ch 4.

Table 6.6 Weight-average molecular weight (M_w), branching level (BL%) and macromonomer level (MM%) of pBA produced via semibatch polymerization at 138 °C.

	In xylene	In DMF	In PeOH
M_w (kg/mol)	5.94	4.66	10.0
BL%	9.78	9.85	5.87
MM%	0.38	0.43	0.21

6.4 Conclusions

PLP-SEC experiments and ^{13}C NMR analysis for HEA and BA in bulk and in solution indicate that intermolecular H-bonding has a disrupting effect on the acrylate backbiting mechanism. The influence of H-bonding on backbiting is shown by the reduced branching that occurs by the addition of BuOH to BA and the increase in branching by the addition of DMF to HEA. The

reduced levels of backbiting make it possible to determine the homopropagation rate coefficient for bulk HEA between 20 and 60 °C using pulse repetition rates of 50 and 100 Hz. To the best of our knowledge, HEA is unique among the acrylate family of monomers in this respect. FT-IR results suggest that H-bonding between solvent and polymer inhibits the intramolecular transfer to polymer reaction. It would be interesting to study whether these new findings are related to the reduced branching observed in controlled-radical polymerization of acrylates[62,63] and in the free-radical polymerization of acrylates in the presence of a powerful chain transfer agent.[64]

Semibatch experiments of BA hompolymerization in xylene and BuOH at 110 °C and in xylene, DMF and PeOH at 138 °C verify the H-bonding effect on branching levels of acrylates. The appropriate choice of solvents, such as BuOH or PeOH, can make it possible to produce polyacrylates with greatly reduced branching by free-radical polymerization.

An experimental study on free radical bulk copolymerization of ST and HEA was also carried out. Copolymer composition, in good agreement with previous literature, is well represented by the terminal model with r_{ST}=0.44±0.03 and r_{HEA}=0.18±0.04; HEA exhibits higher reactivity to ST radicals than do alkyl acrylates such as MA and BA. The PLP-SEC technique is used to measure composition-averaged copolymer propagation rate coefficients ($k_{p,cop}$) at 50 °C, with Mark-Houwink parameters determined via triple-detector SEC, and analysis of the polymer MMDs by two SEC setups in good agreement. Experimental $k_{p,cop}$ results are underpredicted by the terminal model; although well-fit by the IPUE model, estimates of radical reactivity ratios have high uncertainty.

References

1. Tracton, A. A. *Coatings Technology Handbook CRC Press* **2006**.

2. Phuong, Y. G.; David, J. T.; Andrew, K. W. *Biomacromolecules* **2002**, *3*, 554.

3. Bian, K. J.; Cunningham, M. F. *Macromolecules* **2005**, *38*, 695.

4. Montheard, J. P.; Chatzopoulos, M.; Chappard, D. J. *J. Macromol. Sci. Rev. Macromol. Chem. Phys.* **1992**, *32*, 1.

5. Lu, Z. ; Liu, G. ; Duncan, S. *J. Membr. Sci.* **2003**, *221*, 113.

6. Karina, A. G. ; Edeline, W. ; David, J. T. ; Andrew, K. W. *Biomacromolecules* **2004**, *5*, 1194.

7. Cortazar, I. C.; Vidaurre, A.; Ferrer, G. G. ; Pradas, M. M. ; Ribelles, J. L. ; Duenas, J. M. *J. Non-Cryst. Solids* **2001**, *287*, 130.

8. Mohammad, A. C.; David, J. T.; Andrew, K. W.; Michael, B. ; Mangala, P. P. *Biomacromolecules* **2004**, *5*, 1405.

9. Vargun, E. ; Usanmaz, A. *J. Polym. Sci.:Polym. Chem.* **2005**, *43*, 3957.

10. Zhang, L.; Katapodi, K.; Davis, T. P.; Barner- Kowollik, C.; Stenzel, M. H. *J. Polym. Sci.: Polym. Chem.* **2006**, *44*, 2177.

11. Asua, J. M.; Beuermann, S.; Buback, M.; Castignolles, P.; Charleux, B.; Gilbert, R. G.; Hutchinson, R. A.; Leiza, J. R.; Nikitin, A. N.; Vairon, J.-P.; van Herk, A. M. *Macromol. Chem. Phys.* **2004**, *205*, 2151.

12. Barner-Kowollik, C.; Günzler, F.; Junkers, T. *Macromolecules* **2008**, *41*, 8971.

13. van Herk, A. M. *Macromol. Rapid Commun.* **2009**, *30*, 1964.

14. Plessis, C.; Arzamendi, G.; Leiza, J. R.; Schoonbrood, H. A. S.; Charmot, D.; Asua, J. M. *Macromolecules* **2000**, *33*, 4.

15. Nikitin, A. N.; Hutchinson, R. N. *Macromolecules* **2005**, *38*, 1581.

16. Junkers, T.; Theis, A.; Buback, M.; Davis, T. P.; Stenzel, M. H.; Vana, P.; Barner-Kowollik, C. *Macromolecules* **2005**, *38*, 9497.

17. Theis, A.; Davis, T. P.; Stenzel, M. H.; Barner-Kowollik, C. *Macromolecules* **2005**, *38*, 10323.

18. Theis, A.; Feldermann, A.; Charton, N.; Davis, T. P.; Stenzel, M. H.; Barner-Kowollik, C. *Polymer* **2005**, *46*, 6797.

19. Willemse, R. X. E.; van Herk, A. M.; Panchenko, E.; Junkers, T.; Buback, M. *Macromolecules* **2005**, *38*, 5098.

20. Barth, J.; Buback, M.; Hesse, P.; Sergeeva, T. *Macromol. Rapid Commun.* **2009**, *30*, 1969.

21. Barth, J.; Buback, M.; Hesse, P.; Sergeeva, T. *Macromolecules* **2010**, *43*, 4023.

22. Buback, M.; Hesse, P.; Junkers, T.; Sergeeva, T.; Theis, T. *Macromolecules* **2008**, *41*, 288.

23. Yamada, B.; Azukizawa, M.; Yamazoe, H.; Hill, D.; Pomery, P. J. *Polymer* **2000**, *41*, 5611.

24. Azukizawa, M.; Yamada, B.; Hill, D. J. T.; Pomery, P. J. *Macromol. Chem. Phys.* **2000**, *201*,

774.

25. Kajiwara, A. *Macromol. Symp.* **2007**, *248*, 50.
26. Gilbert, B. C.; Lindsay Smith, J. R.; Milne, E. C.; Whitwood, A. C.; Taylor, P. *J. Chem. Soc. Perkin Trans.* **1994**, *2*, 1759.
27. Ahmad, N. M.; Heatley, F.; Lovell, P. A. *Macromolecules* **1998**, *31*, 2822.
28. Peck, A. N. F.; Hutchinson, R. A. *Macromolecules* **2004**, *37*, 5944.
29. Quan, C.; Soroush, M.; Grady, M. C.; Hansen, J. E.; Simonsick, Jr. W. J. *Macromolecules* **2005**, *38*, 7619.
30. Castignolles, P.; Graf, R.; Parkinson, M.; Wilhelm, M.; Gaborieau, M. *Polymer* **2009**, *50*, 2373.
31. Heatley, F.; Lovell, P. A.; Yamashita, T. *Macromolecules* **2001**, *34*, 7636.
32. Beuermann, S.; Buback, M. *Prog. Polym. Sci*. **2002**, *27*, 191.
33. Beuermann, S.; Paquet Jr., D. A.; McMinn, J. H.; Hutchinson, R. A. *Macromolecules* **1996**, *29*, 4206.
34. Couvreur, L.; Piteau, G.; Castignolles, P.; Tonge, M.; Coutin, B.; Charleux, B.; Vairon, J.-P. *Macromol. Symp.* **2001**, *174*, 197.
35. Willemse, R. X. E.; van Herk, A. M. *Macromol. Chem. Phys.* **2010**, *211*, 539.
36. Castignolles, P.; Nikitin, A. N.; Couvreur, L.; Mouraret, G.; Charleux, B.; Vairon, J.-P. *Macromol. Chem. Phys*. **2006**, *207*, 81.
37. Lacík, I.; Beuermann, S.; Buback, M. *Macromolecules* **2003**, *36*, 9355.
38. Buback, M.; Hesse, P.; Lacík, I. *Macromol. Rapid Commun.* **2007**, *28*, 2049.
39. Dervaux, B.; Junkers, T.; Schneider-Baumann, M.; Du Prez, F.; Barner-Kowollik, C. *J. Polym. Sci.: Part A: Polym. Chem.* **2009**, *47*, 6641.
40. Barner-Kowollik, C.; Bennet, F.; Schneider-Baumann, M.; Voll, D.; Rölle, T.; Fäcke, T.; Weiser, M.-S.; Bruder, F.-K.; Junkers, T. *Polym. Chem.* **2010**, *1*, 470.
41. Montheard, J. P. ; Chatzopoulos, M.; Chappard, D. *J. Macromol. Sci.* **1992**, *C32*, 1.
42. Lu, Z.; Liu, G.; Duncan, S. *J. Membr. Sci*. **2003**, *221*, 113.
43. Novak, R. W. In Encyclopedia of Chemical Technology, 4th ed.; Kroschwitz, J. I. Exc. Ed., M. Howe-Grant, Ed.; Wiley&Sons: New York, 1991; Vol 1, 314.
44. Yocum, R.H. E.B. ,*Functional monomers: Their preparation, polymerization, and application.* Marcel Dekker, New York, **1973**.
45. McManus, N. T.; Kim, J. D.; Penlidis, A. *Polym. Bull.* **1998,** *41*, 661.
46. Chow, C. D. *J. Polym. Sci.: Polym. Chem*. **1975**, *13*, 309.
47. Catala, J. M.; Nonn, A.; Pujot, J. M.; Bross, J. *Polym. Bull.* **1986**, *15*, 311.
48. Liang, K.; Dossi, M.; Moscatelli, D.; Hutchinson, R. A. *Macromolecules* **2009**, *42*, 7736.
49. Liang, K.; Hutchinson, R. A. *Macromolecules* **2010**, *43*, 6311.

50. Liang, K.; Hutchinson, R. A. *Macromol. Rapid Commun.* **2011**, *32*, 1090.

51. Li, D.; Li, N.; Hutchinson, R. A. *Macromolecules* **2006**, *39*, 4366.

52. Khutoryanskaya, O. V.; Mayeva, Z. A.; Mun, G. A.; Khutoryanskiy, V. V. *Biomacromolecules* **2008,** *9*, 3353.

53. Beuermann, S.; Buback, M.; Davis, T. P.; Gilbert, R. G.; Hutchinson, R. A.; Olaj, O. F.; Russell, G. T.; Schweer, J.; van Herk, A. M. *Macromol. Chem. Phys.* **1997**, *198*, 1545.

54. Plessis, C.; Arzamendi, G.; Alberdi, J. M.; van Herk, A. M.; Leiza, J. R.; Asua, J. M. *Macromol. Rapid Commun*. **2003**, *24*, 173.

55. Mun, G. A. ; Nurkeeva, Z. S. ; Akhmetkalieva, G. T. ; Shmakov, S. N. ; Khutoryanskiy, V. V. ; Lee, S. C. ; Park, K. *J. Polym. Sci: Polym. Phys.* **2006**, *44*, 195.

56. Beuermann, S. *Macromol. Rapid Commun.* **2009**, *30*, 1066.

57. Beuermann, S.; Nelke, D. *Macromol. Chem. Phys*. **2003**, *204*, 460.

58. Beuermann, S. *Macromolecules* **2004,** *37*, 1037.

59. Dossi, M.; Storti, G.; Moscatelli, D. *Polym. Eng. Sci*. **2011**, *51*, 2109.

60. Li, D.; Hutchinson, R. A. *Macromol. Rapid Commun*. **2007**, *11*, 1213.

61. Davis, T. P.; O'Driscoll, K. F.; Piton, M. C.; Winnik, M. A. *Polym. Int*. **1991**, *24*, 65.

62. Ahmad, N. M.; Charleux, B.; Farcet, C.; Ferguson, C. J.; Gaynor, S. G.; Hawkett, B. S. Heatley, F.; Klumperman, B.; Konkolewicz, D.; Lovell, P. A.; Matyjaszewski, K.; Venaktesh, R. *Macromol. Rapid Commun.* **2009**, *30*, 2002.

63. Reyes, Y.; Asua, J. M. *Macromol. Rapid Commun.* **2011**, *32*, 63.

64. Gaborieau, M.; Koo, S. P. S.; Castignolles, P.; Junkers, T.; Barner-Kowollik, C. *Macromolecules* **2010**, *43*, 5492.

65. Nikitin, A. N.; Hutchinson, R. A.; Wang, W.; Kalfas, G. A.; Richards, J. R.; Bruni, C. *Macromol. React. Eng.* **2010**, *4*, 691.

66. Peck, A. N. F.; Hutchinson, R. A. *Macromolecules* **2004**, *37*, 5944.

67. Grady, M. C.; Simonsick, Jr., W. J.; Hutchinson, R. A. *Macromol. Symp*. **2002**, *182*, 149.

68. Barth, J.; Buback, M.; Hesse, P.; Sergeeva, T. *Macromolecules* **2010**, *43*, 4023.

69. Liang, K.; Hutchinson, R. A.; Barth, J.; Samrock, S.; Buback, M. *Macromolecules* **2011**, *44*, 5843.

Chapter 7 Solvent Effect on BA/HEMA Copolymerization

Preface

Kinetic studies in Ch 6 examine how H-bonding affects the backbiting reaction in BA homopolymerization, while those in Ch 5 examine the relative reactivity of BMA/HEMA as well as the effect of solvent on copolymer MW formed in semibatch reactions, building on the ST/HEMA semibatch study summarized in Ch 4. The surprising increase in ST/HEMA and BMA/HEMA copolymer MW values (compared to ST/BMA copolymerization and BMA homopolymerization) is caused by branching reactions involving dimethacrylate impurity found in commercial HEMA, with the extent of branching also influenced by the combination of solvent choice and temperature. In this chapter, the combined influence of solvent on acrylate branching and HEMA polymerization kinetics is studied for the BA/HEMA system, using both PLP-SEC and semibatch experimentation. The review of previous literature and description of experimental techniques will not be repeated in this chapter.

Results and Discussion

7.1 Kinetic Study on BA/HEMA Copolymerization

Copolymerization of BA and HEMA at 50 °C was carried out in bulk, and in BuOH and DMF solvent, using the PLP-SEC setup coupled with NMR analysis of copolymer composition. Experimental results are shown in Figure 7.1a. Monomer reactivity ratios for BA/HEMA in bulk are estimated as r_{BA}=0.18±0.09, r_{HEMA}=5.54±3.27 assuming the terminal model, very close to the literature values of r_{BA}=0.168 and r_{HEMA}=5.414 reported by Varma et al.[1] In Figure 7.1a, the

terminal model curves plotted with literature values and the best-fit estimates from this work almost coincide.

The introduction of BuOH or DMF solvent into the system has the same effect on HEMA incorporation as observed for its copolymerization with ST and with BMA; the relative reactivity of HEMA monomer to radical addition is reduced compared to its relative reactivity in the absence of solvent, resulting in a decreased level of HEMA incorporation. These results can be interpreted using the same explanations presented in Ch 5 for BMA/HEMA copolymerization: introduction of DMF disrupts the intermolecular H-bonding of HEMA making it less reactive, while the addition of BuOH leads to H-bonding formation with BA, increasing its reactivity to radical addition. To fit the composition data obtained in solution, the monomer reactivity ratios are estimated as r_{BA}=0.29±0.14, r_{HEMA}=3.57±2.17; a single fit was performed to the data obtained in BuOH and in DMF as the results cannot be distinguished. These monomer reactivity ratios are close to values reported by Aerdts et al.[2] for bulk BA/BMA copolymerization, r_{BA}=0.395 and r_{BMA}=2.279. Thus, it is found that BA/HEMA copolymer composition in BuOH or DMF approaches the BA/BMA bulk system.

In Figure 7.1b, the terminal model prediction for BA/BMA copolymer composition using these literature monomer reactivity ratios is compared to experimental data obtained in this study for BA/BMA copolymerization in bulk and BuOH. The very good fit indicates that any H-bonding effect on reactivity that might occur influences both BA and BMA to the same extent, such that the net effect on the reactivity ratios is negligible.

The copolymerization propagation rate coefficients ($k_{p,cop}$) at 50 °C are also determined by PLP-SEC with different monomer compositions; the detailed experimental data are listed in Appendix A.5. Due to the solubility issue of HEMA-rich copolymer in THF, the highest HEMA

monomer composition examined was 50%. Although the $k_{p,cop}$ behavior over the complete composition range cannot be reviewed, the solvent effect on $k_{p,cop}$ is still easy to identify. From Figure 7.2, it is clear that BuOH increases $k_{p,cop}$ significantly. As discussed in previous chapters, the addition of BuOH does not affect HEMA homopropagation, but significantly increases the rate coefficient of BMA homopropagation, and the PLP-SEC results in Ch 6 indicate that BuOH has a similar effect on BA k_p. The addition of DMF decreases the k_p value of HEMA and has no effect on BMA k_p (see Ch 3); assuming that DMF does not influence BA k_p, the decrease in $k_{p,cop}$ seen in Figure 7.2 can be attributed to decreased HEMA reactivity in the presence of H-bonding disruptor DMF. The terminal model prediction with monomer reactivity ratios in bulk is also plotted in Figure 7.2. It fails to describe the $k_{p,cop}$ behavior of BA/HEMA copolymerization, especially at the BA-rich side. The underprediction of $k_{p,cop}$ by the terminal model is in agreement with the findings from a BA/MMA copolymerization study.[3]

Thus, all of the kinetic studies in this thesis provide consistent evidence of how intermolecular H-bonding affects HEMA (or HEA) reactivity during bulk copolymerization relative to the same system with BMA (or BA), and how the influence can be reduced by adding DMF to the system. Similarly, addition of an alcohol to a BMA (or BA) system enhances the monomer reactivity compared to the bulk system.

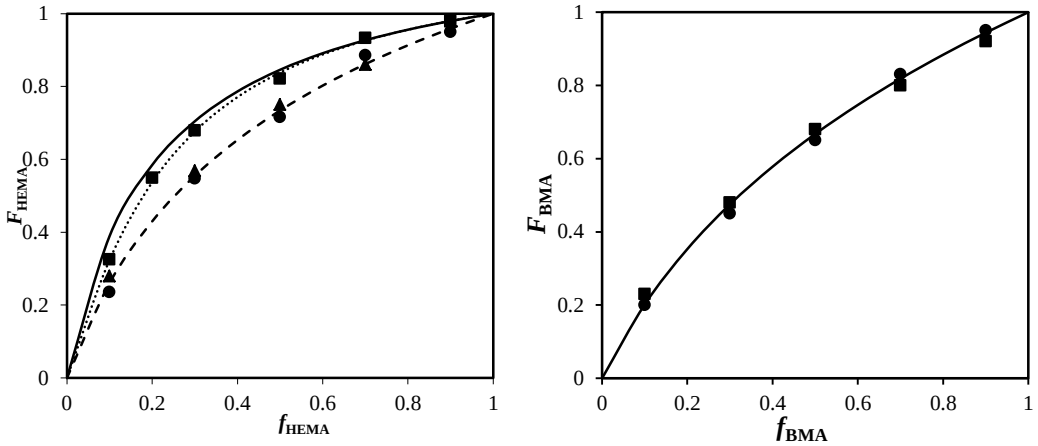

(a) (b)

Figure 7.1 Solvent effects on copolymer compositions from low conversion PLP experiments at 50 °C. (■, in bulk; ●, in BuOH; ▲, in DMF) (a) BA/HEMA copolymerization, described by mole fraction of HEMA in copolymer (F_{HEMA}) as a function of HEMA mole fraction in the monomer phase (f_{HEMA}). Lines are terminal model predictions with literature reactivity values (solid line), experimental values in bulk (dot line) and experimental values in solvents (dash line). (b) BA/BMA copolymerization system, described by mole fraction of BMA in copolymer (F_{BMA}) as a function of BMA mole fraction in the monomer phase (f_{BMA}) compared to predictions with literature reactivity ratios. (See text for further details.)

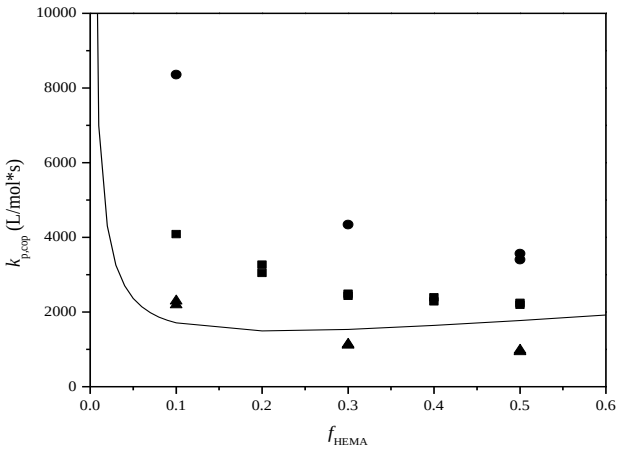

Figure 7.2 Copolymerization propagation rate coefficients ($k_{p,cop}$) data at 50 °C *vs.* 2-hydroxyethyl methacrylate (HEMA) monomer mole fraction (■, in bulk; ●, in BuOH; ▲, in DMF). Terminal model prediction for BA/HEMA in bulk is indicated by the solid curve.

7.2 Semibatch Copolymerization of BA/HEMA

7.2.1 BA/HEMA in 35 wt% solvent at 138 °C

Semibatch experiments of BA/HEMA with 12.5 and 25 wt% HEMA were carried out in 35 wt% xylene, DMF or *n*-pentanol at 138 °C, to study the combined effect of solvent on copolymer MWs and branching levels. Figure 7.3 shows the resultant total monomer concentration $[M]_{tot}$, comonomer compositon f_{HEMA} and copolymer M_w profiles for semibatch copolymerization of BA/HEMA. While containing results for 6 reactions, and thus a bit crowded, these plots are useful to examine the general trends. Later discussion will compare the BA/HEMA profiles to those for BA/BMA copolymerization at identical conditions, as well as branching levels measured on the final copolymer samples.

It is found that the total monomer concentration in PeOH is always lower than that found in xylene or DMF. This result is consistant with the $k_{p,cop}$ results of Figure 7.2: $k_{p,cop}$ of BA/HEMA in BuOH is higher, with the increased reactivity leading to a decreased total monomer concentration under semibatch operation. Following the same reasoning, it would be expected that monomer concentration should be highest for the polymerization in DMF. While the data provide some indication that this is true, the scatter is too great to draw firm conclusions. From Figure 7.1, the HEMA monomer fraction required to produce copolymer with F_{HEMA}=0.25 should be lowered in bulk compared to in BuOH or DMF. Assuming that reaction in xylene is similar to the bulk system, and that PeOH and BuOH provide similar results, the f_{HEMA} semibatch data are consistant with that expectation; while scattered, the values of f_{HEMA} in xylene are lower than measured in the other solvents. As expected, the free HEMA level is lower for the experiments conducted with 12.5% HEMA in the feed.

As found for other HEMA copolymerization systems, polymer MW decreases when HEMA

content is lowered from 25 to 12.5%. However, the magnitude of the decrease is much lower for BA/HEMA, as are the absolute polymer MWs compared to ST/HEMA and BMA/HEMA copolymerizations. It was also found that copolymer MWs produced in xylene and DMF are always higher than in PeOH, a result very different than found for BA homopolymerization (Ch 6). In addition, the large difference in MWs found between ST/HEMA and BMA/HEMA copolymers produced in xylene vs DMF at 138 °C is not found for BA/HEMA. It is a significant challenge to explain all of these observations, which are discussed in more detail below.

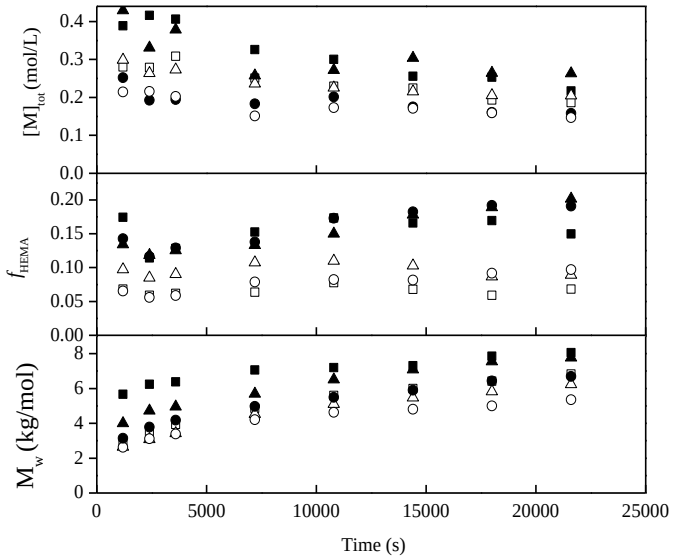

Figure 7.3 Total monomer concentration, HEMA monomer fraction and polymer molecular weight experimental profiles for BA/HEMA semibatch copolymerizations at 138 °C with BA/HEMA mass ratio of 75/25 and 87.5/12.5 with 65 wt% final polymer content and 1.5 mol% TBPA relative to monomer. Solid symbols indicate reactions with 25% HEMA, and empty symbols indicate reactions with 12.5% HEMA. ■□ reactions in xylene, ▲△ reactions in DMF, ●○ reactions in *n*-pentanol.

7.2.2 BA/HEMA *vs.* BA/BMA in 35 wt% solvent at 138 °C

Figure 7.4 compares semibatch reaction results of BA/BMA (a) and BA/HEMA (b) under the same operating conditions, produced with 25% methacrylate. Solvent choice has no effect on

BA/BMA polymer MWs or free monomer levels. While this result was also found for ST/BMA copolymerization (Ch 4), the expectations for BA/BMA were different because of the influence of H-bonding on BA backbiting demonstrated in Ch 6. (PeOH reduces backbiting for BA homopolymerization, thus increasing polymer MW by a factor of 2 at 138 °C.) The M_w values of the final polymers are summarized in Table 7.1, with the branchpoint (^{13}C NMR) and macromer content (proton NMR) data of the final copolymer samples summarized in Table 7.2. Unlike found for homopolymerization of BA, use of PeOH as a solvent (compared to xylene) does not cause a reduction in branchpoint (or macromer) levels. This result may indicate preferred H-bonding formation with methacrylate rather than acrylate units in the copolymer. To test this hypothesis, the intensities of H-bonding signal in FT-IR spectra of pBA and pBMA are compared in Figure 7.5. Both polymers are produced at 138 °C, precipitated and re-dissolved in solvents at 50 wt%. The IR peaks are normalized by the intensity of carbonyl signal at 1720 cm^{-1}, thus it is meaningful to compare the H-bonding signal intensity with the same conditions. Figure 7.5a shows the comparison in xylene and the carbonyl signals of pBA and pBMA present similar shape and intensity. Figure 7.5b compares the spectra in BuOH: while evidence of H-bonding is seen both for pBA and pBMA, the signal intensity of pBMA is about 10% higher than pBA. While this difference is small, it indirectly supports the preference of H-bonding formation with methacrylate over acrylate units in the polymer chain.

For BA/HEMA semibatch copolymerization, the solvent choice affects free monomer concentrations (Figure 7.4), but has little effect on polymer MWs or branching levels (Tables 7.1 and 7.2). The poly(BA/HEMA) MW values are not significantly higher than the values for poly(BA/BMA), a finding very different from the effects found when substituting HEMA for BMA during copolymerization with ST (Ch 4) or BMA (Ch 5). Note that the weight-average

MWs of BA/HEMA (and BA/BMA) copolymers are below 8 kg/mol, which is only one tenth of the maximum value of ST/HEMA copolymer. These differences suggest that the branching reaction caused by dimethacrylate impurity in HEMA, and how it is influenced by solvent choice, is of much reduced importance for the BA/HEMA system.

In order to study the influence of EGDMA on the MW of poly(BA), semibatch experiments of BA homopolymerization (138 °C in xylene) with and without 100 ppm added EGDMA are compared, with MW results plotted in Figure 7.6. In contrast to BMA homopolymerizations, the addition of EGDMA has negligible effect on poly(BA) MWs. This result, while not understood on a mechanistic level, explains why BA/BMA and BA/HEMA copolymers differ little in MW, and why absolute MW levels are so much lower than found for other HEMA-containing copolymers.

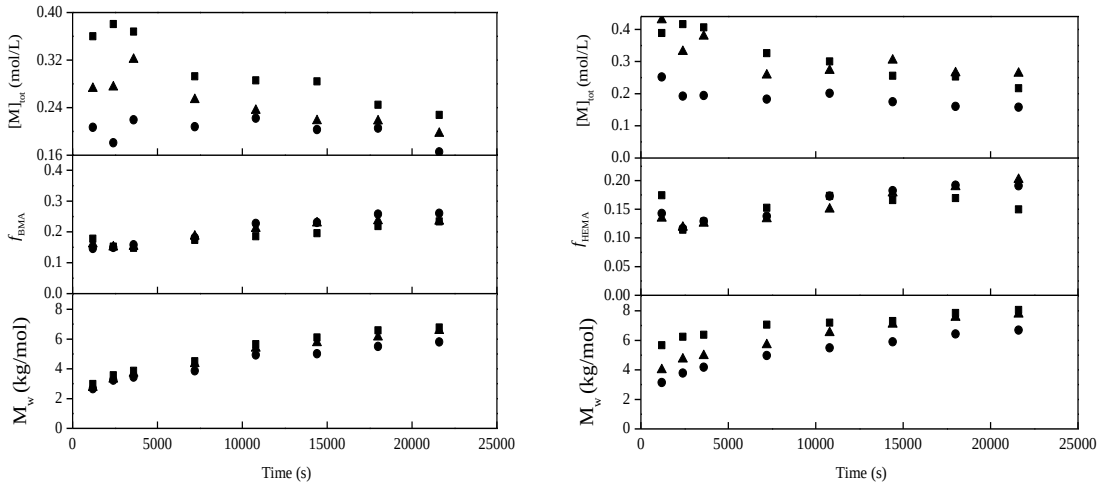

(a) (b)

Figure 7.4 Total monomer concentration, BMA or HEMA monomer fraction and polymer weight-average molecular weight experimental profiles for (a) BA/BMA and (b) BA/HEMA semibatch copolymerizations at 138 °C with BMA or HEMA mass ratio of 25% with 65 wt% final polymer content and 1.5 mol% TBPA relative to monomer. ■ reactions in xylene, ▲ reactions in DMF, ● reactions in *n*-pentanol.

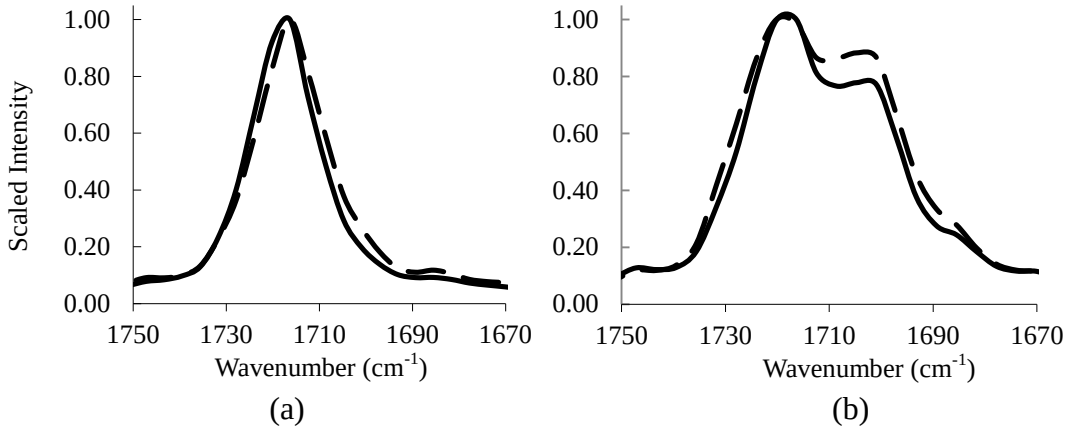

Figure 7.5 FT-IR spectra of the carbonyl stretching region of pBA (solid curve) and pBMA (dash curve) in (a) xylene and (b) BuOH.

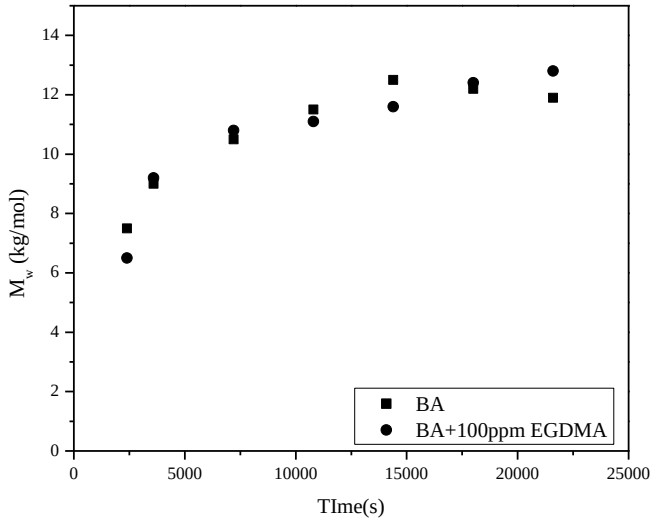

Figure 7.6 Polymer weight-average MW profiles for semibatch homopolymerization of BA with or without 100 ppm added EGDMA at 138 °C with 35 wt% xylene.

7.2.3 BA/HEMA semibatch experiments at 110 °C *vs.* 138 °C

The combined effect of temperature and solvent choice on BA/HEMA copolymerization H-bonding has also been studied. Figure 7.7a plots semibatch experiment profiles at 110 °C with 0.5 mol% BPO, 70 wt% solvent and 12.5 wt% HEMA fed over three hours, while Figure 7.7b

shows experiments at 138 °C with 1.5 mol% TBPA, 35 wt% solvent and 12.5 wt% HEMA fed over six hours. Although the absolute values can not be compared due to different experimental conditions, the relative difference among the three solvents is still distinctive. It is obvious that all the relative difference among three solvents at 138 °C is much smaller than that at 110 °C, indicating that the solvent effect is weakened with increasing temperature, as also seen for the ST/HEMA system discussed in Ch 4.

Table 7.1 and 7.2 summarizes the weight-average MWs, macromonomer level and branching level of final polymers from BA homopolymerization, BA/BMA and BA/HEMA copolymerization in different solvents at 110 °C and 138 °C. The significant solvent effect on BA homopolymerization values disappears in BA copolymerization systems, including the effect of alcohol (BuOH or PeOH) solvent on short chain branching of BA. In addition, the level of branching is only slightly reduced upon the addition of methacrylate (BMA or HEMA), from 10% decrease for homopolymerization of BA to 8% upon addition of 12.5% HEMA and to 6-7% upon addition of 25% HEMA or BMA at 138 °C (Table 7.2). In contrast, González et al.[4] found in the emulsion copolymerization of BA/MMA at 80 °C that the branching level was reduced from 2.6% for pure BA to 0.3% for a 75/25 BA/MMA copolymer. However, in their system, the addition of MMA also reduced the lower instantaneous conversion of the system. The copolymer MWs (Table 7.1) are always highest in xylene and lowest in BuOH or PeOH, which opposite that was found for BA homopolymerization (Ch 6). As hypothesized earlier, solvents may prefer to form H-bonds with methacrylate rather than acrylate units in the polymer chain, thus the H-bonding effect on branching observed in BA homopolymerization disappears in BA/methacrylate copolymerizations.

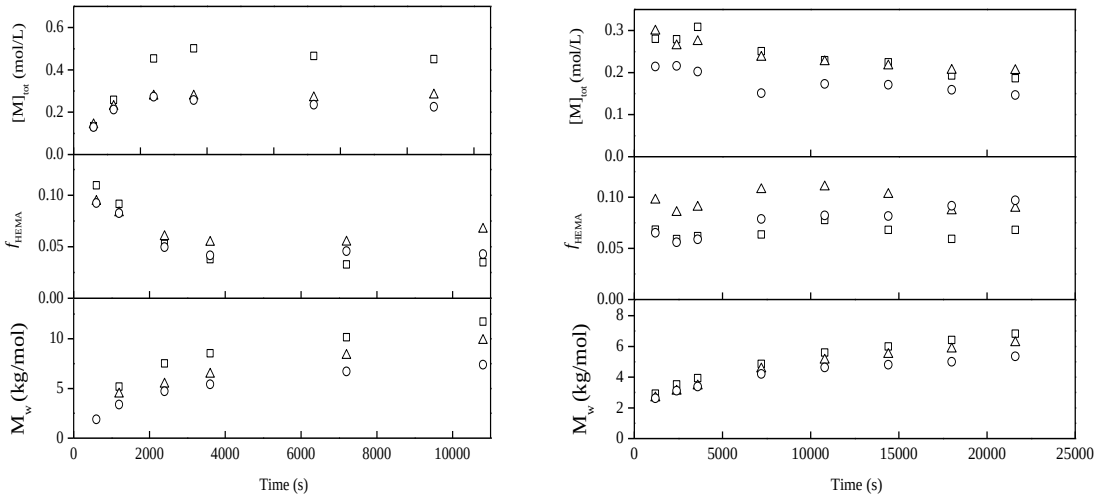

Figure 7.7 Total monomer concentration, HEMA monomer fraction and polymer weight-average molecular weight experimental profiles for BA/HEMA semibatch copolymerization at (a) 110 °C, 0.5 mol% BPO, 70 wt% solvent fraction, 3h feed, 12.5 wt% HEMA; (b) 138 °C, 1.5 mol% TBPA, 35 wt% solvent fraction, 6h feed, 12.5 wt% HEMA monomer fraction. □ reactions in xylene, △ reactions in DMF, ○ reactions in *n*-butanol (110 °C) or *n*-pentanol (138 °C).

Table 7.1 The weight-average MW (kg/mol) of final polymer produced by BA homopolymerization or BA/BMA and BA/HEMA copolymerization under different conditions.

M_w (kg/mol)	BA	BA/BMA (25wt%BMA)	BA/HEMA (12.5wt%HEMA)	BA/HEMA (25wt%HEMA)
30wt%Polymer, 110°C:				
In xylene	11.3	--	11.7	--
In DMF	--	--	9.84	--
In BuOH	55.7	--	7.39	--
65wt%Polymer, 138°C:				
In xylene	5.94	6.77	6.83	8.06
In DMF	4.66	6.56	6.24	7.76
In PeOH	10.0	5.81	5.35	6.70

Table 7.2 The macromonomer level (MM%) and branching level (BL%) of final polymer produced by BA homopolymerization or BA/BMA and BA/HEMA copolymerization under different conditions.

MM%/BL%	BA	BA/BMA (25wt%BMA)	BA/HEMA (12.5wt%HEMA)	BA/HEMA (25wt%HEMA)
30wt%Polymer,110°C:				
In xylene	0.65/6.02	--	0.49/5.15	--
In DMF	--	--	0.59/5.19	--
In BuOH	0.13/1.14	--	0.62/5.36	--
65wt%Polymer,138°C:				
In xylene	0.38/9.78	0.26/7.07	0.28/8.17	0.21/5.98
In DMF	0.43/9.85	0.27/7.14	0.34/8.35	0.23/6.11
In PeOH	0.21/5.87	0.31/7.19	0.32/8.28	0.20/6.05

Conclusions

Solvent effects on BA/HEMA copolymerization have been studied. Kinetic experiments show that HEMA preferentially incorporates into copolymers in bulk, while the terminal model prediction underestimates the $k_{p,cop}$ values. BuOH and DMF influence H-bonding such that BA and HEMA demonstrate the same relative reactivity in both solvents; $k_{p,cop}$ values in DMF are reduced compared to bulk while those in BuOH are increased.

Semibatch experiments have also been conducted with BA/HEMA. As conclusions of all the analysis above, BA/HEMA semibatch copolymerization has the following features.

- The shift in free monomer level and composition measured during semibatch operations with solvent choice are well explained by the kinetic studies.
- The branching reaction leading to increased MWs caused by EGDMA impurity in HEMA when copolymerized with ST or BMA does not occur for HEMA/BA copolymerization.

This result is verified by a BA homopolymerization experiment with 100 ppm added EGDMA.

- H-bonding does not play an important role in BA/HEMA copolymerization, despite the influence of alcohol on backbiting during BA homopolymerization. FT-IR suggests that BuOH and PeOH preferentially form H-bond with methacrylate units in polymer chain rather than acrylate, a possible explanation for this result.

References

1. Varma, I. K.; Patnaik, S. *Euro. Polym. J.* **1976**, *12*, 259.
2. Aerdts, A. M.; German, A. L.; van der Velden, G. P. M. *Magnetic Resonance in Chemistry* **1994**, *32*, S80.
3. Hutchinson, R. A.; McMinn, J. H.; Paquet, D. A.; Jr.; Beuermann, S.; Jackson, C. *Ind. Eng. Chem. Res.* **1997**, *36*, 1103.
4. González, I.; Asua, J. M.; Leiza, J. R. *Polymer* **2007**, *48*, 2542.

Chapter 8 Conclusions and Recommendations

8.1 Conclusions

Kinetic and semibatch studies on free radical copolymerization of hydroxyl-functional monomers have been carried out for a range of monomer and solvent systems and operating conditions. The PLP-SEC-NMR technique has been employed to investigate copolymerization kinetics of HEMA and HEA with ST, HEMA with BMA and HEMA with BA both in bulk and in solution. Semibatch experiments further examine the kinetic behavior of these copolymerization systems and reveal more complex behaviour under industrial conditions. A range of characterization methods, including GC, SEC, ^{1}H NMR, ^{13}C NMR and FT-IR, are used to investigate the kinetics and solvent effects.

8.1.1 Kinetics Studies

PLP studies have been completed on ST/HEMA, BMA/HEMA and BA/HEMA copolymerization both in bulk and in solutions. The comparison studies with ST/BMA and BA/BMA reveal the solvent effect that DMF disrupts the intermolecular H-bonding of HEMA, such that HEMA reactivity decreases towards that of BMA, while BuOH increases the reactivity of BMA and BA. The terminal model can still be used to represent copolymer composition data, with a systematic variation in monomer reactivity ratios with solvent choice and concentration. The copolymer propagation rate coefficients, $k_{p,cop}$, increase in BuOH due to H-bonding formation with BMA or BA and decrease in DMF due to the H-bonding disruption.

A study of ST/HEA copolymerization is also presented in this thesis. HEA exhibits higher

reactivity to ST radicals than do alkyl acrylates such as MA and BA. The unexpected successful PLP study on HEA homopolymerization in bulk draws attention to the H-bonding effect on acrylate polymerization. Thus, PLP-SEC experiments and ^{13}C NMR analysis for pHEA and pBA have been compared in bulk and in solution. The influence of H-bonding on acrylate backbiting mechanism is shown by the reduction of branching by the addition of BuOH to BA and the increase in branching by the addition of DMF to HEA.

8.1.2 Semibatch Studies

A series of semibatch studies has been carried on with copolymerization of ST/HEMA, BMA/HEMA and BA/HEMA with various conditions. In order to have an overview of solvent effect on different systems, the copolymerization profiles at 138 °C with 65 wt% solid content and 25 wt% methacrylate monomer ratio are re-organized and compared. Firstly, ST/BMA and BA/BMA copolymerization are compared in Figure 8.1. No effect of solvent choice is observed in the two systems, which is consistent with PLP-SEC results. However, it is surprising to observe little effect from PeOH on BA/BMA copolymerization, as solvent has a strong effect on backbiting during BA homopolymerization. Finally, it can be seen that total free monomer level and polymer MWs are significantly higher for ST/BMA than BA/BMA semibatch copolymerization. This behaviour is consistent with previous experimentation and is well represented by previous models developed for the systems.

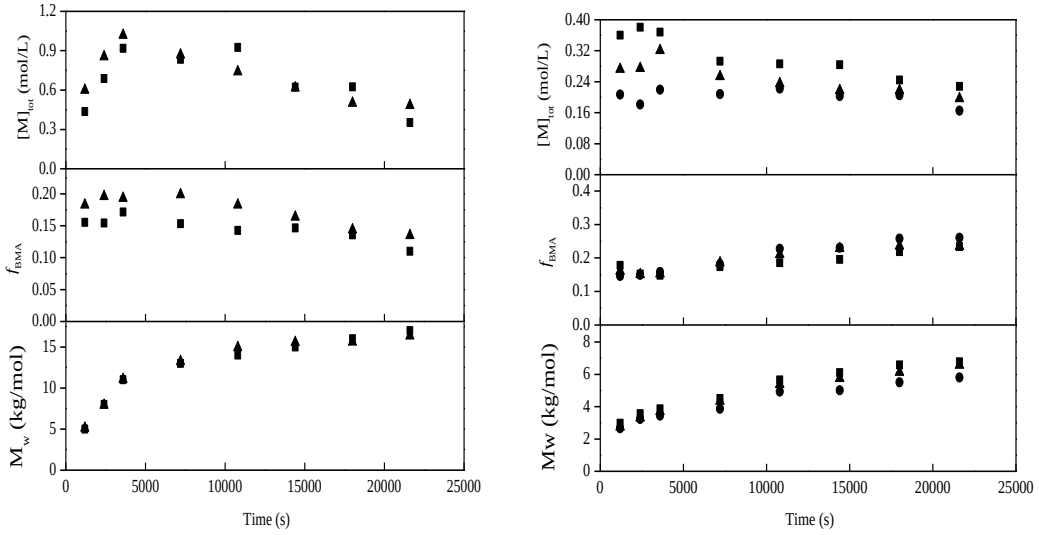

(a) (b)

Figure 8.1 Total monomer concentration, BMA monomer ratio and polymer weight-average molecular weight experimental profiles for (a) ST/BMA and (b) BA/BMA semibatch copolymerizations at 138 °C with BMA mass ratio of 25%. Specified monomer mass ratio in the feed is with 65 wt% final polymer content and 1.5 mol% TBPA relative to monomer. ■ reactions in xylene, ▲ reactions in DMF, ● reactions in *n*-pentanol.

The experimental profiles of semibatch ST/HEMA, BMA/HEMA and BA/HEMA polymerizations are compared in Figure 8.2-8.4. As seen in Figure 8.2, the total monomer concentration in the three systems is always higher for polymerizations conducted in DMF, in agreement with the kinetic studies finding that the HEMA copolymerization systems in DMF always have lower $k_{p,cop}$ values, thus lower reaction rates and higher total free monomer concentrations under semibatch conditions. Similarly, $k_{p,cop}$ was found to be higher for BA/HEMA in butanol, a result consistent with the lower free monomer concentrations observed for the BA/HEMA semibatch polymerization conducted in pentanol. Figure 8.3 plots the HEMA monomer fraction in the three systems for different solvent choices. For ST/HEMA and BMA/HEMA, the f_{HEMA} values are higher in DMF than in xylene, a finding explained by the kinetic studies on copolymer composition that found that HEMA monomer is less reactive (thus

requiring a higher mole fraction to achieve the same copolymer composition) in DMF than in xylene. For BA/HEMA, the values of f_{HEMA} in xylene are lower than measured in the other solvents, while the scatter is too great to draw firm conclusions. It is expected from the kinetic studies that the HEMA monomer fraction required to produce copolymer with F_{HEMA}=0.25 should be lowered in bulk (xylene) compared to in BuOH or DMF. Thus, it is seen that the effect of solvent on semibatch HEMA copolymerization free monomer levels and composition is well understood and predictable from the kinetic studies.

The comparison of weight-average MWs of HEMA copolymers is shown as Figure 8.4. The polymer M_w values for ST/HEMA and BMA/HEMA are significantly higher than those produced in ST/BMA and BMA semibatch systems. Experiments conducted have shown that this large increase in MW is related to the dimethacrylate impurity found in HEMA monomer. The polymer MWs produced in DMF solution are higher than those from polymerization in xylene, due to the higher free monomer levels. Such lower MWs are observed for BA/HEMA copolymers and no effect of EGDMA is found. The former result is consistent with BA/BMA results (see Figure 8.1), and the latter finding was confirmed by experiments run with EGDMA added to BA homopolymerization. The reduced influence of EGDMA impurities on acrylate polymerization is a surprising result that requires further study. Also surprisingly, the H-bonding effect on acrylate short chain branching disappears in copolymerization, with BA/HEMA polymer MWs produced in PeOH lower than the values for polymer produced in xylene and DMF.

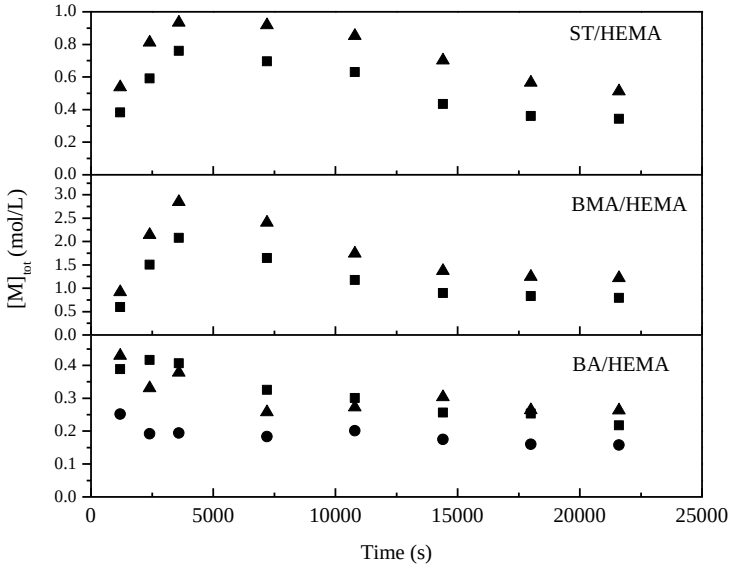

Figure 8.2 The comparison of total monomer concentration, $[M]_{tot}$ (mol/L), in the semibatch experiments of ST/HEMA, BMA/HEMA and BA/HEMA at 138 °C with HEMA mass ratio of 25%. Specified monomer mass ratio in the feed is with 65 wt% final polymer content and 1.5 mol% TBPA relative to monomer. ■ reactions in xylene, ▲ reactions in DMF ● reactions in *n*-pentanol.

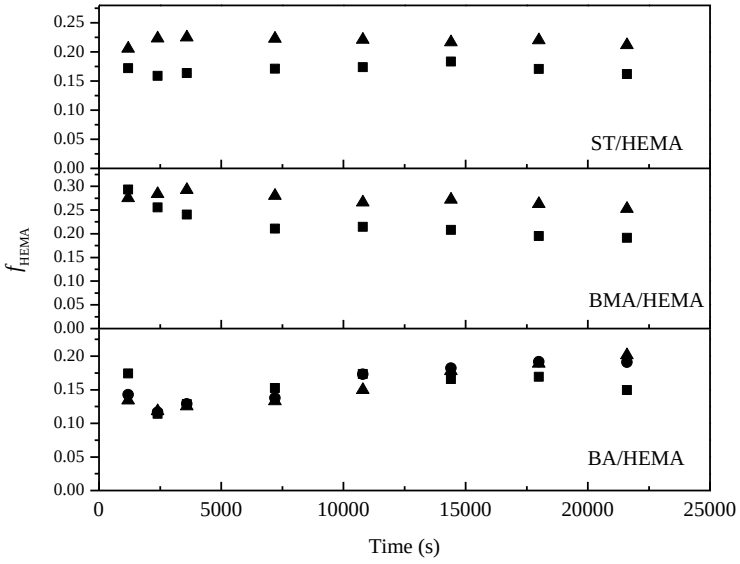

Figure 8.3 The comparison of HEMA monomer fraction, f_{HEMA}, in the semibatch experiments of ST/HEMA, BMA/HEMA and BA/HEMA at 138 °C with HEMA mass ratio of 25%. Specified monomer mass ratio in the feed is with 65 wt% final polymer content and 1.5 mol% TBPA relative to monomer. ■ reactions in xylene, ▲ reactions in DMF, ● reactions in *n*-pentanol.

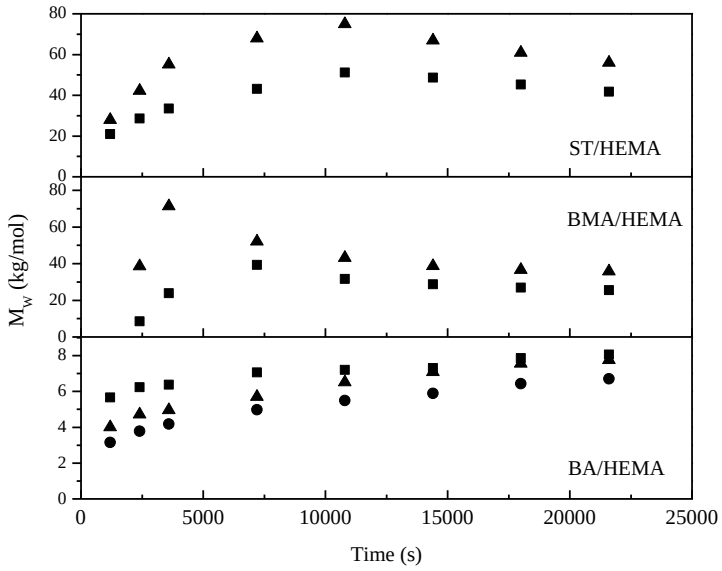

Figure 8.4 The comparison of weight-average molecular weight of polymers in the semibatch experiments of ST/HEMA, BMA/HEMA and BA/HEMA at 138 °C with HEMA mass ratio of 25%. Specified monomer mass ratio in the feed is with 65 wt% final polymer content and 1.5 mol% TBPA relative to monomer. ■ reactions in xylene, ▲ reactions in DMF, ● reactions in *n*-pentanol.

8.2 Recommendations

The general understanding of solvent effects on free radical polymerization kinetics has been furthered by this work. However, some unexpected results still need to be clarified.

- In ST/HEMA copolymerization kinetic study, the fact that *s* and *r* values determined in bulk provide a good representation of $k_{p,cop}$ curves for H-bonding systems but not copolymer composition is surprising.
- It has been verified experimentally that 100 ppm dimethacrylate impurity in HEMA leads to a significant increase of polymer MWs in semibatch reactions when copolymerized with ST or BMA, but not with BA. Furthermore, the magnitude of the effect with EGDMA is dependent on solvent choice. These mechanisms need to be further explored

and, if possible, modeled.

- A hypothesis to explain the disappearance of the H-bonding effect on acrylate short chain branching in copolymerization has been proposed in Ch 7. However, the supporting evidence is weak; thus, it is strongly recommended to develop a new experimental method to monitor the H-bonding in situ, such as online FT-IR or NMR.
- Further studies can be extended to copolymerization of methacrylates and HEA, a system important to industry. An increase of copolymer MW is expected, as EGDMA impurity also is found in HEA monomer. It is also interesting to look at the branching level of BMA/HEA copolymers.

Finally, this work provides a solid basis for understanding of copolymerization kinetics utilizing HEMA as a hydroxyl-functional monomer. Future work may concentrate on the modeling of these H-bonding effects within the framework of Predici.

Appendices

Appendix A.1: PLP/SEC/NMR Results for Styrene/Methacrylate Systems (Ch 3)

Table A.1.1 50-120℃ Bulk Styrene/HEMA PLP experimental conditions and results with [DMPA]=5mmol·L^{-1}

T (℃)	Pulse Repetition Rate (Hz)	Monomer Mole Fraction f_{HEMA}	Polymer Mole Fraction F_{HEMA}	Conversion %	SEC Result						
					RI			LS			$k_{p,cop,LS}/k_{p,cop,RI}$
					M_1 (g·mol^{-1})	M_2/M_1	$k_{p,cop}$ from M_1 (L·mol^{-1}·s^{-1})	M_1 (g·mol^{-1})	M_2/M_1	$k_{p,cop}$ from M_1 (L·mol^{-1}·s^{-1})	
50	50	0	0	2.0	4365	2.00	246	4266	2.00	241	0.98
				2.2	4365	2.00	246	4266	2.00	241	0.98
50	33	0	0	1.8	6457	2.00	243	6310	2.00	237	0.98
				1.9	6607	2.00	248	6310	2.00	237	0.95
50	50	0.1	0.24	2.0	4898	2.00	276	4786	2.00	270	0.98
				1.8	5012	1.95	283	4786	2.00	270	0.95
50	33	0.1	0.24	1.8	7413	1.95	279	7079	1.95	266	0.95
				1.6	7413	2.00	279	7244	2.00	273	0.98
50	50	0.2	0.35	1.7	5888	2.00	326	5623	2.09	312	0.95
				2.0	5888	2.00	326	5754	2.04	319	0.98
50	33	0.2	0.35	2.1	8710	2.00	321	8511	1.95	314	0.98
				2.2	8913	2.00	329	8511	2.00	314	0.95
50	50	0.3	0.43	1.9	6918	2.00	376	6607	2.00	360	0.95
				2.3	6918	1.91	376	6761	1.95	368	0.98
50	33	0.3	0.43	2.1	10233	1.95	371	10000	2.00	362	0.98
				1.7	10471	1.91	380	10000	2.00	362	0.95

Table A.1.1 (Continued).

T (℃)	Pulse Repetition Rate (Hz)	Monomer Mole Fraction f_{HEMA}	Polymer Mole Fraction F_{HEMA}	Conversion %	SEC Result						
					RI			LS			$k_{p,cop,LS}/k_{p,cop,RI}$
					M_1 ($g \cdot mol^{-1}$)	M_2/M_1	$k_{p,cop}$ from M_1 ($L \cdot mol^{-1} \cdot s^{-1}$)	M_1 ($g \cdot mol^{-1}$)	M_2/M_1	$k_{p,cop}$ from M_1 ($L \cdot mol^{-1} \cdot s^{-1}$)	
50	50	0.4	0.49	2.0	8511	1.95	455	8128	1.95	435	0.95
				1.8	8318	2.00	445	8128	1.95	435	0.98
50	33	0.4	0.49	1.9	12303	2.00	439	12023	1.95	429	0.98
				2.3	12303	2.00	439	12023	2.00	429	0.98
50	50	0.7	0.66	2.1	14791	2.00	765	14125	2.00	731	0.95
				1.9	14454	1.95	748	14125	2.00	731	0.98
50	33	0.7	0.66	1.6	20893	2.00	720	20417	2.04	704	0.98
				2.1	21380	1.95	737	20417	2.00	704	0.95
50	50	0.9	0.84	2.0	n/d	n/d	n/d	n/d	n/d	n/d	n/d
				1.9	n/d	n/d	n/d	n/d	n/d	n/d	n/d
50	33	0.9	0.84	2.0	n/d	n/d	n/d	n/d	n/d	n/d	n/d
				1.9	n/d	n/d	n/d	n/d	n/d	n/d	n/d
70	50	0	0	2.1	8511	2.00	488	8318	2.00	477	0.98
				2.5	8511	2.00	488	8318	2.00	477	0.98
70	50	0.1	0.24	2.0	10000	1.95	563	9772	2.00	550	0.98
				2.3	9772	2.00	550	9550	2.04	537	0.98
70	50	0.2	0.35	2.1	11749	1.91	650	11220	1.95	620	0.95
				2.2	11482	1.95	635	11220	2.00	620	0.98
70	50	0.3	0.43	2.0	13804	2.00	750	13490	2.00	733	0.98
				2.5	13804	2.00	750	13490	2.00	733	0.98

TableA.1.1 (Continued).

T (℃)	Pulse Repetition Rate (Hz)	Monomer Mole Fraction f_{HEMA}	Polymer Mole Fraction F_{HEMA}	Conversion %	SEC Result						
					RI			LS			$k_{p,cop,LS}/k_{p,cop,RI}$
					M_1 ($g\cdot mol^{-1}$)	M_2/M_1	$k_{p,cop}$ from M_1 ($L\cdot mol^{-1}\cdot s^{-1}$)	M_1 ($g\cdot mol^{-1}$)	M_2/M_1	$k_{p,cop}$ from M_1 ($L\cdot mol^{-1}\cdot s^{-1}$)	
70	50	0.4	0.49	2.6	16596	2.00	887	15849	1.91	848	0.95
				2.0	16596	1.95	887	16218	2.00	867	0.98
70	50	0.5	0.54	2.1	19055	2.00	1003	18621	2.00	980	0.98
				2.2	19498	2.00	1026	18621	2.00	980	0.95
70	50	0.7	0.66	2.2	28184	1.95	1439	26915	2.00	1374	0.95
				2.3	28184	2.00	1439	27542	1.95	1406	0.98
70	50	0.9	0.84	2.1	n/d	n/d	n/d	n/d	n/d	n/d	n/d
				2.7	n/d	n/d	n/d	n/d	n/d	n/d	n/d
90	50	0	0	2.0	14125	2.00	822	13804	2.00	803	0.98
				2.4	14125	2.00	822	13804	2.00	803	0.98
90	50	0.1	0.24	2.2	16982	2.00	970	16218	1.95	927	0.95
				2.3	16982	2.00	970	16596	2.00	948	0.98
90	50	0.2	0.35	2.1	20417	2.00	1146	19953	2.00	1120	0.98
				2.0	20417	1.95	1146	19953	2.00	1120	0.98
90	50	0.3	0.43	2.2	25704	2.00	1417	24547	2.04	1353	0.95
				2.2	25704	2.00	1417	25119	2.00	1385	0.98
90	50	0.4	0.49	2.1	30903	2.00	1675	30200	2.00	1637	0.98
				2.4	31623	2.00	1714	30903	1.95	1675	0.98
90	50	0.5	0.54	2.1	38905	1.95	2074	37154	2.00	1981	0.95
				2.1	38019	1.95	2027	36308	2.00	1936	0.95

Table A.1.1 (Continued).

T (℃)	Pulse Repetition Rate (Hz)	Monomer Mole Fraction f_{HEMA}	Polymer Mole Fraction F_{HEMA}	Conversion %	SEC Result						
					RI			LS			$k_{p,cop,LS}/k_{p,cop,RI}$
					M_1 ($g \cdot mol^{-1}$)	M_2/M_1	$k_{p,cop}$ from M_1 ($L \cdot mol^{-1} \cdot s^{-1}$)	M_1 ($g \cdot mol^{-1}$)	M_2/M_1	$k_{p,cop}$ from M_1 ($L \cdot mol^{-1} \cdot s^{-1}$)	
90	50	0.7	0.66	2.0	50119	2.00	2589	47863	1.95	2472	0.95
				2.3	50119	2.00	2589	48978	1.95	2530	0.98
90	50	0.9	0.84	2.0	n/d	n/d	n/d	n/d	n/d	n/d	n/d
				2.1	n/d	n/d	n/d	n/d	n/d	n/d	n/d
120	50	0	0	2.0	14125	2.00	822	13804	2.00	803	0.98
				2.5	14125	2.00	822	13804	2.00	803	0.98
120	50	0.1	0.24	2.4	16982	2.00	970	16218	1.95	927	0.95
				2.3	16982	2.00	970	16596	2.00	948	0.98
120	50	0.2	0.35	2.1	20417	2.00	1146	19953	2.00	1120	0.98
				2.0	20417	1.95	1146	19953	2.00	1120	0.98
120	50	0.3	0.43	2.2	25704	2.00	1417	24547	2.04	1353	0.95
				2.2	25704	2.00	1417	25119	2.00	1385	0.98
120	50	0.4	0.49	2.1	30903	2.00	1675	30200	2.00	1637	0.98
				2.4	31623	2.00	1714	30903	1.95	1675	0.98
120	50	0.5	0.54	2.3	38905	1.95	2074	37154	2.00	1981	0.95
				2.1	38019	1.95	2027	36308	2.00	1936	0.95
120	50	0.7	0.66	2.0	50119	2.00	2589	47863	1.95	2472	0.95
				2.1	50119	2.00	2589	48978	1.95	2530	0.98
120	50	0.9	0.84	2.0	n/d	n/d	n/d	n/d	n/d	n/d	n/d
				2.2	n/d	n/d	n/d	n/d	n/d	n/d	n/d

Table A.1.2. ST/HEMA solution copolymerization : PLP experimental conditions and results with [DMPA]=5mmol·L^{-1} at 90 ℃

T (℃)	Pulse Repetition Rate (Hz)	Solvent	Monomer Mole Fraction f_{HEMA}	Polymer Mole Fraction F_{HEMA}	Conversion %	SEC Result						
						RI			LS			
						M_1 (g·mol^{-1})	M_2/M_1	$k_{p,cop}$ from M_1 (L·mol^{-1}·s^{-1})	M_1 (g·mol^{-1})	M_2/M_1	$k_{p,cop}$ from M_1 (L·mol^{-1}·s^{-1})	$k_{p,cop,LS}/k_{p,cop,RI}$
90	50	50% Tol	0	0	2.1	15488	2.00	931	14791	2.00	889	0.95
					2.2	15136	2.00	910	14791	1.95	889	0.98
90	33	50% Tol	0	0	2.0	22387	1.95	898	21878	2.00	877	0.98
					1.9	22387	2.00	898	21878	2.00	877	0.98
90	25	50% Tol	0	0	2.2	30200	2.00	908	28840	2.00	867	0.95
					1.8	29512	1.95	887	28840	2.00	867	0.98
90	50	25% Tol	0	0	2.1	15488	1.95	916	15136	1.95	895	0.98
					2.2	15849	2.00	937	15136	2.00	895	0.95
90	50	25% DMF	0	0	1.9	12303	1.95	711	12023	1.95	695	0.98
					2.0	12303	1.95	711	12023	1.95	695	0.98
90	33	25% DMF	0	0	1.8	18197	2.00	702	17783	1.95	686	0.98
					1.8	18197	2.00	702	17783	1.95	686	0.98
90	25	25% DMF	0	0	1.9	24547	1.95	710	23988	2.00	694	0.98
					1.7	24547	2.00	710	23442	2.00	678	0.95
90	50	50% DMF	0	0	2.0	12303	2.00	707	12023	2.00	691	0.98
					1.7	12303	2.00	707	12023	1.95	691	0.98
90	50	50% BuOH	0	0	2.0	14791	2.00	920	14454	2.00	899	0.98
					1.8	14791	2.00	920	14454	1.95	899	0.98

Table A.1.2 (Continued)

T (℃)	Pulse Repetition Rate (Hz)	Solvent	Monomer Mole Fraction f_{HEMA}	Polymer Mole Fraction F_{HEMA}	Conversion %	SEC Result						
						RI			LS			$k_{p,cop,LS}/k_{p,cop,RI}$
						M_1 ($g\cdot mol^{-1}$)	M_2/M_1	$k_{p,cop}$ from M_1 ($L\cdot mol^{-1}\cdot s^{-1}$)	M_1 ($g\cdot mol^{-1}$)	M_2/M_1	$k_{p,cop}$ from M_1 ($L\cdot mol^{-1}\cdot s^{-1}$)	
90	50	50% Tol	0.1	0.27	2.0	18197	2.00	1085	17783	1.95	1060	0.98
					2.2	18197	2.00	1085	17378	2.00	1036	0.95
90	33	50% Tol	0.1	0.27	1.8	26303	1.95	1045	25119	1.95	998	0.95
					1.9	26915	1.95	1070	25704	1.95	1021	0.95
90	25	50% Tol	0.1	0.27	2.0	35481	1.95	1057	33884	2.00	1010	0.95
					1.8	35481	2.00	1057	34674	1.95	1033	0.98
90	50	25% Tol	0.1	0.25	1.8	19498	1.95	1035	19055	1.95	1012	0.98
					1.9	19953	1.95	1059	19498	1.95	1035	0.98
90	50	25% DMF	0.1	0.21	1.8	14454	1.95	825	13804	2.00	788	0.95
					2.0	14125	1.95	806	13804	2.00	788	0.98
90	33	25% DMF	0.1	0.21	2.1	20893	1.95	795	19953	2.00	759	0.95
					2.2	20417	1.95	777	19498	2.00	742	0.95
90	25	25% DMF	0.1	0.21	1.9	26915	2.00	768	26303	1.95	750	0.98
					2.3	27542	1.95	786	26915	1.95	768	0.98
90	50	50% DMF	0.1	0.17	2.1	13490	1.95	769	13183	1.95	751	0.98
					1.9	13804	2.00	786	13490	2.00	769	0.98
90	50	50% BuOH	0.1	0.17	2.0	16218	1.95	999	15849	1.95	976	0.98
					1.8	16596	2.00	1022	16218	2.00	999	0.98

Table A.1.2 (Continued)

T (℃)	Pulse Repetition Rate (Hz)	Solvent	Monomer Mole Fraction f_{HEMA}	Polymer Mole Fraction F_{HEMA}	Conversion %	SEC Result						
						RI			LS			$k_{p,cop,LS}/k_{p,cop,RI}$
						M_1 ($g \cdot mol^{-1}$)	M_2/M_1	$k_{p,cop}$ from M_1 ($L \cdot mol^{-1} \cdot s^{-1}$)	M_1 ($g \cdot mol^{-1}$)	M_2/M_1	$k_{p,cop}$ from M_1 ($L \cdot mol^{-1} \cdot s^{-1}$)	
90	50	50% Tol	0.2	0.40	2.1	21878	1.95	1292	20893	2.00	1234	0.95
					2.0	21380	1.95	1263	20893	2.00	1234	0.98
90	33	50% Tol	0.2	0.40	2.0	31623	2.00	1245	30903	2.00	1217	0.98
					1.9	31623	2.00	1245	30903	1.95	1217	0.98
90	25	50% Tol	0.2	0.40	2.0	41687	1.95	1231	40738	2.00	1203	0.98
					1.8	42658	2.00	1260	40738	2.00	1203	0.95
90	50	25% Tol	0.2	0.35	1.8	23442	2.00	1261	22909	2.00	1233	0.98
					1.9	23442	2.00	1261	22909	2.00	1233	0.98
90	50	25% DMF	0.2	0.31	1.8	16218	2.00	913	15849	1.95	892	0.98
					2.0	16218	1.95	913	15488	2.00	872	0.95
90	33	25% DMF	0.2	0.31	2.1	23442	2.00	880	22909	2.00	860	0.98
					2.0	23442	1.95	880	22909	2.00	860	0.98
90	25	25% DMF	0.2	0.31	1.9	31623	1.95	890	30903	2.00	870	0.98
					2.0	31623	2.00	890	30200	1.95	850	0.95
90	50	50% DMF	0.2	0.29	2.1	15488	2.00	875	15136	1.95	855	0.98
					1.9	15488	1.95	875	15136	2.00	855	0.98
90	50	50% BuOH	0.2	0.29	2.0	19498	2.00	1189	19055	1.95	1162	0.98
					1.9	19498	1.95	1189	19055	2.00	1162	0.98

Table A.1.2 (Continued)

T (℃)	Pulse Repetition Rate (Hz)	Solvent	Monomer Mole Fraction f_{HEMA}	Polymer Mole Fraction F_{HEMA}	Conversion %	SEC Result						
						RI			LS			$k_{p,cop,LS}/k_{p,cop,RI}$
						M_1 ($g \cdot mol^{-1}$)	M_2/M_1	$k_{p,cop}$ from M_1 ($L \cdot mol^{-1} \cdot s^{-1}$)	M_1 ($g \cdot mol^{-1}$)	M_2/M_1	$k_{p,cop}$ from M_1 ($L \cdot mol^{-1} \cdot s^{-1}$)	
90	50	50% Tol	0.3	0.48	2.0	26303	2.00	1540	25119	2.00	1471	0.95
					2.2	25704	2.00	1505	24547	2.00	1437	0.95
90	33	50% Tol	0.3	0.48	1.8	37154	2.00	1450	36308	1.95	1417	0.98
					2.0	38019	1.95	1484	37154	2.00	1450	0.98
90	25	50% Tol	0.3	0.48	2.0	50119	2.00	1467	48978	1.95	1434	0.98
					1.8	50119	2.00	1467	47863	2.00	1401	0.95
90	50	25% Tol	0.3	0.44	1.9	26915	1.95	1466	26303	2.00	1433	0.98
					2.2	27542	1.95	1501	26915	2.00	1466	0.98
90	50	25% DMF	0.3	0.40	1.9	18197	2.00	1011	17378	2.00	965	0.95
					2.0	18197	1.95	1011	17378	2.00	965	0.95
90	33	25% DMF	0.3	0.40	2.1	26303	2.00	974	25704	2.00	952	0.98
					2.2	26915	2.00	997	26303	2.00	974	0.98
90	25	25% DMF	0.3	0.40	1.9	35481	1.95	986	33884	1.95	941	0.95
					2.3	34674	2.00	963	33884	2.00	941	0.98
90	50	50% DMF	0.3	0.37	2.1	17783	2.00	995	17378	2.00	973	0.98
					1.9	18197	1.95	1019	17783	2.00	995	0.98
90	50	50% BuOH	0.3	0.37	2.0	22387	2.00	1353	21878	2.00	1322	0.98
					2.1	22909	1.95	1384	22387	2.00	1353	0.98

Table A.1.2 (Continued)

T (℃)	Pulse Repetition Rate (Hz)	Solvent	Monomer Mole Fraction f_{HEMA}	Polymer Mole Fraction F_{HEMA}	Conversion %	SEC Result						
						RI			LS			$k_{p,cop,LS}/k_{p,cop,RI}$
						M_1 ($g \cdot mol^{-1}$)	M_2/M_1	$k_{p,cop}$ from M_1 ($L \cdot mol^{-1} \cdot s^{-1}$)	M_1 ($g \cdot mol^{-1}$)	M_2/M_1	$k_{p,cop}$ from M_1 ($L \cdot mol^{-1} \cdot s^{-1}$)	
90	50	50% Tol	0.4	0.57	2.1	28840	2.00	1674	28184	2.00	1636	0.98
					2.0	28840	1.95	1674	28184	2.00	1636	0.98
90	33	50% Tol	0.4	0.57	2.0	42658	2.00	1651	41687	1.95	1614	0.98
					1.9	43652	2.00	1690	41687	2.00	1614	0.95
90	25	50% Tol	0.4	0.57	2.0	56234	1.95	1632	54954	2.00	1595	0.98
					1.8	56234	2.00	1632	54954	2.00	1595	0.98
90	50	25% Tol	0.4	0.51	1.8	30903	2.00	1702	30200	2.00	1664	0.98
					1.8	30903	2.00	1702	30200	1.95	1664	0.98
90	50	25% DMF	0.4	0.47	1.9	22387	2.00	1228	21380	2.00	1172	0.95
					2.0	21878	1.95	1200	20893	2.00	1146	0.95
90	33	25% DMF	0.4	0.47	2.1	31623	2.00	1156	30903	2.00	1130	0.98
					2.0	31623	2.00	1156	30200	2.00	1104	0.95
90	25	25% DMF	0.4	0.47	1.9	42658	2.00	1170	41687	1.95	1143	0.98
					2.1	42658	1.95	1170	41687	2.00	1143	0.98
90	50	50% DMF	0.4	0.45	2.1	21878	2.00	1214	21380	2.00	1187	0.98
					1.9	21878	2.00	1214	20893	2.00	1159	0.95
90	50	50% BuOH	0.4	0.45	2.0	27542	2.00	1649	26303	2.00	1575	0.95
					2.0	27542	2.00	1649	26915	1.95	1611	0.98

Table A.1.2 (Continued)

T (℃)	Pulse Repetition Rate (Hz)	Solvent	Monomer Mole Fraction f_{HEMA}	Polymer Mole Fraction F_{HEMA}	Conversion %	SEC Result						
						RI			LS			
						M_1 ($g \cdot mol^{-1}$)	M_2/M_1	$k_{p,cop}$ from M_1 ($L \cdot mol^{-1} \cdot s^{-1}$)	M_1 ($g \cdot mol^{-1}$)	M_2/M_1	$k_{p,cop}$ from M_1 ($L \cdot mol^{-1} \cdot s^{-1}$)	$k_{p,cop,LS}/k_{p,cop,RI}$
90	50	50% Tol	0.5	0.64	2.0	33113	2.00	1906	32359	2.00	1863	0.98
					2.2	32359	2.00	1863	31623	2.00	1821	0.98
90	33	50% Tol	0.5	0.64	1.8	48978	2.00	1880	47863	2.00	1837	0.98
					1.9	47863	1.95	1837	46774	2.00	1795	0.98
90	25	50% Tol	0.5	0.64	2.0	66069	2.00	1902	63096	2.00	1816	0.95
					1.8	64565	1.95	1859	61660	1.95	1775	0.95
90	50	25% Tol	0.5	0.57	1.8	33884	2.00	1885	33113	2.00	1842	0.98
					1.6	34674	1.95	1929	33884	2.04	1885	0.98
90	50	25% DMF	0.5	0.53	1.7	24547	2.00	1329	23988	2.00	1299	0.98
					2.0	24547	2.00	1329	23988	2.00	1299	0.98
90	33	25% DMF	0.5	0.53	2.1	37154	2.00	1341	36308	2.00	1311	0.98
					2.2	38019	1.95	1373	36308	1.95	1311	0.95
90	25	25% DMF	0.5	0.53	1.9	48978	1.95	1326	47863	2.00	1296	0.98
					2.3	47863	2.00	1296	46774	2.00	1267	0.98
90	50	50% DMF	0.5	0.51	2.1	25119	1.95	1382	24547	2.00	1351	0.98
					1.7	25704	1.95	1415	24547	2.00	1351	0.95
90	50	50% BuOH	0.5	0.51	2.0	30903	2.00	1833	30200	2.00	1792	0.98
					1.8	31623	2.00	1876	30200	2.00	1792	0.95

Table A.1.2 (Continued)

T (℃)	Pulse Repetition Rate (Hz)	Solvent	Monomer Mole Fraction f_{HEMA}	Polymer Mole Fraction F_{HEMA}	Conversion %	SEC Result						
						RI			LS			$k_{p,cop,LS}/k_{p,cop,RI}$
						M_1 ($g \cdot mol^{-1}$)	M_2/M_1	$k_{p,cop}$ from M_1 ($L \cdot mol^{-1} \cdot s^{-1}$)	M_1 ($g \cdot mol^{-1}$)	M_2/M_1	$k_{p,cop}$ from M_1 ($L \cdot mol^{-1} \cdot s^{-1}$)	
90	50	50% Tol	0.7	0.76	1.9	n/d	n/d	n/d	n/d	n/d	n/d	n/d
					2.1	n/d	n/d	n/d	n/d	n/d	n/d	n/d
90	50	25% Tol	0.7	0.70	2.0	45709	2.00	2591	43652	2.00	2474	0.95
					2.2	45709	2.00	2591	44668	2.00	2532	0.98
90	50	25% DMF	0.7	0.65	2.0	36308	1.95	1919	35481	2.00	1876	0.98
					1.9	36308	1.95	1919	34674	2.04	1833	0.95
90	50	50% DMF	0.7	0.65	2.0	34674	2.00	1877	33884	2.00	1835	0.98
					1.8	34674	1.95	1877	33884	2.00	1835	0.98
90	50	50% BuOH	0.7	0.65	1.8	43652	1.95	2585	42658	1.95	2526	0.98
					1.9	43652	1.95	2585	41687	2.00	2469	0.95
90	50	50% Tol	0.9	0.92	1.8	n/d	n/d	n/d	n/d	n/d	n/d	n/d
					2.1	n/d	n/d	n/d	n/d	n/d	n/d	n/d
90	50	25% Tol	0.9	0.87	2.2	n/d	n/d	n/d	n/d	n/d	n/d	n/d
					2.1	n/d	n/d	n/d	n/d	n/d	n/d	n/d
90	50	25% DMF	0.9	0.83	1.8	n/d	n/d	n/d	n/d	n/d	n/d	n/d
					2.0	n/d	n/d	n/d	n/d	n/d	n/d	n/d
90	50	50% DMF	0.9	0.85	2.1	n/d	n/d	n/d	n/d	n/d	n/d	n/d
					2.0	n/d	n/d	n/d	n/d	n/d	n/d	n/d

Table A.1.3. ST/GMA solution copolymerization : PLP experimental conditions and results with [DMPA]=5mmol·L^{-1} at 90 ℃

T (℃)	Pulse Repetition Rate (Hz)	Solvent	Monomer Mole Fraction f_{GMA}	Polymer Mole Fraction F_{GMA}	Conversion %	SEC Result						
						RI			LS			
						M_1 (g·mol^{-1})	M_2/M_1	$k_{p,cop}$ from M_1 (L·mol^{-1}·s^{-1})	M_1 (g·mol^{-1})	M_2/M_1	$k_{p,cop}$ from M_1 (L·mol^{-1}·s^{-1})	$k_{p,cop,LS}/k_{p,cop,RI}$
90	50	50% Tol	0	0	2.0	15136	2.00	910	14791	2.00	889	0.98
					2.2	15136	2.00	910	14791	2.00	889	0.98
90	50	25% Tol	0	0	2.0	15488	2.00	916	15136	2.00	895	0.98
					1.8	15488	2.00	916	15136	1.95	895	0.98
90	50	50% DMF	0	0	2.2	12303	2.00	707	12023	2.00	691	0.98
					1.8	12303	2.00	707	12023	2.00	691	0.98
90	50	25% DMF	0	0	2.1	12303	2.00	711	12023	2.00	695	0.98
					2.2	12303	2.00	711	12023	2.00	695	0.98
90	50	50% BuOH	0	0	1.8	14791	2.00	920	14454	2.00	899	0.98
					2.0	14791	2.00	920	14454	2.00	899	0.98
90	50	50% Tol	0.1	0.22	1.8	14125	1.95	841	13490	2.00	804	0.95
					1.8	13804	2.00	822	13490	2.00	804	0.98
90	50	25% Tol	0.1	0.22	2.1	14791	1.95	863	14125	2.00	824	0.95
					1.9	14454	2.00	843	13804	2.00	805	0.95
90	50	50% DMF	0.1	0.22	2.0	11220	1.95	639	10965	1.95	625	0.98
					1.9	11482	2.00	654	10965	2.00	625	0.95
90	50	25% DMF	0.1	0.22	2.2	11220	1.95	640	10715	2.00	611	0.95
					2.0	10965	2.00	625	10715	2.00	611	0.98

Table A.1.3 (Continued)

T (℃)	Pulse Repetition Rate (Hz)	Solvent	Monomer Mole Fraction f_{GMA}	Polymer Mole Fraction F_{GMA}	Conversion %	SEC Result						
						RI			LS			$k_{p,cop,LS}/k_{p,cop,RI}$
						M_1 ($g\cdot mol^{-1}$)	M_2/M_1	$k_{p,cop}$ from M_1 ($L\cdot mol^{-1}\cdot s^{-1}$)	M_1 ($g\cdot mol^{-1}$)	M_2/M_1	$k_{p,cop}$ from M_1 ($L\cdot mol^{-1}\cdot s^{-1}$)	
90	50	50% BuOH	0.1	0.22	13804	1.95	850	13490	1.95	831	0.98	0.98
					13804	2.00	850	13183	2.00	812	0.95	0.95
90	50	25% Tol	0.2	0.34	2.0	14791	2.00	851	14454	2.00	832	0.98
					1.9	14791	1.95	851	14454	2.00	832	0.98
90	50	50% DMF	0.2	0.34	2.1	12023	2.00	679	11749	2.00	663	0.98
					1.9	12023	1.95	679	11482	2.00	648	0.95
90	50	25% DMF	0.2	0.34	2.0	11749	2.00	661	11482	2.00	646	0.98
					2.0	12023	1.95	677	11749	2.00	661	0.98
90	50	50% BuOH	0.2	0.34	1.9	14454	1.95	882	14125	2.00	862	0.98
					2.0	14791	2.00	902	14125	2.00	862	0.95
90	50	50% Tol	0.3	0.42	1.8	16596	2.00	971	16218	2.00	949	0.98
					1.9	16596	1.95	971	15849	2.00	927	0.95
90	50	25% Tol	0.3	0.42	1.9	16596	2.00	942	16218	2.00	921	0.98
					1.8	17378	2.04	987	16596	2.00	942	0.95
90	50	50% DMF	0.3	0.42	2.0	13490	2.00	755	13183	2.04	738	0.98
					1.7	13804	2.04	773	13183	2.00	738	0.95
90	50	25% DMF	0.3	0.42	2.2	13183	2.00	733	12882	2.00	716	0.98
					2.0	13183	2.00	733	12882	2.00	716	0.98

Table A.1.3 (Continued)

T (℃)	Pulse Repetition Rate (Hz)	Solvent	Monomer Mole Fraction f_{GMA}	Polymer Mole Fraction F_{GMA}	Conversion %	SEC Result						
						RI			LS			
						M_1 ($g \cdot mol^{-1}$)	M_2/M_1	$k_{p,cop}$ from M_1 ($L \cdot mol^{-1} \cdot s^{-1}$)	M_1 ($g \cdot mol^{-1}$)	M_2/M_1	$k_{p,cop}$ from M_1 ($L \cdot mol^{-1} \cdot s^{-1}$)	$k_{p,cop,LS}/k_{p,cop,RI}$
90	50	50% BuOH	0.3	0.42	2.0	15849	2.00	958	15136	1.95	915	0.95
					1.8	15849	1.95	958	15488	2.00	936	0.98
90	50	50% Tol	0.4	0.47	1.8	18197	2.00	1055	17783	2.00	1031	0.98
					2.0	18621	2.04	1080	18197	2.00	1055	0.98
90	50	25% Tol	0.4	0.47	2.1	18621	2.00	1044	18197	2.00	1021	0.98
					1.9	18621	2.00	1044	18197	2.00	1021	0.98
90	50	50% DMF	0.4	0.47	2.0	15136	2.00	841	14791	2.00	821	0.98
					1.8	15136	2.00	841	14454	1.95	803	0.95
90	50	25% DMF	0.4	0.47	2.1	14791	2.04	812	14454	2.00	794	0.98
					2.2	15136	2.00	831	14454	2.00	794	0.95
90	50	50% BuOH	0.4	0.47	1.8	17783	2.00	1065	17378	2.00	1041	0.98
					2.0	18197	2.04	1090	17378	2.00	1041	0.95
90	50	50% Tol	0.5	0.54	1.8	20893	2.00	1202	20417	2.00	1174	0.98
					2.0	21380	2.00	1230	20417	2.00	1174	0.95
90	50	25% Tol	0.5	0.54	2.1	21380	2.00	1185	20893	2.00	1158	0.98
					1.9	21380	1.95	1185	20417	2.00	1131	0.95
90	50	50% DMF	0.5	0.54	2.0	16982	2.00	936	16596	2.00	914	0.98
					2.2	17378	1.95	957	16596	2.00	914	0.95

Table A.1.3 (Continued)

T (℃)	Pulse Repetition Rate (Hz)	Solvent	Monomer Mole Fraction f_{GMA}	Polymer Mole Fraction F_{GMA}	Conversionà %	SEC Result						
						RI			LS			
						M_1 ($g \cdot mol^{-1}$)	M_2/M_1	$k_{p,cop}$ from M_1 ($L \cdot mol^{-1} \cdot s^{-1}$)	M_1 ($g \cdot mol^{-1}$)	M_2/M_1	$k_{p,cop}$ from M_1 ($L \cdot mol^{-1} \cdot s^{-1}$)	$k_{p,cop,LS}/k_{p,cop,RI}$
90	50	25% DMF	0.5	0.54	2.1	17783	2.00	965	16982	2.00	922	0.95
					1.9	17378	1.95	943	16982	2.00	922	0.98
90	50	50% BuOH	0.5	0.54	2.0	19953	2.00	1185	19055	1.95	1132	0.95
					1.9	19953	2.00	1185	19498	2.00	1158	0.98
90	50	50% Tol	0.7	0.66	2.2	26915	1.95	1524	26303	2.00	1489	0.98
					2.0	26915	2.00	1524	25704	2.00	1456	0.95
90	50	25% Tol	0.7	0.66	2.1	27542	2.00	1492	26915	2.00	1458	0.98
					1.9	28184	2.00	1527	26915	2.00	1458	0.95
90	50	50% DMF	0.7	0.66	1.8	22909	2.00	1244	22387	2.00	1215	0.98
					1.9	23442	2.00	1273	22909	1.95	1244	0.98
90	50	25% DMF	0.7	0.66	2.1	23442	2.00	1244	22909	2.00	1216	0.98
					2.2	23988	2.00	1273	23442	2.00	1244	0.98
90	50	50% BuOH	0.7	0.66	2.0	26303	1.95	1537	25704	2.00	1502	0.98
					2.1	26303	2.00	1537	25119	2.00	1468	0.95
90	50	50% Tol	0.9	0.84	1.9	37154	2.00	2074	36308	2.00	2026	0.98
					1.8	37154	1.95	2074	36308	2.00	2026	0.98
90	50	25% Tol	0.9	0.84	1.9	38019	1.95	2018	37154	2.00	1972	0.98
					1.9	38905	2.00	2065	38019	2.00	2018	0.98

Table A.1.3 (Continued)

T (℃)	Pulse Repetition Rate (Hz)	Solvent	Monomer Mole Fraction f_{GMA}	Polymer Mole Fraction F_{GMA}	Conversion %	SEC Result						
						RI			LS			
						M_1 ($g \cdot mol^{-1}$)	M_2/M_1	$k_{p,cop}$ from M_1 ($L \cdot mol^{-1} \cdot s^{-1}$)	M_1 ($g \cdot mol^{-1}$)	M_2/M_1	$k_{p,cop}$ from M_1 ($L \cdot mol^{-1} \cdot s^{-1}$)	$k_{p,cop,LS}/k_{p,cop,RI}$
90	50	50% DMF	0.9	0.84	2.0	33884	1.95	1814	32359	2.00	1732	0.95
					1.9	33884	2.00	1814	33113	2.00	1773	0.98
90	50	25% DMF	0.9	0.84	2.2	35481	1.95	1846	34674	2.00	1804	0.98
					2.1	35481	2.00	1846	33884	2.00	1763	0.95
90	50	50% BuOH	0.9	0.84	2.0	35481	2.00	2043	34674	1.95	1996	0.98
					1.8	36308	1.95	2091	34674	2.00	1996	0.95
90	50	50% Tol	1.0	1.0	2.1	47863	2.00	2653	45709	2.00	2534	0.95
					2.2	46774	1.95	2593	45709	2.00	2534	0.98
90	50	25% Tol	1.0	1.0	2.0	50119	2.00	2634	47863	2.00	2516	0.95
					1.9	50119	2.00	2634	48978	2.00	2574	0.98
90	50	50% DMF	1.0	1.0	2.2	48978	2.00	2605	47863	2.00	2546	0.98
					1.8	48978	1.95	2605	47863	2.00	2546	0.98
90	50	25% DMF	1.0	1.0	2.1	50119	2.00	2583	48978	1.95	2524	0.98
					2.2	51286	2.00	2643	50119	2.00	2583	0.98
90	50	50% BuOH	1.0	1.0	1.9	46774	2.00	2674	44668	2.00	2554	0.95
					2.0	46774	1.95	2674	45709	2.00	2613	0.98

Table A.1.4 ST/BMA solution copolymerization : PLP experimental conditions and results with [DMPA]=5mmol·L^{-1} at 90 ℃

T (℃)	Pulse Repetition Rate (Hz)	Solvent	Monomer Mole Fraction f_{BMA}	Polymer Mole Fraction F_{BMA}	Conversion %	SEC Result						
						RI			LS			$k_{p,cop,LS}/k_{p,cop,RI}$
						M_1 (g·mol^{-1})	M_2/M_1	$k_{p,cop}$ from M_1 (L·mol^{-1}·s^{-1})	M_1 (g·mol^{-1})	M_2/M_1	$k_{p,cop}$ from M_1 (L·mol^{-1}·s^{-1})	
90	50	50% Tol	0	0	1.9	15136	2.00	910	14791	2.00	889	0.98
					2.1	15136	2.00	910	14791	2.00	889	0.98
90	50	25% Tol	0	0	2.2	15488	2.00	916	15136	2.00	895	0.98
					1.9	15488	2.00	916	15136	2.00	895	0.98
90	50	50% DMF	0	0	2.1	12303	2.00	707	12023	2.00	691	0.98
					1.9	12303	2.00	707	12023	2.00	691	0.98
90	50	25% DMF	0	0	2.2	12303	2.00	711	12023	2.00	695	0.98
					2.0	12303	2.00	711	12023	2.00	695	0.98
90	50	50% BuOH	0	0	1.9	14791	2.00	920	14454	2.00	899	0.98
					2.1	14791	2.00	920	14454	2.00	899	0.98
90	50	50% Tol	0.1	0.14	1.9	14791	1.95	892	14454	2.00	872	0.98
					1.9	14791	2.00	892	14454	1.95	872	0.98
90	50	25% Tol	0.1	0.14	2.2	15136	1.95	899	14454	1.95	858	0.95
					1.8	15136	2.00	899	14791	2.00	878	0.98
90	50	50% DMF	0.1	0.14	2.1	12023	1.95	693	11749	2.00	677	0.98
					1.8	12303	2.00	709	12023	1.95	693	0.98
90	50	25% DMF	0.1	0.14	2.1	12023	1.95	698	11749	2.00	682	0.98
					2.1	12023	2.00	698	11749	1.95	682	0.98

Table A.1.4 (Continued)

T (℃)	Pulse Repetition Rate (Hz)	Solvent	Monomer Mole Fraction f_{BMA}	Polymer Mole Fraction F_{BMA}	Conversion %	SEC Result						
						RI			LS			$k_{p,cop,LS}/k_{p,cop,RI}$
						M_1 ($g\cdot mol^{-1}$)	M_2/M_1	$k_{p,cop}$ from M_1 ($L\cdot mol^{-1}\cdot s^{-1}$)	M_1 ($g\cdot mol^{-1}$)	M_2/M_1	$k_{p,cop}$ from M_1 ($L\cdot mol^{-1}\cdot s^{-1}$)	
90	50	50% BuOH	0.1	0.27	2.2	14454	1.95	901	14125	2.00	881	0.98
					1.9	14454	2.00	901	13804	1.95	861	0.95
90	50	50% Tol	0.2	0.24	2.0	15136	1.95	915	14791	2.00	894	0.98
					2.1	15136	2.00	915	14791	2.00	894	0.98
90	50	25% Tol	0.2	0.24	2.2	15488	2.00	923	15136	2.00	902	0.98
					1.8	15849	1.95	944	15136	2.00	902	0.95
90	50	50% DMF	0.2	0.24	2.0	12589	2.00	727	12023	2.00	695	0.95
					1.8	12589	1.95	727	12303	2.00	711	0.98
90	50	25% DMF	0.2	0.24	2.1	12589	2.00	733	12023	2.00	700	0.95
					2.2	12589	1.95	733	12303	2.00	717	0.98
90	50	50% BuOH	0.2	0.37	1.8	15488	1.95	968	15136	2.00	946	0.98
					2.1	15136	2.00	946	14791	2.00	925	0.98
90	50	50% Tol	0.3	0.42	1.9	15488	2.00	938	14791	1.95	896	0.95
					1.8	15849	1.95	960	15136	2.00	917	0.95
90	50	25% Tol	0.3	0.42	2.0	15849	2.00	947	15488	2.04	926	0.98
					1.9	15488	2.04	926	15136	2.00	905	0.98
90	50	50% DMF	0.3	0.42	2.1	12882	2.00	746	12589	1.00	729	0.98
					1.8	13183	2.04	763	12589	2.00	729	0.95

Table A.1.4 (Continued)

T (℃)	Pulse Repetition Rate (Hz)	Solvent	Monomer Mole Fraction f_{BMA}	Polymer Mole Fraction F_{BMA}	Conversion %	SEC Result						
						RI			LS			$k_{p,cop,LS}/k_{p,cop,RI}$
						M_1 ($g\cdot mol^{-1}$)	M_2/M_1	$k_{p,cop}$ from M_1 ($L\cdot mol^{-1}\cdot s^{-1}$)	M_1 ($g\cdot mol^{-1}$)	M_2/M_1	$k_{p,cop}$ from M_1 ($L\cdot mol^{-1}\cdot s^{-1}$)	
90	50	25% DMF	0.3	0.42	2.1	12882	2.00	753	12589	2.00	736	0.98
					2.2	12882	2.00	753	12303	1.95	719	0.95
90	50	50% BuOH	0.3	0.33	2.0	16982	2.00	1064	16218	1.95	1016	0.95
					1.9	16596	1.95	1040	16218	2.00	1016	0.98
90	50	50% Tol	0.4	0.40	1.9	15849	2.00	962	15488	2.00	940	0.98
					2.2	16218	2.04	984	15849	1.95	962	0.98
90	50	25% Tol	0.4	0.40	2.0	16218	2.00	972	15849	2.00	950	0.98
					1.8	16596	2.00	995	15849	2.00	950	0.95
90	50	50% DMF	0.4	0.40	2.1	13490	2.00	782	13183	2.00	765	0.98
					1.9	13490	2.00	782	13183	2.00	765	0.98
90	50	25% DMF	0.4	0.40	2.2	13490	2.04	791	12882	2.00	755	0.95
					2.1	13490	2.00	791	13183	2.00	773	0.98
90	50	50% BuOH	0.4	0.49	1.9	17378	2.00	1091	16982	2.00	1066	0.98
					2.1	17378	2.04	1091	16982	1.95	1066	0.98
90	50	50% Tol	0.5	0.47	1.9	16596	2.00	1009	16218	2.00	986	0.98
					2.2	16596	2.00	1009	15849	2.00	964	0.95
90	50	25% Tol	0.5	0.47	2.1	16596	2.00	998	16218	1.95	975	0.98
					1.8	16982	1.95	1021	16596	1.95	998	0.98

Table A.1.4 (Continued)

T (℃)	Pulse Repetition Rate (Hz)	Solvent	Monomer Mole Fraction f_{BMA}	Polymer Mole Fraction F_{BMA}	Conversion %	SEC Result						
						RI			LS			
						M_1 ($g \cdot mol^{-1}$)	M_2/M_1	$k_{p,cop}$ from M_1 ($L \cdot mol^{-1} \cdot s^{-1}$)	M_1 ($g \cdot mol^{-1}$)	M_2/M_1	$k_{p,cop}$ from M_1 ($L \cdot mol^{-1} \cdot s^{-1}$)	$k_{p,cop,LS}/k_{p,cop,RI}$
90	50	50% DMF	0.5	0.47	2.1	14454	2.00	840	14125	2.04	821	0.98
					2.0	14125	1.95	821	13804	2.00	802	0.98
90	50	25% DMF	0.5	0.47	1.8	14125	2.00	830	13804	1.95	811	0.98
					1.8	14125	1.95	830	13804	2.00	811	0.98
90	50	50% BuOH	0.5	0.53	2.1	18621	2.00	1171	18197	2.00	1144	0.98
					1.8	19055	2.00	1198	18621	2.00	1171	0.98
90	50	50% Tol	0.7	0.61	2.1	18621	1.95	1136	18197	2.00	1110	0.98
					2.1	18621	2.00	1136	18197	2.00	1110	0.98
90	50	25% Tol	0.7	0.61	2.2	19055	2.00	1151	18621	2.00	1125	0.98
					1.8	19055	2.00	1151	18621	2.00	1125	0.98
90	50	50% DMF	0.7	0.61	1.9	16218	2.00	946	15849	2.00	924	0.98
					1.9	16596	2.00	968	16218	2.00	946	0.98
90	50	25% DMF	0.7	0.61	2.2	16218	2.00	958	15849	2.04	936	0.98
					2.1	16596	2.00	980	16218	2.00	958	0.98
90	50	50% BuOH	0.7	0.63	2.2	21380	1.95	1349	20893	2.00	1318	0.98
					2.0	21380	2.00	1349	20417	2.00	1288	0.95

Table A.1.4 (Continued)

T (℃)	Pulse Repetition Rate (Hz)	Solvent	Monomer Mole Fraction f_{BMA}	Polymer Mole Fraction F_{BMA}	Conversion %	SEC Result						
						RI			LS			$k_{p,cop,LS}/k_{p,cop,RI}$
						M_1 ($g\cdot mol^{-1}$)	M_2/M_1	$k_{p,cop}$ from M_1 ($L\cdot mol^{-1}\cdot s^{-1}$)	M_1 ($g\cdot mol^{-1}$)	M_2/M_1	$k_{p,cop}$ from M_1 ($L\cdot mol^{-1}\cdot s^{-1}$)	
90	50	50% Tol	0.9	0.82	1.8	23988	2.00	1468	23442	2.04	1434	0.98
					2.1	23442	1.95	1434	22909	2.00	1402	0.98
90	50	25% Tol	0.9	0.82	1.8	24547	1.95	1490	23442	2.00	1423	0.95
					1.9	23442	2.00	1423	22909	1.95	1391	0.98
90	50	50% DMF	0.9	0.82	2.1	21878	1.95	1279	21380	2.00	1250	0.98
					1.9	22387	2.00	1309	21380	1.95	1250	0.95
90	50	25% DMF	0.9	0.82	2.1	21878	1.95	1298	21380	2.00	1269	0.98
					2.0	22387	2.00	1328	21380	2.00	1269	0.95
90	50	50% BuOH	0.9	0.81	2.0	28840	2.00	1825	28184	2.04	1784	0.98
					1.9	29512	1.95	1868	28840	2.00	1825	0.98
90	50	50% Tol	1.0	1.0	2.2	33113	2.00	2029	31623	2.00	1938	0.95
					2.2	32359	1.95	1983	31623	2.00	1938	0.98
90	50	25% Tol	1.0	1.0	2.1	32359	2.00	1968	31623	2.00	1923	0.98
					2.0	32359	2.00	1968	31623	2.00	1923	0.98
90	50	50% DMF	1.0	1.0	2.1	33884	2.00	1984	33113	2.00	1939	0.98
					1.9	33884	1.95	1984	33113	2.00	1939	0.98
90	50	25% DMF	1.0	1.0	2.0	33113	2.00	1969	32359	2.00	1924	0.98
					2.1	33884	2.00	2015	33113	2.00	1969	0.98
90	50	50% BuOH	1.0	1.0	1.8	41687	2.00	2642	39811	2.00	2523	0.95

Appendix A.2 Semibatch experimental reproducibility

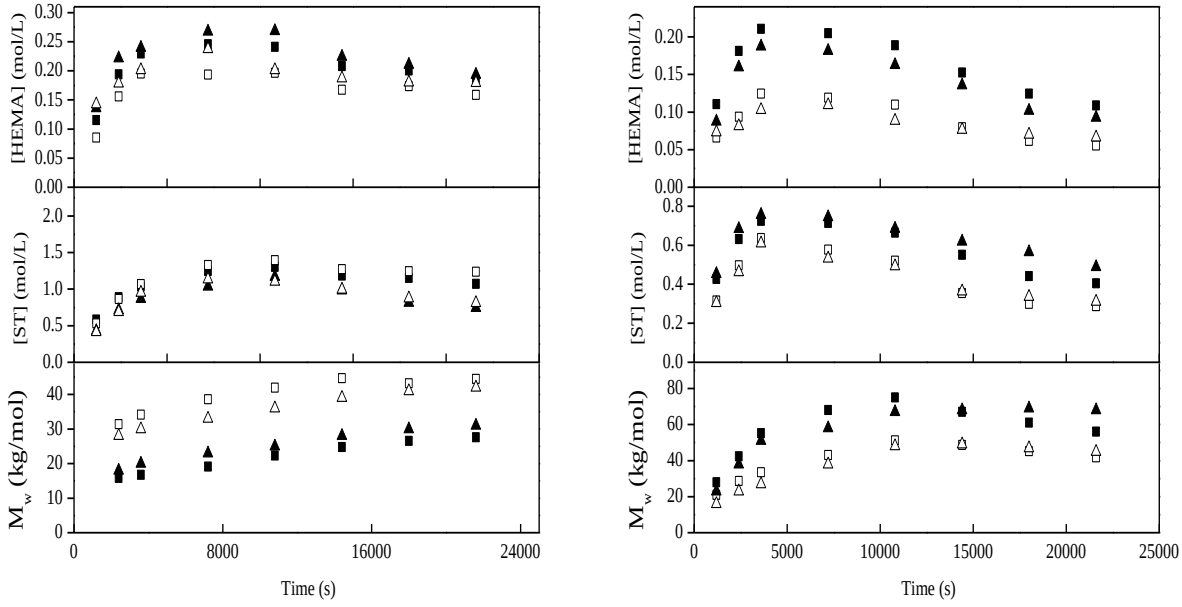

(a) (b)

Figure A.2.1 Experimental results of [ST], [HEMA] and weight-average MW (M_w) for two HEMA/ST 75/25 copolymerization experiments in xylene (empty symbol) and DMF (solid symbol) at (a) 110 °C and (b) 138 °C, respectively. See Ch 4 for experimental details.

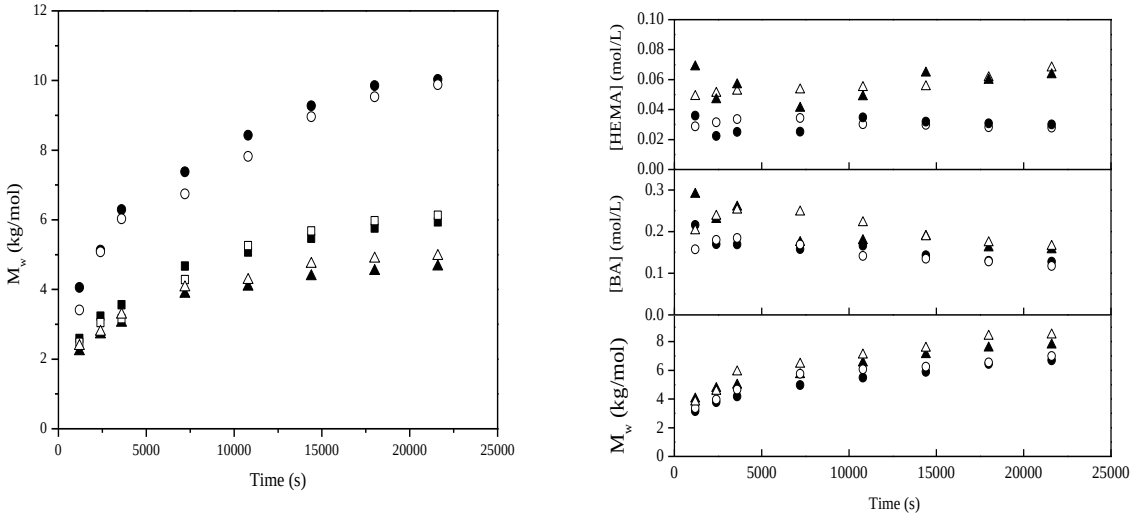

(a) (b)

Figure A.2.2 Experimental results of [BA], [HEMA] and weight-average MW (M_w) for (a) BA homopolymerization and (b) HEMA/BA 75/25 copolymerization experiments at 138 °C in xylene (■□), DMF (▲△) and *n*-pentanol (●○).

Appendix A.3: PLP/SEC/NMR Results for Methacrylate Copolymerization (Ch 5)

Table A.3.1 HEMA/BMA solution copolymerization : PLP experimental conditions and results with [DMPA]=5mmol·L^{-1}

T (℃)	Pulse Repetition Rate (Hz)	Solvent	Monomer Mole Fraction f_{HEMA}	Polymer Mole Fraction F_{HEMA}	Conversion %	SEC Result						
						RI			LS			$k_{p,cop,LS}/k_{p,cop,RI}$
						M_1 (g·mol^{-1})	M_2/M_1	$k_{p,cop}$ from M_1 (L·mol^{-1}·s^{-1})	M_1 (g·mol^{-1})	M_2/M_1	$k_{p,cop}$ from M_1 (L·mol^{-1}·s^{-1})	
90	50	Bulk	0.1	-	2.2	39365	2.00	2807	37402	1.95	2667	0.95
90	50	Bulk	0.4	-	1.8	65083	1.95	4404	63782	2.00	4316	0.98
90	50	Bulk	0.5	-	2.1	70758	2.00	4503	69343	2.00	4413	0.98
					2.2	73430	2.00	4877	69759	1.95	4633	0.95
90	50	Bulk	0.7	0.78	2.8	-	-	-	-	-	-	-
90	50	Bulk	0.8	0.82	2.4	-	-	-	-	-	-	-
100	50	Bulk	0	0	2.2	36033	2.00	2569	35312	2.00	2518	0.98
100	50	Bulk	0.2	-	2.0	63696	2.00	4310	62422	1.95	4224	0.98
100	50	Bulk	0.3	0.48	1.8	70936	1.95	4711	69518	2.00	4617	0.98
100	50	Bulk	0.4	0.58	2.8	-	-	-	-	-	-	-
100	50	Bulk	0.6	0.74	2.2	-	-	-	-	-	-	-
100	50	Bulk	0.7	0.80	2.2	120011	2.00	6451	117611	2.04	6322	0.98
					2.1	126685	2.04	6809	120351	2.04	6469	0.95
90	50	50% BuOH	0	0	2.0	40623	1.95	2574	39811	2.00	2523	0.98
90	50	50% BuOH	0.1	0.11	1.8	46241	2.04	2930	45317	2.00	2872	0.98
90	50	50% BuOH	0.2	-	1.6	52270	2.04	3312	49657	2.00	3147	0.95
90	50	50% BuOH	0.3	0.31	2.0	55276	1.95	3503	52513	2.00	3328	0.95

Table A.3.1 (Continued)

T (℃)	Pulse Repetition Rate (Hz)	Solvent	Monomer Mole Fraction f_{HEMA}	Polymer Mole Fraction F_{HEMA}	Conversion %	SEC Result						
						RI			LS			$k_{p,cop,LS}/k_{p,cop,RI}$
						M_1 ($g\cdot mol^{-1}$)	M_2/M_1	$k_{p,cop}$ from M_1 ($L\cdot mol^{-1}\cdot s^{-1}$)	M_1 ($g\cdot mol^{-1}$)	M_2/M_1	$k_{p,cop}$ from M_1 ($L\cdot mol^{-1}\cdot s^{-1}$)	
90	50	50% BuOH	0.4	-	2.0	56600	2.04	3590	55527	2.00	3519	0.98
90	50	50% BuOH	0.5	0.51	2.2	-	-	-	-	-	-	-
90	50	50% BuOH	0.7	0.71	2.0	-	-	-	-	-	-	-
90	50	50% BuOH	0.9	0.91	2.8	-	-	-	-	-	-	-
90	50	50% DMF	0.1	-	1.8	35214	1.95	2062	33454	2.00	1959	0.95
					1.9	33038	2.00	1934	32378	1.95	1896	0.98
90	50	50% DMF	0.2	-	2.1	36907	1.95	2229	36169	2.00	2118	0.98
					1.9	4.991	2.04	2345	38942	1.95	2228	0.95
90	50	50% BuOH	0	0	2.0	40623	1.95	2574	39811	2.00	2523	0.98
90	50	50% DMF	0.3	0.31	2.4	41161	2.00	2353	39103	2.04	2236	0.95
90	50	50% DMF	0.4	0.40	2.8	41897	2.00	2380	41060	2.00	2333	0.98
90	50	50% DMF	0.6	0.61	1.8	50249	1.95	2804	47737	2.04	2664	0.95

Appendix A.4: PLP/SEC/NMR Results for Acrylate and Acrylate/Styrene Systems (Ch 6)

Table A.4.1 50℃, 50Hz Bulk ST/HEA PLP experimental conditions and results with [DMPA]=5mmol·L^{-1}

Monomer Mole Fraction f_{HEA}	Polymer Mole Fraction F_{HEA}	Conversion %	SEC-Waters				SEC-Viscotek			
			RI		LS		Universal Calibration		Multiple Detector	
			M_1 (g·mol^{-1})	$k_{p,cop}$ from M_1 (L·mol^{-1}·s^{-1})	M_1 (g·mol^{-1})	$k_{p,cop}$ from M_1 (L·mol^{-1}·s^{-1})	M_1 (g·mol^{-1})	$k_{p,cop}$ from M_1 (L·mol^{-1}·s^{-1})	M_1 (g·mol^{-1})	$k_{p,cop}$ from M_1 (L·mol^{-1}·s^{-1})
0	0	2.8	4169	235	4074	230	-	-	-	-
		2.5	4169	235	4074	230	-	-	-	-
0.1	0.1724	3.2	9772	546	10965	612	8710	486	11220	626
		2.8	9772	546	10965	612	8710	486	11220	626
0.3	0.3409	3.5	17783	972	18621	1018	15849	867	18621	1018
		3.1	18197	995	18197	995	16218	887	19055	1042
0.5	0.4347	3.2	28840	1545	26915	1442	25704	1377	28840	1545
		2.8	29512	1581	28184	1510	25704	1377	28840	1545
0.7	0.5555	3.4	53703	2821	53703	2821	47863	2514	54954	2886
		2.9	51286	2694	51286	2694	48978	2572	56234	2954
0.9	0.7143	2.8	83176	4284	83176	4284	74131	3819	85114	4384
		3.3	83176	4284	81283	4187	74131	3819	85114	4384
1.0	1.0	3.1	-	-	-	-	562341	28691	691831	35297
		2.9	-	-	-	-	549541	28038	676083	34494

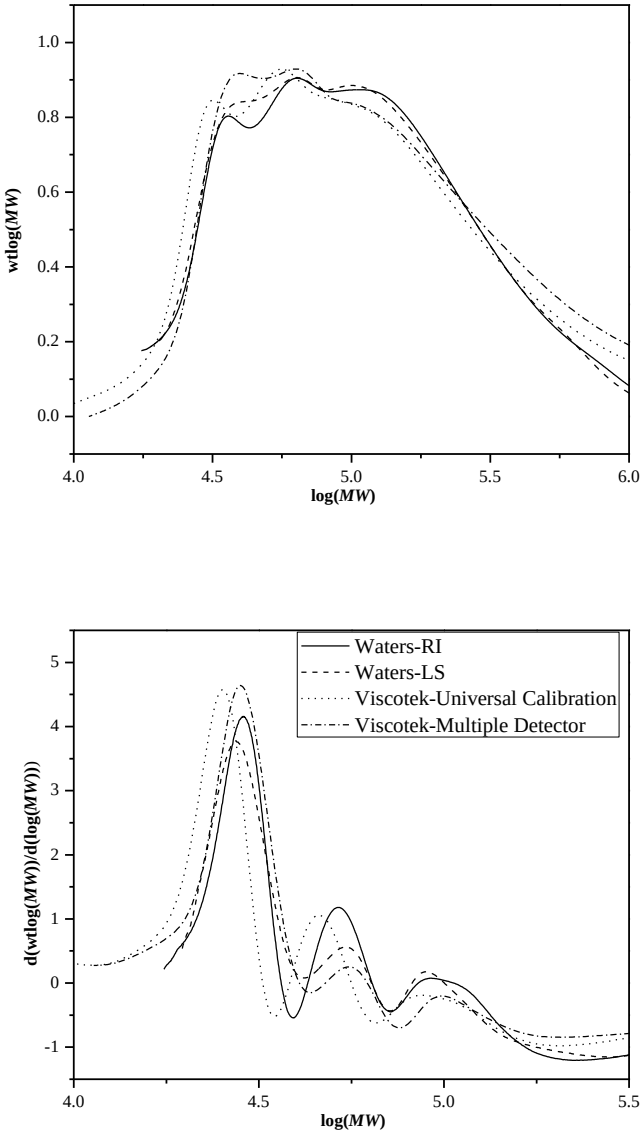

Figure A.4.1 MMDs (top) and corresponding first derivative (bottom) plots obtained for styrene/2-hydroxyethyl acrylate (HEA) copolymer produced by PLP at 50 °C and 50 Hz, as measured by RI, LS, Universal Calibration and Multiple Detector. HEA monomer composition is 50%.

Table A.4.2 ^{13}C NMR peak assignments for PLP-generated pBA at 50 °C

Peak(ppm)	Assignment	Integration	
		Bulk (Fig 2a)	In BuOH (Fig 4a)
14	-CH3	100.00	100.00
20	-CH2CH2CH2CH3	100.08	100.02
30	-CH2CH2CH2CH3	100.05	100.00
67	-CH2CH2CH2CH3	99.97	100.03
29	CH2 in branch	0.77	-
33-37	CH2 in main chain/backbone	99.47	99.98
39	CH in branch	0.26	-
40-41	CH in main chain/backbone	99.53	99.96
48	Quaternary carbon	0.25	-
172	C=O in branch	0.48	-
174	C=O in main chain/backbone	99.53	100.02

Table A.4.3 ^{13}C NMR peak assignments for PLP-generated pHEA at 50 °C

Peak(ppm)	Assignment	Integration	
		Bulk (Fig 2b)	In DMF (Fig 4b)
58	-OCH2CH2OH	100.00	100.00
66	-OCH2CH2OH	99.98	100.07
29	CH2 in branch	-	0.66
32-36	CH2 in main chain	100.03	99.46
37.5	CH in branch	-	0.19
38	CH in main chain	99.97	99.65
48	Quaternary carbon	-	0.18
172	C=O in branch	-	0.38
174	C=O in main chain	100.02	99.68

Table A.4.4 Experimental conditions and results for bulk pulsed-laser polymerization of HEA between 20 and 60 °C with [DMPA]=5mmol·L^{-1}

T (℃)	Pulse Repetition Rate (Hz)	Pulsed Time (s)	Conversion %	SEC Result		
				M_1 (g·mol^{-1})	M_2/M_1	k_p from M_1 (L·mol^{-1}·s^{-1})
20	100	120	2.5	173780	2.00	17733
		120	2.0	169824	2.00	17329
27	100	100	2.3	204174	2.04	20834
30	100	80	2.1	218776	1.95	22324
		80	2.2	223872	2.00	22844
40	100	60	2.6	275423	2.00	28104
		60	2.2	269153	2.00	27465
50	100	40	2.1	323594	1.95	33020
		40	2.3	331131	1.91	33789
50	50	60	2.5	660693	2.04	33709
		60	2.1	676083	2.04	34494
60	100	20	2.2	389045	2.00	39698
		20	2.3	398107	2.00	40623

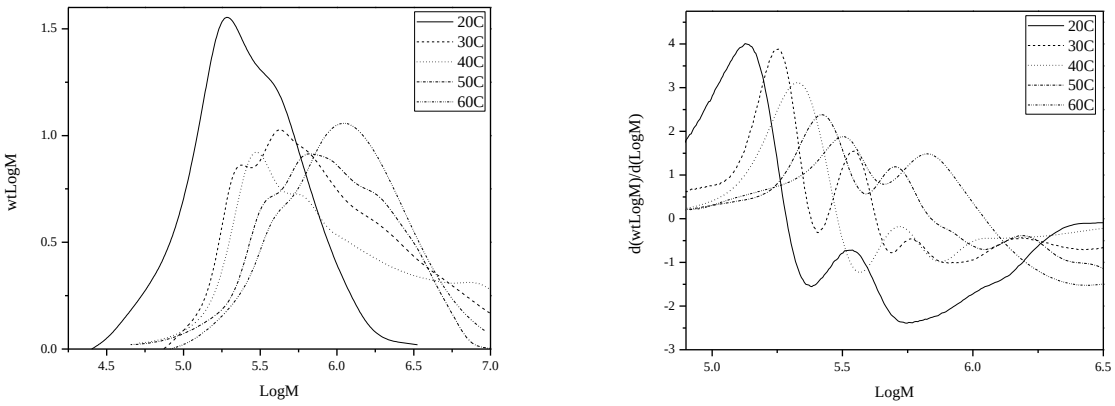

Figure A.4.2 MMDs (left) and first derivative plots (right) of samples produced by bulk PLP of HEA homopolymerization between 20 and 60 °C at 100 Hz.

Appendix A.5: PLP/SEC/NMR Results for Acrylate/Methacrylate Systems (Ch 7)

Table A.5.1 HEMA/BA bulk and solution copolymerization: PLP experimental results at 50℃ with [DMPA]=5mmol·L^{-1}

Pulse Repetition Rate (Hz)	Solvent	Monomer Mole Fraction f_{HEMA}	Polymer Mole Fraction F_{HEMA}	Conversion %	SEC Result						
					RI			LS			
					M_1 (g·mol^{-1})	M_2/M_1	$k_{p,cop}$ from M_1 (L·mol^{-1}·s^{-1})	M_1 (g·mol^{-1})	M_2/M_1	$k_{p,cop}$ from M_1 (L·mol^{-1}·s^{-1})	$k_{p,cop,LS}/k_{p,cop,RI}$
50	Bulk	0.1	0.325	2.0	75858	1.98	4277	72444	2.00	4085	0.95
				2.2	75858	2.00	4277	72444	1.98	4085	0.95
50	Bulk	0.2	0.554	1.8	60256	2.00	3340	58884	1.98	3264	0.98
				1.9	57544	2.00	3190	54954	1.98	3046	0.95
50	Bulk	0.3	0.683	2.0	46774	2.04	2549	45709	2.04	2491	0.98
				1.8	47863	2.00	2608	44668	2.00	2434	0.93
50	Bulk	0.4	-	1.8	44668	2.00	2392	42658	1.98	2284	0.95
				1.6	45709	2.00	2447	44668	1.98	2392	0.98
50	Bulk	0.5	0.821	1.7	43652	2.00	2296	41687	2.00	2193	0.95
				2.0	44668	1.98	2350	42658	1.98	2244	0.95
50	Bulk	0.7	0.933	2.6	-	-	-	-		-	-
50	Bulk	0.9	0.985	2.8	-	-	-	-	-	-	-

Table A.5.1 (Continued)

Pulse Repetition Rate (Hz)	Solvent	Monomer Mole Fraction f_{HEMA}	Polymer Mole Fraction F_{HEMA}	Conversion %	SEC Result						
					RI			LS			
					M_1 ($g \cdot mol^{-1}$)	M_2/M_1	$k_{p,cop}$ from M_1 ($L \cdot mol^{-1} \cdot s^{-1}$)	M_1 ($g \cdot mol^{-1}$)	M_2/M_1	$k_{p,cop}$ from M_1 ($L \cdot mol^{-1} \cdot s^{-1}$)	$k_{p,cop,LS}/k_{p,cop,RI}$
50	50% BuOH	0.1	0.35	2.1	77625	2.04	8754	74131	2.00	8360	0.95
				2.2	75858	1.98	8555	74131	1.98	8360	0.98
50	50% BuOH	0.3	0.43	1.9	40738	1.98	4439	39811	2.00	4338	0.98
				2.3	41687	2.00	4543	39811	2.04	4338	0.95
50	50% BuOH	0.5	0.43	2.1	33884	2.04	3565	32359	2.00	3404	0.95
				1.7	34674	2.00	3648	33884	1.98	3565	0.98
50	50% BuOH	0.7	0.861	2.2	-	-	-	-	-	-	-
50	50% BuOH	0.9	0.974	2.0	-	-	-	-	-	-	-
50	50% DMF	0.1	0.236	2.0	40738	2.04	2297	38905	2.00	2194	0.95
				2.2	41687	2.00	2351	40738	2.04	2297	0.98
50	50% DMF	0.3	0.548	2.0	21380	2.00	1165	20417	2.00	1112	0.95
				1.8	21380	2.04	1165	20893	2.04	1138	0.98

Table A.5.1 (Continued)

Pulse Repetition Rate (Hz)	Solvent	Monomer Mole Fraction f_{HEMA}	Polymer Mole Fraction F_{HEMA}	Conversion %	SEC Result						
					RI						$k_{p,cop,LS}/k_{p,cop,RI}$
					M_1 ($g \cdot mol^{-1}$)	M_2/M_1	$k_{p,cop}$ from M_1 ($L \cdot mol^{-1} \cdot s^{-1}$)	M_1 ($g \cdot mol^{-1}$)	M_2/M_1	$k_{p,cop}$ from M_1 ($L \cdot mol^{-1} \cdot s^{-1}$)	
50	50% DMF	0.5	0.716	1.9	18621	1.98	979	17783	2.00	935	0.95
				2.3	19055	4.17	1002	18621	1.98	979	0.98
50	50% DMF	0.7	0.886	2.0	-	-	-	-	-	-	-
50	50% DMF	0.9	0.958	1.8	-	-	-	-	-	-	-

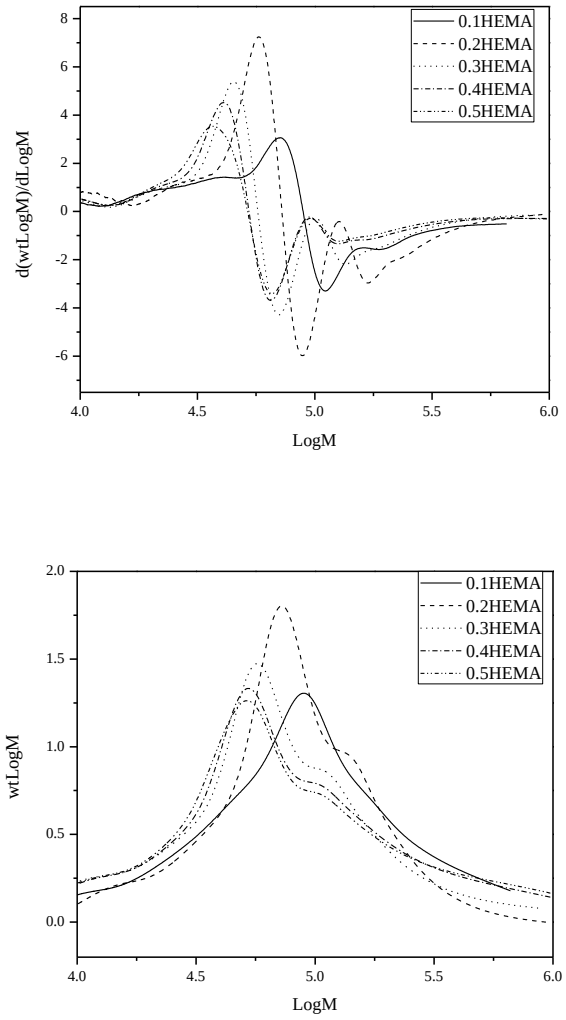

Figure A.5.1 MMDs (top) and first derivative plots (bottom) of samples produced by bulk PLP of HEMA/BA copolymerization at 50 °C and 50 Hz